INVESTIGATION OF THE DOPAMINERGIC NEURONS OF THE ZEBRAFISH OLFACTORY BULB
THROUGH IMMUNOHISTOCHEMISTRY, BEHAVIOURAL ANALYSIS AND EFFECTS OF
ENVIRONMENTAL TOXINS

by

Jillian Marie Doyle

Submitted in partial fulfilment of the requirements
for the degree of Doctor of Philosophy

at

Dalhousie University
Halifax, Nova Scotia
May 2024

For Henry, my other thesis

Table of Contents

List Of Tables

Chapter 2

Chapter 4

Chapter 5

List Of Figures

Chapter 1

Chapter 2

Chapter 3

Chapter 4

Chapter 5

Abstract

The sense of smell is integral to almost every aspect of life and its loss can be detrimental. Therefore, understanding how the olfactory system functions is essential to investigating potential solutions for its dysfunction. Zebrafish present a unique opportunity for study due to the relative simplicity of their already extensively examined olfactory system. However, the zebrafish olfactory bulb contains other less studied cells, such as dopaminergic (tyrosine hydroxylase positive; TH+) interneurons, which are of particular interest, as they potentially modulate communication between various regions/glomeruli of the bulb, although it is unknown whether or how this occurs. The purpose of this thesis was to characterize these interneurons and examine their role in olfactory behaviour.

First, I described the normal anatomy of the TH+-cells in the olfactory bulb and changes during development. I identified four distinct cell types/subtypes which appear to have specific functions and noted differences in the lateral and medial regions of the bulb, namely the uniquely dopaminergic innervation to the medial olfactory tract. Then, I developed a successful appetitive olfactory learning paradigm, which trained fish to respond to an odour after four days of conditioning. I then used the apparatus and baseline food odour response to demonstrate that manganese exposure causes reduced and inappropriate responses to different odours. In addition, I showed that manganese exposure reduced the number of TH+-cells in the olfactory bulb by 50% and disrupted the olfactory sensory neurons (OSNs) of the bulb. Prompted by the observed disruption of the OSNs, I investigated the isolated effects of metronidazole (Mtz), an antibiotic used in a new chemogenetic ablation technique claiming to specifically target only TH+-cells. I found that Mtz alone not only caused a 30% reduction in the number of TH+-cells in the bulb and variably disrupted OSNs but also caused reduced responses to odourants. Collectively, these findings indicated that TH+-cells in the olfactory bulb have several different morphologies and seem to uniquely innervate the medial olfactory tract. Furthermore, specific ablation for investigating behavioural changes is difficult, as various methods cause stress and adversely affect other olfactory cells.

List of Abbreviations and Symbols

ΔAIC   Change in Akaike information criterion

°C   Degrees Celsius

%   Percent

μm   Micrometer

3D   Three-dimensional

ANOVA   Analysis of variance

AOB   Accessory olfactory bulb

cm   Centimeter

CS   Conditioned stimulus

dpf   Days post-fertilisation

fps   Frames per Second

GABA   γ-aminobutyric acid

GFP   Green fluorescent protein

hr   Hour

hrs   Hours

hpf   Hours post-fertilisation

KLH   Keyhole limpet hemocyanin

LED   Light-emitting diode

L   Liter

LOT   Lateral olfactory tract

MOB   Main olfactory bulb

MOT	Medial olfactory tract
mg	Milligram
mL	Milliliter
mm	Millimeter
Mn	Manganese
$MnCl_2$	Manganese chloride
min	Minute
mpf	Months post-fertilisation
Mtz	Metronidazole
OSN	olfactory sensory neurons
pH	Potential of hydrogen
psu	Practical Salinity Units
ROI	Region of Interest
sec	Seconds
S.E.M	Standard error of mean
TH	Tyrosine hydroxylase
UCS	Unconditioned Stimulus

Acknowledgements

Chapter 1: Introduction

A portion of this chapter has been modified from Doyle and Croll (2022). See Appendix III for the Copyright release.

1.1 Olfactory Importance

The sense of smell is integral to almost every aspect of life. Animals rely on olfaction for finding food, social relationships and detecting predators (Doty, 1976; Stoddart, 1980; Hara, 1994). As humans, we often overlook our sense of smell, thinking that we are less reliant on it than other animals. However, olfaction still plays a critical role in our daily lives. While modern humans seldom use olfaction to track down prey, it is still a major component in gustation and the enjoyment of food. However, despite these critical functions, the importance of olfaction is often not noticeable until it is lost. This has become a widespread issue since the advent of the COVID-19 pandemic, as one of the common symptoms is anosmia, the loss of olfactory ability (Hajikhani et al., 2020; Han et al., 2020; Xydakis et al., 2021). Anosmia can be the result of disease, for instance Alzheimer's and Parkinson's Disease, or exposure to certain chemicals, like insecticides or heavy metals (Sunderman, 2001; Gobba and Abbacchini, 2012; Ruan et al., 2012). It is known to cause a lack of appetite, due to olfaction's contribution to the sense of taste (Mathis et al., 2021). This is a large problem in the elderly population, as anosmia can also occur as a natural side effect of the aging process (Attems et al., 2015). Anosmia can also negatively impact mental health and can even worsen pre-existing anxiety and depression (Boesveldt et al., 2017). Anosmia can have fatal consequences, because of the inability to detect dangerous stimuli, like spoiled food, smoke or gas leaks (Scangas and Bleier, 2017).

Despite the importance of olfaction, it is one of the less studied senses. Much of the existing olfactory research in vertebrates is conducted in rodents, a standard medical model, which can present some complications when drawing parallels to human physiology. Rodents rely heavily on their sense of smell and therefore have a more complex olfactory system than that of humans (Buck and Axel, 1991; Potter et al., 2001; Schaefer et al., 2001; Mombaerts, 2006; Jones et al., 2008; Oliva et al., 2008). Zebrafish, on the other hand, possess an olfactory system that is similarly organized to mammals yet is much simpler than that of rodents (Baier and Korsching, 1994; Friedrich and Korsching, 1997).

1.2 Zebrafish Background

The general organization of the zebrafish brain is comparable to the mammalian brain, with fore-, mid- and hindbrain regions also containing a diencephalon and telencephalon (See Fig. 1), the primary neurotransmitters used, and their functions are also generally similar to those in humans (Wullimann et al., 1996). For example, sensory systems including olfaction and vision primarily rely on glutaminergic transmission, the neuromuscular junction is cholinergic, and the autonomic system has adrenergic sympathetic and cholinergic parasympathetic divisions (Panula et al., 2006; Lieschke and Currie, 2007; Toledo-Ibarra et al., 2013; Stoyek et al., 2015; Caramillo and Echevarria, 2017). Like mammals, zebrafish possess a blood brain barrier, and permeability tests indicate that its physiological properties are conserved between zebrafish and humans (Cuoghi and Mola, 2007; Wager and Russell, 2013). In addition to their physiological benefits, zebrafish also exhibit sophisticated cognitive behaviours, such as learning and

retaining associations (See Chapter 3), and they manifest well-documented anxiety

behaviours (Lieschke and Currie, 2007).

One of the key advantages of zebrafish is their suitability for experimental

genetic manipulation, which has led to the development of thousands of mutant,

transgenic and otherwise genetically-altered strains (Ruzicka et al., 2019). For example,

adult zebrafish of some mutant strains are optically transparent, enabling *in vivo*

imaging of internal tissues and even individual cells (White et al., 2008). These

transparent mutations extend the optical transparency that is already a useful trait of all

larval zebrafish into adulthood (Parichy et al., 2009). Genetically altered zebrafish

featuring a genotype or phenotype of interest can be produced with less effort than

their rodent counterparts, as DNA or RNA can more easily be injected at the single cell

stage, due to external fertilisation and development of the fish (Clark et al., 2011).

Fluorescent reporters linked to specific promoters provide an array of imaging

opportunities (Halpern et al., 2008). Besides traditional reporters, like green fluorescent

protein (GFP), genetically encoded calcium indicators like GCaMP and the optogenetic

reporter channel rhodopsin can be incorporated into transgenic zebrafish lines (Halpern

et al., 2008; Howe et al., 2017). Combining the ability to create custom transgenic lines

with current imaging techniques presents a unique opportunity to study the functions of

genes in a living animal, something not easily achieved with many other current models.

With advanced microscopic techniques, the imaging of live transgenic lines is becoming

more accessible. Light sheet microscopy enables the user to illuminate and image entire

planes of tissue, which has advantages over traditional point-scanning methods like

confocal and two-photon microscopy (Hillman et al., 2019). Fluorescence lifetime imaging microscopy (FLIM) offers the ability to perform *in vivo* observations of zebrafish over the temporal lifespan of the fluorophore and can provide additional data on overlapping emission spectra and the intensity of the fluorophore (Zhang et al., 2021). In addition to the advantages described above, zebrafish are becoming increasingly popular for use in high-throughput screens due to their prolific reproduction and cost-efficient size (Briggs, 2002; Meyers, 2018). Based on these factors, potential therapeutics and genes can be identified relatively quickly, taking a fraction of the time required for rodents.

Despite the many benefits of using zebrafish as a model for biomedical research, there are also drawbacks stemming from their aquatic environment, their physiological differences from humans, and their nascent role as a model organism. The aquatic environment of the zebrafish presents some unique challenges related to their care and experimental design. Difficulties may arise when administering or determining dosages of water-insoluble chemicals (Rubinstein, 2006). For example, dimethylsulfoxide (DMSO) is often used to dissolve the desired chemicals and therefore its potential effect on fish must be considered (De Koning et al., 2015; Christou et al., 2019; Hoyberghs et al., 2021). The quality of the water itself plays a large role in the well-being and normal behaviour of fish; therefore water parameters like temperature, salinity, pH, and nitrate levels must be carefully monitored (Velez et al., 2024). Notwithstanding the similarities between zebrafish and mammalian physiology, there are also notable differences. Brain regions are not always directly and fully comparable or as well developed in zebrafish,

however it has been fully mapped and has equivalent functional regions (Wullimann et al., 1996; Wullimann and Mueller, 2004). Genetic research presents further differences, as the zebrafish has a duplicated genome; in cases where humans have a single gene, zebrafish may have two, which may obscure the function of the gene (Lieschke and Currie, 2007). Regardless of the proliferation of the zebrafish as a model, it has not yet achieved the widespread acceptance of other model organisms, particularly rodents. Despite more than two decades of mainstream use, published literature on zebrafish overwhelmingly continues to include justification on their suitability as a model organism (Vaz et al., 2018).

1.3 Overview Of Zebrafish Olfactory System

The zebrafish olfactory system is a prime target for study due to its similarities to mammalian systems, in combination with the ease of accessibility. Zebrafish possess two olfactory pits containing rosette-shaped olfactory epithelia, which are the sites of first odour contact (Byrd and Brunjes, 1995). Olfactory sensory neurons (OSNs) lining the rosettes project their axons along the olfactory nerves to the olfactory bulbs (Miyasaka et al., 2012). OSNs express olfactory receptor (OR) proteins, which bind to specific moieties in odourant molecules that have entered the nares (Shao et al., 2017). Regardless of the locations of the OSNs expressing each OR protein in the olfactory epithelium, each type of OSN projects to a single area in the olfactory bulb, known as a glomerulus (Weiss et al., 2020). Any one odour can activate many ORs, such that even a simple odour can activate a combinatorial code of specific glomerular activity in the olfactory bulb (Mori et al., 1999).

6

The olfactory bulb itself is a popular topic for study; although organized like a mammalian bulb, the zebrafish olfactory system has fewer OSNs and glomeruli in general, allowing for whole bulb characterization. The zebrafish olfactory bulb is roughly separated into three layers. The outermost layer, the olfactory nerve layer, is formed by the axons of OSNs coming from the rosette and wrapping around the outside of the bulb (Baier and Korsching, 1994; Braubach et al., 2012). Just underneath the olfactory nerve layer is the glomerular layer made up of about 140 glomeruli but also including some accessory cells including periglomerular cells. The core of the bulb comprises the internal cell layer with mitral cells and granule cell dendrites (Byrd, 2000).

The glomeruli of the zebrafish have been extensively studied with about 140 being identified. These are organized into nine regions, and each region responds to a different category of odours related to the type of OSN innervating the corresponding glomerulus. For instance, microvillous OSNs are activated by amino-acids and project to the lateral glomeruli, while ciliated OSNs, activated by bile salts, innervate dorsal, medial and ventral glomeruli (Hansen and Zeiske, 1993; Braubach et al., 2012). Crypt, kappe and pear OSNs are unique in that they only innervate one glomerulus each: mdG2, mdG5 & lG2, respectively (Ahuja et al., 2015; Biechl et al., 2016; Imamura et al., 2020). Previous studies have shown that glomeruli in particular areas of the bulb are also innervated by specific types of mitral cells, either uni- or multi-dendritic (Fuller et al., 2006; Braubach and Croll, 2021) (See Chapter 2 for greater detail).

1.4 Olfactory Behaviour

A practical method of assessing experimental effects on a normal phenotype in the nervous system is to examine changes in behaviour (Khan et al., 2017). For rodents, there is a wide range of paradigms available to examine the effects of experimental treatment on behaviour, ranging from simple evaluation of locomotion to complex cognitive abilities involving learning and memory (Sousa et al., 2006). Zebrafish also possess a wide range of behaviours, and many normal and abnormal behaviours have been catalogued (Kalueff et al., 2013). Zebrafish are inherently communal animals, living in shoals, so they display a wide variety of social behaviours. They also express well-documented fear and anxiety behaviours and can learn complex associations (Lieschke and Currie, 2007). Consequently, there have been many behavioural tests developed for zebrafish that are suitable for understanding neural function.

Several zebrafish paradigms are analogous to well established ones developed for rodents (Champagne et al., 2010). For instance, the novel tank test is an assessment of anxiety-like behaviour in zebrafish reacting to a new, stark environment and can be compared to the open-field test in rodents (Blaser and Rosemberg, 2012; Harro, 2018). There are also many paradigms that test cognitive behaviours, as the fish can rapidly learn associations using various unconditioned stimuli (Karnik and Gerlai, 2012). Zebrafish are highly visual animals and can differentiate between basic colours or patterns, but they can also form associations using olfactory or auditory stimuli (Colwill et al., 2005; Braubach et al., 2009; Avdesh et al., 2012; Doyle et al., 2017). Many common apparatuses used for studying cognitive behaviours in rodents have also been

adapted for zebrafish, including shuttle boxes, Y-mazes, T-mazes and plus-mazes (Pather

and Gerlai, 2009; Gerlai, 2010; Sison and Gerlai, 2010). Zebrafish training is highly

reproducible and can therefore be automated and performed using groups of animals

(Wyeth et al., 2011; Miller and Gerlai, 2012; Doyle et al., 2017). Moreover,

commercially-available software offers three-dimensional, automated tracking of

multiple fish simultaneously (Stewart et al., 2015).

Most of these learning paradigms are suitable for use with adult zebrafish;

however, only the simplest behavioural assays are suitable for larvae (Colwill and

Creton, 2011; Kalueff et al., 2013). Larvae can be examined for general behavioural

abnormalities, but larvae under 5 days post fertilisation (dpf) do not swim well enough

to perform many behaviours exhibited by adult zebrafish (Lindsey et al., 2010). By 30

dpf, however, juvenile fish can generally perform in adult-appropriate paradigms

(Kalueff et al., 2013; Merovitch, 2016).

1.5 Olfactory Development

The olfactory system begins development 17 hours after fertilization with the

appearance of the olfactory placode, which develops as a thickening of the ectoderm

(Whitlock and Westerfield, 1998, 2000). Pioneering neurons begin to extend axons into

the developing forebrain at approximately 22 hours post-fertilization (Hansen and

Zeiske, 1993; Whitlock and Westerfield, 1998). After about 32 hours post-fertilization

(hpf) the placode invaginates to form the nares and after roughly 48 hpf OSN axons

grow using the pioneer neurons as a guideline and begin to form rudimentary glomeruli,

known as protoglomeruli (Miyasaka et al., 2007). After the establishment of the OSN

pathways the pioneering neurons undergo programmed cell death (Whitlock and

Westerfield, 1998). It appears that these protoglomeruli are already functional at 2.5

dpf even though the larvae are still unhatched, as Ca^{2+} imaging indicates activity in

response to odour mixtures, like amino acids, bile salts and food odour (Li et al., 2005).

Although these responses were small, by the time the larvae hatched (3 dpf) and

reached 5 dpf, the activity was more substantial and consistent. The authors suggest

that the odourant receptors responsible for detecting these odours start to be

expressed between 2 and 5 dpf (Barth et al., 1996; Byrd et al., 1996; Argo et al., 2003; Li

et al., 2005). In free swimming larvae, odours elicit swimming behaviour in newly

hatched 3 dpf larvae, which seems to confirm the findings of Li et al. (2005). It appears

that even though most of the differentiation in the olfactory system occurs between 3

and 30 dpf, zebrafish have the capacity for basic olfaction even before hatching

(Braubach et al., 2013).

1.6 Olfactory Disruption

Due to its proximity to the external environment, the olfactory system is

particularly sensitive to environmental pathogens and pollution. Pathogens like bacteria,

viruses and funguses can be introduced to the nose through unsanitary hygiene

practices such as rhinotillexomania (nose picking) (Zhou et al., 2023). Bacteria such as

Chlamydophila pneumoniae, which causes respiratory tract infections, can be

transported up the olfactory nerve and infect the central nervous system, which is

linked to Alzheimer's Disease-like pathology in rodents (Chacko et al., 2022). Several

viruses, including but not limited to herpes, polio and West Nile can use the olfactory

nerve to gain access to the central nervous system and lead to severe

neurodegenerative disease (Riel et al., 2015). The precise mechanism of how these

pathogens are transported up the olfactory nerve is poorly understood, and may vary

depending on the type.

Environmental pollutants have also been known to disrupt the olfactory system.

Herbicides and pesticides routinely contaminate soil and waterways, affecting both

aquatic and terrestrial animals and causing serious consequences (Wiens, 1980; Goetz

and Zilberman, 2000; Müller et al., 2020). Rotenone and paraquat (N,N'-dimethyl-4-4'-

bipiridinium) are widely used industrial pesticides and environmental contaminants

(Dinis-Oliveira et al., 2006). They are both thought to impair mitochondrial Complex I,

leading to problems with the electron transport chain and consequently the

overproduction of reactive oxygen species (Sherer et al., 2003; Bové et al., 2005; Wang

et al., 2018b). This causes cell death, mainly in dopaminergic neurons, and therefore can

mimic Parkinsonian-like symptoms (Manning-Bog et al., 2003; Doyle and Croll, 2022).

Other major disruptors of the olfactory system are heavy metals, which routinely

contaminate air, soil and water near mining operations and other industrial production

facilities (Mohammed et al., 2011). Workers in battery factories using nickel (Ni) and

cadmium (Cd) reported both anosmia and hyposmia from prolonged exposure to the

metal dust, and exposure to chromium (Cr) and arsenic (As) has even been linked to

cancers of the nose (Sunderman, 2001). Outside of the concentrated exposure seen in

factories and mines, heavy metals pollute water and soil where they cannot be broken

down or removed, given their inorganic nature (Musilova et al., 2016; Gong et al., 2018).

Heavy metals can also travel up the olfactory nerve into the olfactory bulb (Sunderman, 2001). Animals exposed to aluminium (Al), cadmium (Cd), cobalt (Co), mercury (Hg), manganese (Mn), nickel (Ni) and zinc (Zn) have shown increased levels of these metals in the olfactory bulb and Mn, Ni and Zn have been shown to cross synapses in the bulb and migrate to other areas of the brain (Sunderman, 2001; Tjälve and Tallkvist, 2003). It is, therefore, not surprising to learn that disruption of the nose by various pathogens and chemicals has been linked to the development of several neurodegenerative diseases (Harrass et al., 2021; Fatuzzo et al., 2023; Reid, 2023).

1.7 Olfactory Disruption In Neurodegenerative Disease

Olfactory dysfunction is one of the earliest signs of both Alzheimer's and Parkinson's diseases (Fatuzzo et al., 2023). Alzheimer's Disease (AD) is the most common neurodegenerative disease, accounting for approximately 70% of all dementias in humans and afflicting millions of people worldwide (Cummings, 2004; Newman et al., 2014). It typically affects those over the age of 65 as Late Onset Alzheimer's Disease (LOAD), but it can rarely be found in those younger than 65 as Early Onset Alzheimer's Disease (EOAD) (Nussbaum and Ellis, 2003). Hallmark symptoms include problems with memory, attention span, executive functions, language and spatial orientation. The exact cause of AD is unknown, but it is characterized by a loss of neurons, mostly in the cerebral cortex and hippocampus (Nussbaum and Ellis, 2003). The pathophysiology of AD may appear in the brain decades before clinical symptoms become evident, and it can only officially be confirmed during autopsy (Villemagne et al., 2013; Caramillo and Echevarria, 2017). Olfactory symptoms are thought to be some of the earliest

manifestations of the disease, which is confirmed by pathology as AD first affects the

entorhinal cortex before spreading to the rest of the brain (Zou et al., 2016). Early

deficits are typically related to difficulty in olfaction recognition, although they can be

hard to differentiate from general age-related deficits (Zou et al., 2016).

Parkinson's Disease (PD) is the second most common neurodegenerative disease

after AD and similarly affects individuals over the age of 65. Symptoms mainly affect

movement, including tremors, bradykinesia (slow movements), rigidity and postural

instability, but it also has many cognitive symptoms, like impaired memory and

executive dysfunction (Rana et al., 2015). It is characterized by a loss of dopaminergic

neurons in the substantia nigra and the development of Lewy bodies: intracytoplasmic

inclusions. Several genes have been implicated, including LRRK2 and α-synuclein, and

DJ-1, PINK1 and PARKIN have been specifically linked to early-onset PD (EOPD). It has

also been suggested that environmental factors may play a role (Best and Alderton,

2008). As with AD, PD pathology indicates that the disease begins in the olfactory bulb

and then progresses to other regions of the brain (Fullard et al., 2017). Patients with PD

also exhibit impairment of both odour detection and identification (Sobel et al., 2001).

With both AD and PD, much research is focused on using olfaction function tests to

predict the onset of disease in the hope that early intervention can slow the progress of

the disease (Tissingh et al., 2001; Whitcroft and Hummel, 2019; Winchester and Martyn,

2020; Bang et al., 2021).

1.8 Goals Of The Thesis

Given the research mentioned above, it is clear that olfaction comprises an integral part of survival and its loss can be detrimental to quality of life. Therefore, understanding how every aspect of the olfactory system functions is essential to investigating potential solutions for its dysfunction. Zebrafish present a unique opportunity for study due to the relative simplicity of their olfactory system when compared to rodents, while still maintaining a mammalian-like organization of its structures. Other works have extensively examined the glomerular network of the zebrafish olfactory bulb; however, the bulb contains many other cells with different functions. Dopaminergic interneurons are a point of particular interest as they potentially modulate communication between various regions or glomeruli of the bulb, although it is unknown if this is accurate or how it occurs (Wullimann and Rink, 2001; Rink and Wullimann, 2002; Chen et al., 2009; Kosaka and Kosaka, 2009).

The goal of this thesis was to characterize these interneurons of the zebrafish olfactory bulb and examine their role in olfactory behaviour. First the normal anatomy of these neurons was characterized (Chapter 2) using antibodies raised against tyrosine hydroxylase (TH), the rate limiting step in the dopamine pathway, including their distribution, morphology and development. Four cell types or subtypes were identified and differences in the lateral and medial regions of the bulb were noted, specifically the uniquely dopaminergic innervation of the medial olfactory tract. Then in Chapter 3, an efficient and feasible odour-based learning paradigm was used to investigate olfactory behaviour (Chapter 3), which successfully trained fish to respond to the odour,

phenylethyl alcohol after four days of conditioning. Finally, to determine the possible

functions of the TH-immunoreactive neurons, the zebrafish were environmentally

exposed to two chemicals manganese, and metronidazole (Chapter 4 and 5). Anatomy

of the chemical-exposed bulbs was examined, using techniques and baselines from

Chapter 2, and then effects on behaviour were analyzed, using techniques drawn from

Chapter 3. The result was a significant reduction in the number TH+ cells and noted

olfactory deficits. However, off-target disruption the olfactory sensory neurons (OSNs)

was noted, along with anxiogenic behaviour, thereby questioning the specificity of these

two ablation techniques.

Figure 1: A lateral view of the adult zebrafish brain. The brain is generally divided into four areas: telencephalon, mesencephalon, diencephalon and rhombencephalon. This thesis mainly focuses on the telencephalon, which consists of the olfactory bulbs and the forebrain (pallium and subpallium).
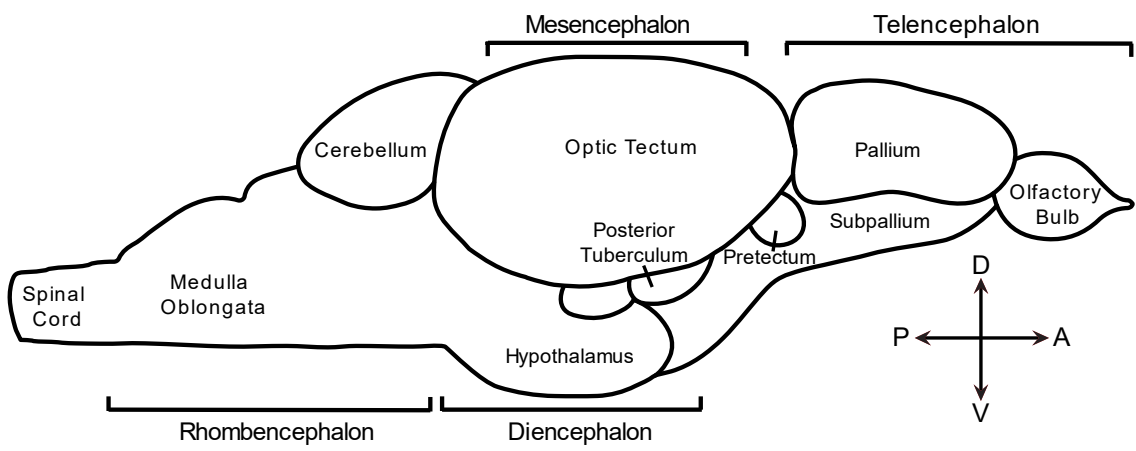
Figure 1: A lateral view of the adult zebrafish brain

Chapter 2: Description Of TH+ Cells Of The Zebrafish Olfactory Bulb From

Embryo To Adult

2.1 Introduction

The olfactory bulb is the initial site of sensory processing in vertebrates, where

inputs from peripheral olfactory sensory neurons (OSNs) are segregated into receptor-

specific glomeruli. Mitral, tufted and ruffed cells then relay patterns of glomerular

activities to the olfactory cortex for further analysis (Stoddart, 1980). The olfactory bulbs

in different species are all comparable in function, but their organization can differ in

detail between and within different taxa. In the main olfactory bulb (MOB), which

processes most odours in mammals, the OSNs innervate only single glomeruli

(Mombaerts et al., 1996). In the accessory olfactory bulb (AOB), which processes

pheromones, however, each OSN can innervate multiple glomeruli (Larriva-Sahd, 2008).

This multi-glomerular innervation is also evident in amphibians in both the MOB and

AOB, but in teleosts, which do not possess separate MOB and AOB, each OSN innervates

a single glomerulus, as in the MOB of mammals (Hassenklöver and Manzini, 2013; Biechl

et al., 2017; Silva and Antunes, 2017; Weiss et al., 2020). Some literature suggests that

the medial glomeruli of fish may act in place of the AOB, as they are innervated by crypt

cells, an OSN type known to process pheromones specifically (Hussain et al., 2013;

Gerlach et al., 2019).

The projection neurons of the olfactory bulb also exhibit significant interspecies

diversity. Most mitral cells in the mammalian MOB possess a single primary dendrite

and only innervate one glomerulus (Macrides and Schneider, 1982). By contrast, mitral

cells in the mammalian AOB possess multiple primary dendrites and can innervate more

than one glomerulus (Wagner et al., 2006; Yonekura and Yokoi, 2008). Like the

mammalian AOB, amphibian mitral cells have multiple primary dendrites which

innervate multiple glomeruli (Jiang and Holley, 1992). This is also a trait shared with

most teleost fishes; however, zebrafish may be an exception (Kosaka and Hama, 1982;

Oka, 1983; Satou, 1990; Fujita et al., 1991). Fuller et al., (2006) classified zebrafish mitral

cells into two categories: those possessing a single primary dendrite and those with

multiple primary dendrites. While both unidendritic and multidendritic types were

found throughout the bulb, the majority of the multidendritic mitral cells project to the

medial olfactory tract (MOT) and most unidendritic cells project to the lateral olfactory

tract (LOT). This again supports the idea that the medial bulb in teleosts has similar

function to the AOB in higher vertebrates. Fuller et al (2006) also stated that most

unidendritic mitral cells in the zebrafish olfactory bulb only innervate single glomeruli

and indicated that even multidendritic can innervate only a single glomerulus. They

therefore concluded that this wiring is comparable to mammals and differs from the

typical teleost organization. However, Braubach and Croll (2021) showed that while

mitral cells typically innervate single glomeruli (uniglomerular), there are also many

mitral cells that each innervate two or more glomeruli (multiglomerular). For instance,

lateral glomeruli are only innervated by uniglomerular mitral cells while the medial

glomeruli are innervated by a mixture of uniglomerular and multiglomerular cells. This

again highlights the differences between the lateral and medial regions of the zebrafish

olfactory bulb.

The niche occupied by tufted cells exhibits even greater interspecies diversity

than with mitral cells (Imamura et al., 2020). In mammals and amphibians, tufted cells

innervate only single glomeruli (Macrides and Schneider, 1982; Mori et al., 1983; Jiang

and Holley, 1992). However, in some species like zebrafish, there is no evidence of

tufted cells at all. Instead, ruffed cells, which are found throughout teleost fish species,

including zebrafish, are generally thought to perform the function of vertebrate tufted

cells (Fuller and Byrd, 2005). Since being reported in zebrafish these cells have not been

studied in detail, however they appear to have an even distribution throughout the

olfactory bulb (Fuller and Byrd, 2005).

Other cells in the olfactory bulb are not as extensively studied as mitral/tufted

cells. Periglomerular interneurons and the axonless, GABAergic granular cells are

thought to be involved in feedback inhibition and regulating projection (mainly mitral

cell) neuron activity (Pressler and Strowbridge, 2020). Periglomerular cells vary widely

between species and are often classified based on both innervation and

immunoreactivity (Kosaka and Kosaka, 2007). In mammals, reptiles and amphibians,

dopamine is thought to regulate mitral cell activity via D2 receptors (Bundschuh et al.,

2012). A study in rats showed that the activation of the D2 receptors caused a

depression in the synaptic transmission between olfactory receptor cells and the mitral

cells (Hsia et al., 1999). Therefore, dopaminergic periglomerular interneurons are of

particular interest. In mice and rats, dopaminergic interneurons, as indicated by tyrosine

hydroxylase (TH) immunoreactivity, co-express the transmitter γ-aminobutyric acid

(GABA), and reside mainly in the glomerular layer of the olfactory bulb (Kosaka et al.,

2020). There is variety even within these neurons, and they can be further divided into

subtypes based on cell size, number of dendrites and where they innervate. In reptiles,

almost all TH immunoreactive interneurons also expressed GABA, which were classified into two types based on number of dendrites and cell size. However, both types of interneurons were found throughout the MOB and AOB without notable differences (Kosaka et al., 1991). Conversely, a study of two frog species found that no TH immunoreactive interneurons in the MOB or AOB bulb co-expressed GABA and these cells could generally be divided into two types based on number of dendrites and the presence of a prominent axon (Boyd and Delaney, 2002). In zebrafish, TH immunoreactive interneurons have also been identified but have not yet been extensively researched, making them a prime target for further study (Braubach, 2011; Fuller et al., 2006)

Our lab has thoroughly investigated the glomeruli in zebrafish as they differentiate from protoglomeruli in larvae into the final adult organization (Braubach et al., 2012, 2013) and most recently also examined the relationship between the glomeruli and mitral cells (Braubach and Croll, 2021). With this project, I now aim to specifically catalogue the TH immunoreactive interneurons of the zebrafish olfactory bulb, noting their morphology and location, and categorizing them into separate types, if appropriate. I also examine possible changes in these cells as the fish mature from larva to adult. In addition, Braubach and Croll (2021) and Fuller et al. (2006) found that mitral cell innervation of glomeruli differs between the medial and lateral regions of the zebrafish olfactory bulb. Therefore, I will also examine the relationship of these TH immunoreactive interneurons to glomeruli in both the medial and lateral regions to determine if differences exist in innervation or morphology. This includes neurite length,

direction and whether cells innervate locally or across regions. By obtaining this information, I endeavour to document the similarities and differences between zebrafish TH immunoreactive interneurons and those of other species. Also, I aim to determine if our findings further the hypothesis that variations exist between the medial and lateral regions of the bulb.

2.2 Methods

2.2.1 Animals

Mixed sex fish were obtained from the Zebrafish Core Facility (Faculty of

Medicine, Dalhousie University, Halifax, NS, CAN). Animals younger than 7 days post-

fertilisation (dpf) were maintained in groups of fifty embryos in Petri dishes containing

E3 medium (Cold Spring Harbor Protocols, 2011). The medium was changed daily, and

Petri dishes were placed in an incubator at 28.0°C in 24-hour darkness. Older fish were

maintained in 3 or 10 L tanks (Pentair Aquatic Eco-Systems, Apopka, FL, USA) on a 14:10

hour light/dark cycle in treated, reverse osmosis water (28°C, pH 7.3 and salinity at 0.20

PSU). They were fed twice daily with GEMMA fish food (Skretting, St. Andrew's, NB,

CAN).

Fish were maintained in the Core Facility until just before collection for use in

this study. I utilized both AB (wild-type) and SAGFF(LF)27A;GFP fish at 7 – 28 dpf and 3+

months (for adults). SAGFF(LF)27A;GFP is a transgenic line of zebrafish which was

developed by Koide et al., (2009) and expresses GPF only in the amino acid-sensitive

OSNs that innervate the lateral glomeruli and the medial dorsal glomeruli. All

experiments were conducted in accordance with the Canadian Council on Animal Care

standards and guidelines (Dalhousie Protocol 21-117).

2.2.2 Dissection and Tissue Preparation

Zebrafish were sacrificed by immersion in cold water (<4°C) for 10 min, by which

time they had stopped all spontaneous movements and were unresponsive to fin

pinches (Chen et al., 2014; Wallace et al., 2018). Due to the transparency and small size

of larval zebrafish, 7 dpf fish were fixed and processed whole for immunocytochemistry. In the 14 dpf fish, the dorsal cranium was removed with a fine forceps, but otherwise they were processed whole. Both the 21 and 28 dpf fish had the dorsal cranium removed, were fixed overnight, and then the forebrains with attached olfactory bulbs were removed for processing. In adult fish, the forebrains and olfactory bulbs were removed immediately and then fixed overnight before further processing.

All fish and isolated tissues were fixed in 4% paraformaldehyde (PFA; Electron Microscopy Sciences, Hartfield, PA, USA) dissolved in phosphate-buffered saline (PBS: 100 mM Na_2HPO_4, 140 mM NaCl, pH 7.4) at 4°C. After fixation, the whole fish or dissected brains were subjected to four 20 min washes in PBS before being placed in blocking solution (PBS-Block; 0.25% Triton X-100, 2% dimethyl sulfoxide, 1% bovine serum albumin, 1% normal donkey serum and 1% normal goat serum in PBS; all ingredients from Sigma-Aldrich, St. Louis, MO, USA) for 24 hours at 4°C. The samples were again washed for four times at 20 min each before application of antibodies.

2.2.3 Antibody Characterization

Table 1: List of Primary Antibodies

Antibody	Antigen/Host	Source
Anti-keyhole-limpet-hemocyanin (KLH) (1:100 dilution)	keyhole limpet hemocyanin/rabbit	Sigma-Aldrich H0892 (St. Louis, MO, USA)
Anti-tyrosine-hydroxylase (TH) (1:200 dilution)	TH purified from rat PC12 cells LNC1 clone/ mouse	Immunostar 22941 (Hudson, WI, USA)
Anti-tyrosine-hydroxylase (TH) (1:200 dilution)	Denatured TH from rat PC cells/rabbit	EMD Millipore AB152 (Burlington, MA, USA)
Anti-γ-aminobutyric acid (GABA) (1:200 dilution)	γ-aminobutyric acid-bovine serum albumin/rabbit	Sigma-Aldrich A2052 (St. Louis, MO, USA)

A number of primary antibodies were used in this study as listed in Table 1. To label the putative dopaminergic interneurons, antibodies raised against tyrosine hydroxylase (TH), the rate-limiting enzyme in the catecholaminergic pathway, were used. Zebrafish possess two isoforms of TH, known as *th1* and *th2*, but Chen et al., (2009) reported that antibodies raised against rodent TH only label cells expressing *th1*. They also determined that only *th1* is present in the olfactory bulb of the zebrafish. In the present study, I primarily used a mouse monoclonal antibody raised against TH purified from rat PC12 cells, as it labelled all TH in the zebrafish bulb. This antibody had been previously used to label numerous cells in the zebrafish brain. Fuller et al (2006) performed a Western blot analysis and determined that this antibody did not crossreact with other proteins and that the immunoreactivity was consistent with other studies (Edwards and Michel, 2002; Fuller and Byrd, 2005). A rabbit polyclonal antibody raised against rodent TH was used in order to confirm that antibodies from different companies label TH immunoreactive interneurons consistently. Zebrafish brains double-labelled with both anti-TH antibodies showed complete overlap in olfactory bulbs, forebrains and midbrains, indicating that both antibodies are labelling the same cells (See Supp Fig. 1).

To label the terminals of the OSNs in the glomeruli, a rabbit polyclonal antibody raised against keyhole limpet hemocyanin (KLH) was employed. The antibody has been used previously in teleosts because it labels an unknown epitope in or on OSN axons of

fish (Riddle and Oakley, 1992; Starcevic and Zielinski, 1997; Fuller et al., 2006; Gayoso et al., 2011; Braubach et al., 2012).

In many species, TH immunoreactive interneurons also express GABA; therefore a rabbit polyclonal antibody raised against GABA conjugated to KLH was also employed. This antibody had been successfully used by Edwards and Michel (2002) to label GABA-expressing cells in the zebrafish brain. Whereas the antibodies employed here have been formerly used for immunohistochemistry in zebrafish and related species, it was determined that they were the appropriate ones for this study. Omission controls without the primary antibodies were performed with all secondary antibodies and no staining was noted.

Table 2: List of Secondary Antibodies

Antibody	Source
Donkey anti-Rabbit IgG (H+L) Highly Cross-Adsorbed Secondary Antibody, Alexa Fluor™ 555	Invitrogen (Waltham, MA, USA)
Donkey anti-Rabbit IgG (H+L) Highly Cross-Adsorbed Secondary Antibody, Alexa Fluor™ 488	Invitrogen (Waltham, MA, USA)
Donkey anti-Mouse IgG (H+L) Highly Cross-Adsorbed Secondary Antibody, Alexa Fluor™ 555	Invitrogen (Waltham, MA, USA)
Donkey anti-Mouse IgG (H+L) Highly Cross-Adsorbed Secondary Antibody, Alexa Fluor™ 488	Invitrogen (Waltham, MA, USA)

2.2.4 *Immunocytochemistry*

Forebrains of AB zebrafish were double labelled with anti-KLH rabbit polyclonal antibody and anti-TH mouse monoclonal antibody, both diluted 1:200 in PBS blocking solution. Specimens were incubated in primary antibodies for two to five days at 4°C with gentle agitation on a rocker. After incubation in the primary antibodies, the whole

fish or forebrains were washed in PBS (4x 20 min) as described before. Samples were

then placed in a solution of secondary antibodies diluted 1:200 in PBS-Block for another

2-5 days at 4°C. Secondary antibodies were donkey anti-rabbit and donkey anti-mouse

conjugated to either Alexa Fluor 488 or Alexa Fluor 555 (Table 2). In addition to using

immunohistochemistry to label cells and neurites, the lateral glomeruli of

SAGFF(LF)27A;GFP fish express GFP; and therefore, all these fish were only incubated in

anti-TH mouse monoclonal antibody dilution 1:200 in PBS-Block.

   After incubation in antibodies, samples were again washed (4x 20 min) in PBS

and then immersed in CUBIC based clearing agent for 24 hours before mounting (Susaki

et al., 2014, 2015). Whole fish or isolated brains fish were mounted in the clearing agent

ventral side down (7 and 14 dpf) or dorsal side down (21 & 28 dpf, adult) on glass slides,

and then small dots of silicon grease (Dow-Corning, Midland, MI, USA) were applied to

the four corners of a 18mm x 18mm glass coverslip before it was placed over the

specimen and lightly compressed. The coverslips were then sealed to the slide with nail

polish and viewed with a confocal microscope.

2.2.5 *Imaging*

   Specimens were viewed either with a Zeiss LSM 710 or LSM 880 laser scanning

confocal microscope (Carl Zeiss, Thornwood, NY, USA). Whole olfactory bulbs were

initially imaged using either a 10x objective for adult brains or 20x-40x objective for

brains from 7-28 dpf fish and the final magnification was adjusted using the digital zoom

until the bulb filled the field of view. Optical sections were obtained at the "optimal"

intervals (0.5 µm – 3.5 µm) suggested by the acquisition software, Zen (Carl Zeiss,

Thornwood, NY, USA) at a resolution of 1024 x 1024 on the LSM 710 or 1764 x 1764 on

the LSM 880. Higher magnification images were then obtained using 25x, 40x, or 63x oil

immersion lenses depending on the thickness of the sample. Image stacks were

imported into ImageJ (National Institute of Health, Bethesda, MD, USA;

https://imagej.nih.gov/ij/) for further analysis.

2.2.6 *Analysis*

Low power images were used for general cell counts and noting prominent

neurites. Cell counts were performed using the "Cell Counter" function in ImageJ, which

enabled the tagging of the cell bodies in each optical section while advancing through

the image stack and outputting the X, Y and Z coordinates of each cell. The tag was

placed in the middle of each cell's nucleus and denoted it as the "center" of the cell

body. The images were converted to maximum intensity projections to provide a view of

the entire olfactory bulb, enabling division into anterior medial, anterior lateral,

posterior medial and posterior lateral quadrants. X and Y coordinates bounding each of

the quadrants were recorded in an Excel (Microsoft, Redmond WA, USA) spreadsheet

containing a macro that sorted all the cell locations coordinates into the appropriate

quadrants.

The higher power images were then examined to determine the number of

neurites per bulb and the location of the cell body. The "Simple Neurite Tracer" plug-in

in ImageJ then allowed the tracing of cell neurites and yielded the starting and ending

coordinates of each path. Due to the density of cells, only clearly visible neurites that

exited the cell body in a narrow tapering of the soma were traced, as not to be confused

with neurites running beneath cells. Using these data, the number of neurites per cell and whether visible branching occurred were catalogued. Neurite coordinates were logged into another spreadsheet which determined the quadrant that each of the neurites started and ended within, therefore providing information on where the cells were projecting.

Statistical analyses of all these measures were performed as described. Two-way ANOVAs were performed for the neurite analysis, with post-hoc pairwise comparisons using a Bonferroni correction in SPSS 28 (IBM, Armonk, NY, USA). Simple comparisons of two means were analysed using a Student's t-test.

2.3 Results

2.3.1 Adults /General trends

In the adult animals, the olfactory bulb (OB) was generally ovoid in shape, measuring approximately 520 μm along the minor axis and ~630 μm along the major axis. The TH+ cells were plentiful and appeared evenly distributed throughout the bulb. Anti-KLH labelled glomeruli throughout the bulb, but green fluorescent protein (GFP) was specifically expressed in lateral glomeruli and the medial-dorsal glomeruli of the SAGFF(LF)27A;GFP fish (Fig. 2A&B). The division between left and right bulbs was identifiable with left and right OBs not strictly symmetrical, however, they had comparable cell counts (t-test; $p < 0.05$) and apparent distribution (Fig. 2C). The OB/Forebrain (FB) division was harder to identify, becoming contiguous with the medial olfactory tract (Fig. 2D). A few multipolar cells near either side of the OB/FB border had neurites running in both directions, back into the bulb and into the forebrain. An overview of the olfactory bulbs and forebrain clearly showed the continuity of the medial side of the bulb and the MOT, as TH+ cells could be seen lining the tract all the way back into the forebrain (Fig. 2E).

Numerous puncta obscured cell bodies and neurites, making analysis difficult. These puncta were largely believed to be TH-containing synapses because they were co-localized in the same layer as the olfactory sensory nerve (OSN) terminals stained with anti-KLH or expressing GFP at this stage, and in comparable regions occupied by protoglomeruli and developing glomeruli in earlier stages (Fig.3). Higher magnification investigation of a glomerulus revealed that though the puncta were found in proximity

to the OSN terminals (Fig. 3A), there were also extra-glomerular puncta, which may indicate synapses with other olfactory cells. TH+ cells were not always found precisely inside of glomeruli but were located near the perimeter (Fig. 3B&C). Others did not appear to be closely associated with glomeruli at all, as they were located in the intraglomerular space possibly to synapse with other olfactory cells (Fig.3A).

Inspection of higher magnification images revealed that the number of cells in the adult bulb was 913 (±14.0) (Fig. 4A & Table 3) and the number in each quadrant was nearly equal with 29.6%, 26.0%, 25.0% and 19.4% in the AL, AM, PL and PM quadrants, respectively (Fig. 4B). This was the most even distribution of all the developmental stages studied. The cells were generally ovoid in shape with the major axis measuring 7.59 ±0.096 μm and the minor axis 5.40 ±0.072 μm. The majority of cells possessed no visible neurites, even at higher magnifications. It was possible the neurites were extremely short or that they projected through the z-axis and were therefore difficult to visualize or resolve. Most other cells had a single long neurite which averaged 67.0 ±1.49 μm in length (Fig. 5A), but there was a small population (<50) of multipolar cells with two (rarely three) neurites that were found in all areas of the bulb.

There were general differences between the regions of the bulb as well. There were more neurites originating on the medial side of the bulb, which was consistent throughout development (Fig. 5B; ANOVA; p<0.05). A further post-hoc analysis revealed this difference was significant at 7, 14 and 21 dpf (Post-hoc t-test; p<0.05). Neurites in the posterior region tended to be longer than anterior neurites (Fig. 6A; ANOVA; p<0.05), however, this was only significant at the 14 and 21 dpf ages (Post-hoc t-test;

p<0.05). The length of neurites was in the lateral and medial regions was similar throughout development until adulthood when the average medial neurite was longer, however this difference was not significant (ANOVA; p>0.05)

Brains were also stained with anti-GABA, in addition to anti-TH (Fig. 7A), however, very few GABA+ cells were identified; approximately 50 per bulb (Fig. 7B). They were located in small clusters near the posterior of the bulb. While these cells possessed the same size and soma morphology as the TH+ cells, (Fig. 7C&D) no neurites were noted and there was no double labelling of cells with anti-TH and anti-GABA (Fig. 7E).

Table 3: Mean number of cells found in each of the four quadrants and total number of cells in the bulbs at each age. (Rounded to nearest cell; N=10 for each age; ±SEM)

	AL	AM	PL	PM	BULB
7 dpf	3 ±1	9 ±1	11 ±1	10 ±1	32 ±2
14 dpf	5 ±1	19 ±2	16 ±1	14 ±2	55 ±2
21 dpf	31 ±3	61 ±2	31 ±2	29 ±1	152 ±4
28 dpf	47 ±3	65 ±2	54 ±5	65 ±11	230 ±13
Adult	177± 39	251 ±29	248 ±10	237 ±21	913 ±14

2.3.2 7 DPF

In 7 dpf fish, the bulb measured ~82 µm along the major axis and ~58 µm at the minor axis. Most TH immunoreactive cells were located medially along the division between the OBs (Fig. 8). Although cells along the medial borders of two bulbs were closely positioned, the division between the bulbs was easily discerned as neurites of these cells were clearly visible and distinctly innervated only the ipsilateral bulb (Fig. 9).

Similarly, the posteromedial cells in each bulb appeared to be continuous with those underlying the medial olfactory tract running through the FB, but again cells could be categorized as being present in the bulb or in the forebrain because at this stage their neurites clearly projected either anteriorly or posteriorly, respectively (Fig. 10). Cells were counted in views of the entire bulbs and the 7 dpf larvae possessed 32.4 ± 2.09 cells per bulb (Fig. 4A & Table 3) at this age with 27.9% of cell bodies located in the Anterior Medial (AM) quadrant, while only 8.1% were present in the Anterior Lateral (AL) quadrant (Fig. 4B & 11). The Posterior Lateral (PL) and the Posterior Medial (PM) quadrants contained 34.2% and 29.8% of the cell bodies, respectively (Fig. 11).

Additionally, the AL quadrant was occupied by numerous puncta thought to be synapses that contained TH, as stated above. Approximately 30% of visible cells had a neurite of at least one-half cell length, and of those neurites the average length in 7 dpf fish was 13.0 μm or roughly 1.5 cell length (Fig. 5A). The rest of the cells either had no discernable neurites emanating from the soma or neurites less than 0.5 μm in length. Again, it should be noted that it is possible that some neurites may have been missed due to the way the bulb was imaged, for example running dorso-ventrally through the bulb (z-axis). The majority of neurites began (68.1%) and ended (67.0%) within the posterior region of the bulb, which was supported by the fact that most cells are also in the posterior region at this age and the average neurite length was small. There was, however, a significant difference between the percentage of neurites originating in the lateral and medial sides of the bulb, with more beginning on the medial side of the bulb (Fig. 5B; Post-hoc t-test; $p < 0.05$).

The SAGFF(LF)27A;GFP fish allowed us to further investigate the relationship between the TH+ cells and specific sets of glomeruli, as OSNs projecting to both the lateral glomeruli and the media dorsal glomeruli (mdG) were labelled with GFP in these cells. Dopaminergic innervation to the lateral protoglomeruli viewed in the SAGFF(LF)27A;GFP animals appeared minimal at this age, with ~5 TH+ cells having neurites terminating near them or cell bodies within 10 µm of the lateral protoglomeruli (Fig. 12). There were also numerous puncta present in the same area occupied by these lateral glomeruli. In contrast, ~10 TH+ cells were either innervating near or located within one cell length of the medial protoglomeruli visible in the SAGFF(LF)27A;GFP fish and puncta, while present, were fewer than those seen near the lateral glomeruli.

2.3.2 14 DPF

The 14 dpf measured ~155 µm in the major axis and ~86 µm in the minor. The number of TH+ neurons doubled, with most still located in the medial region of the bulb but with more now present in the posterior regions. Juvenile fish had 55.2 ±2.49 TH+ cells per bulb and the percentage of each per quadrant largely remained the same, with the AM quadrant increasing slightly to 32.0%, while the percentages of cell bodies found in the PL and PM quadrants were 27.8% and 24.4%, respectively (Fig. 4A&B). The AL quadrant contained 8.8% of the cells, with again most of the puncta found in this quadrant (Fig. 13). The division between bulbs was still very clear, although the division between OB and forebrain was becoming increasingly populated by soma and neurites which obscured finer details of anatomy. Despite the increase in cell bodies, most neurites could still be traced back to the appropriate region (OB or Forebrain). Very long

neurites were visible on the forebrain side of the division projecting posteriorly into the

forebrain, possibly indicating the assembly of the medial olfactory tract (Fig. 14).

Average neurite length within the bulb increased slightly to 17.6 µm (Fig. 5A) and 28% of

cells had neurites of at least one-half cell length. Similar to the 7 dpf fish most (56.9%) of

the neurites at this stage began in the posterior quadrants; however, there was

increased innervation to the anterior quadrant with 33.4% of neurites ending there

despite only 14.0% originating from there. There was no difference between neurite

lengths (Fig. 5B; Post-hoc t-test; p>0.05) in the lateral and medial region; however, there

was a significant difference (Fig. 5A; Post-hoc t-test; p<0.05) between posterior and

anterior neurite lengths. Like the 7 dpf fish, there is a significant difference (Fig.4B; Post-

hoc t-test; p<0.05) between the percentage of neurites beginning in the lateral and

medial sides of the bulb. Approximately 10 TH+ cells were now innervating or had cell

bodies within one cell length of the lateral protoglomeruli (Fig. 15) of the

SAGFF(LF)27A;GFP larvae. The medial protoglomeruli had ~15 TH+ cells that are

innervating or possessed cell bodies within one cell length.

2.3.3 21 DPF

At three weeks, the bulb measured ~196 µm on the major axis and ~133 µm on

the minor axis. More cells were present in the rest of the OB, as they were now filling

out from the medial-posterior to the lateral-anterior portion of the OB. These fish had

152 ±3.6 (Fig. 4A & Table 3) TH+ cells and the quadrant composition began to even out

with decreased relative proportions in the PL and PM regions and an increase in the AL

(Fig.4B). By far the most growth was seen in the AM quadrant which now accounted for

37.5% of all TH+ cells and more than tripling the number of neurons from 14 dpf (19.1 to 61.2). The lateral and anterior edges still only possessed few cells and seemed to be mostly populated by puncta, possibly synapses of TH+ cells and glomeruli, as discussed previously (Fig. 16). As in the 14 dpf fish, the division between the left and right bulbs was clearly defined; however, the OB/forebrain border became harder to discern due to the increased number of cells and puncta. At higher magnification, cells with a single branch in the neurite within one cell body length begin to appear around the OB/forebrain border. Typically, only 1 or 2 of these cells per bulb were identified and usually one branch projected anteriorly into the bulb, while the other projected posteriorly into the forebrain (Fig. 17). At this point, multipolar cells, usually with two neurites, also became evident, usually in the medial side of the bulb. These cells had long neurites and possibly project between regions of the bulb (Fig. 18). Neurites of TH+ cells were still visible at this age, but they were becoming obscured by the increased number of puncta present, and after this age, higher magnification images were required to trace neurites in detail. The average neurite length roughly doubled to 30.3 µm and 33% of cells had neurites of at least one-half cell length (Fig. 5A). The AM region continued to have the highest percentage of neurites that began (38.7%) and ended (40.1%) in that quadrant (Fig. 4B). There was no significant difference (Fig. 5B; Post-hoc t-test; p>0.05) between neurite lengths in the lateral and medial regions; however, there was a difference (Fig. 5A; Post-hoc t-test; p<0.05) between anterior and posterior lengths, being 27.5 µm and 33.1 µm, respectively. There was a difference in the percentage of cells beginning in the lateral versus medial regions of the bulb (Fig. 4B;

37

Post-hoc t-test; p<0.05); like in the 7 dpf fish, there were more neurites originating in

the medial region. Innervation to the lateral glomeruli had changes, with approximately

20 TH+ cells now associated with the lateral glomeruli in the SAGFF(LF)27A;GFP fish. The

medial glomeruli visible in the SAGFF(LF)27A;GFP fish had ~15 TH+ cells that innervated

or possessed cell bodies within one cell length.

2.3.4 28 DPF

The bulb now measured ~283 μm on the major axis and ~189 μm on the minor.

The TH cells continued to fill out the anterior and lateral areas of the bulb, and cells

were now clearly visible along the lateral edges of the OB. The puncta were now more

numerous in the posterior and medial regions of the bulb (Fig. 19A). As with the 21 DPF

fish, the division between left and right bulbs was clear, although there were 1-2 bipolar

cells with neurites that crossed between the left and right bulbs, possibly indicating

communication between the two (Fig. 19C); however, it became increasingly difficult to

differentiate between the OB and the medial olfactory tract in the forebrain as cells

developed in that area (Fig. 19B). The number of TH+ cells increased to 208 ± 13.0 by 28

dpf with, again, most of the growth in the AM quadrant (~30% of the cell bodies; Fig.

4B). The other three regions contained a similar percentage of the cells (14-17%). TH+

cell neurites were present but becoming more difficult to measure due to the number of

cells and the numerous puncta. Higher magnification images were required to visualize

neurites in detail as overviews were overwhelmed by puncta. Due to these constraints,

in 28 dpf and adult fish, the neurite analysis was based on the most visible neurites in

each of the quadrants at higher power, as this was the most that could be accurately

traced. The average neurite was 38.6 ±2.7 μm in length, with 27.9% originating in the

medial region and 21.5% in the lateral. There was no significant difference between

neurite lengths in the lateral and medial regions (Fig.5B; Post-hoc t-test; p<0.05); or

anterior and posterior regions (Fig.5A; Post-hoc t-test; p>0.05). There was also no

difference in the percentage of cells beginning in the lateral versus medial regions of the

bulb (Fig. 4B; Post-hoc t-test; p>0.05). At this age, the lateral glomeruli in the

SAGFF(LF)27A;GFP fish had 50 TH+ cells with neurites terminating near them or cell

bodies within 10 μm while the medial glomeruli had ~30 cells.

2.4 Discussion

2.4.1 Changing Olfactory Requirements

The number of TH+ cells in the olfactory bulbs increased dramatically from 7 dpf to adulthood. Braubach et al. (2013) stated that the organization of the glomeruli of olfactory bulb was largely complete by 30 dpf, but I have demonstrated that a significant portion of the adult complement of TH+ cells appeared after that timepoint, and the complexity of their neuritic morphology increased. Therefore, the question arises as to the function of these additional cells. Firstly, the zebrafish experienced a 6-7-fold increase in length from roughly 4.5 mm as a 7 dpf larvae to 30-35 mm as an adult (Kimmel et al., 1995). The olfactory bulb also increased in length, from 82 μm to 630 μm in the major axis and from 58 μm to 520 μm in the minor, which allowed for more room for cells. Existing glomeruli enlarged and differentiated to contain all the terminals of the developing OSNs. As the glomeruli developed, it was probable that more supporting cells were required and therefore developed in all areas of the bulbs as the fish grew. Due to their small size, the TH+ cells can probably only produce a limited number of synapses each; therefore, many cells are needed to innervate larger glomeruli (Modney and Hatton, 1989; Coggeshall and Lekan, 1996).

This growth was possibly due in part to the changing olfactory requirements of the zebrafish as they mature. By 7 dpf, the larvae have barely begun feeding and remain close to the surface, opportunistically eating tiny food particles (Lucore and Connaughton, 2021). The reliance on the olfactory system for food location is therefore likely to be minimal in early life. By this age, however, fish demonstrated a basic fear

40

response, freezing, when exposed to the alarm substance, *Schreckstoff* (Jesuthasan and Mathuru, 2008; Jesuthasan et al., 2021). *Schreckstoff* is known to activate the dorsomedial glomeruli specifically, through the crypt-type OSNs (Chia et al., 2019). These crypt cells are also directly involved in kin recognition, as larvae imprint visually and olfactorily on their surroundings at 6 dpf (Biechl et al., 2016; Gerlach et al., 2019). The medial glomeruli in the 7 dpf fish had more associated TH+ cells than the lateral ones up until 21 dpf, which supports this hypothesis that some pheromonal and alarm recognition is more important than food detection at this age. Despite being able to recognize related conspecifics, other social behaviours at this age are greatly limited, with only the most rudimentary shoaling evident (Engeszer et al., 2007). The 7 dpf fish form only loosely cohesive groups and will not form tighter shoals until after 30 dpf (Buske and Gerlai, 2011). There are several theories for this development, but the most popular is that larvae are more likely to be targeted by predators as a group when small and therefore it is more beneficial to be farther apart (Buske and Gerlai, 2011). In addition, the microorganisms favoured as food by larvae are prone to an even distribution in the environment (Buske and Gerlai, 2011). Hence, it is probable that complex odour analysis is not necessary for optimal survival, and therefore not many cells are required at this stage.

By 21 dpf, the larvae have fully inflated swim bladders and can navigate the water column to find food (Parichy et al., 2009; Lindsey et al., 2010). This age marks increased complexity of TH+ cell innervation in the bulb with the appearance of multipolar cells and increased innervation of the forebrain/olfactory border. At this

stage, multipolar cells appeared and long axon cells projecting toward both the forebrain and olfactory bulb were present. It was reasonable to assume that the more complicated behaviours require increased olfactory ability and therefore increased communication in the bulb. The number of TH+ cells more than doubled from 28 dpf to adulthood, possibly indicating more sophistication of odour detection.

One of the main differences between the juvenile and the adult fish is the development of social behaviour. Zebrafish reach sexual maturity at approximately three months post fertilisation (Parichy et al., 2009). Therefore, it is possible that the neural wiring required for mating behaviour does not develop until this age. Adults possess well-developed social behaviours and can easily discriminate between a wide variety of odours (Valentinčič et al., 1994; Namekawa et al., 2018). There are well over 900 TH+ cells present in the bulb at this age, which are even more numerous than mitral cells (Fuller et al., 2006). However, it is unclear whether all the TH+ neurons belong to the same group or should be separated into smaller subcategories based on morphology.

2.4.2 Cell Morphology

Cell body size was largely consistent throughout development and across individuals. This was unlike the variation in cell sizes seen in reptiles and rodents (Kosaka et al., 1991; Kosaka and Kosaka, 2009). Also, there was no co-localization of TH and GABA seen in rodents and reptiles. This was similar to the findings of Boyd and Delaney (2002), in the TH+ cells of two species of frog. But the TH+ cells in zebrafish differ in axon morphology from the frog species. Therefore, it seems that zebrafish possess

unique characteristics among lower and higher vertebrates. Cell morphology did differ

as the fish aged but by adulthood there were four noted cell morphologies. By far the

most common were the unipolar cells having no discernable neurites. The second most

numerous possessed a single neurite that did not branch within 10 μm of the cell body.

In fact, these cells rarely had detectable branches at all. The cells were found in all

regions of the bulb and did not appear to be associated with any particular regions. The

other two types were much less numerous than the first. There was one distinct

subpopulation of unipolar cells that did possess a neurite branch within 10 μm of the

cell body. Less than a dozen of these were typically associated with the division between

the forebrain and olfactory bulb, with the cell body usually near the division between

the two regions and the two branches projecting into both the olfactory bulb and the

forebrain. Given the location and morphology it is likely that these cells are involved in

relaying information between the bulb and the medial olfactory tract (MOT). This is

supported by the fact that they become more numerous and intertwined with each

other becoming indistinguishable from the medial olfactory tract by adulthood.

Multipolar cells were also noted in the bulb beginning to appear between 21 and 28 dpf.

The cells typically had two neurites, however several cells with three neurites were

observed. Initially multipolar cells seemed to be located mostly in the medial bulb,

however, in older animals about 50 were noted all over the bulb. These cells typically

had longer neurites and presumably projected between different glomeruli and possibly

different regions.

As mentioned in the results section, there were puncta located throughout the bulb, both within glomeruli and outside of glomeruli. Therefore, it is probable that TH+ neurons also synapse with cells other than OSNs, most likely mitral cells and/or other intra- or inter-glomerular TH+ cells. While the puncta are found mostly in the olfactory nerve and glomerular layers of the bulb, they were also some located in the internal cell layer. The TH+ cells could synapse with any of the other olfactory cells, including other TH+ cells or mitral cells.

2.4.3 Medial Vs Lateral Innervation

As discussed in the introduction, there were clear differences between medial and lateral regions with respect to other olfactory cells, like with OSNs and mitral cells. Therefore, I hypothesized that there would be differences in the TH+ cells as well. Although there were no particular types of cells associated with the medial versus lateral side of the bulb, there were differences in innervation. There were more cells on the medial side when compared to lateral and more neurites originate on the medial side. The largest difference was the clear dopaminergic innervation of the MOT, as no TH+ cells were noted in the lateral tract at all. In rats, dopaminergic interneurons are thought to modulate mitral cell activity via D2 receptors (Hsia et al., 1999; Bundschuh et al., 2012). Therefore, it is possible that modulation of mitral cells via TH+ cells is occurring in the MOT. In rodents, dopaminergic interneurons were noted to have a dampening effect on synaptic transmission with mitral cells (Hsia et al., 1999). Activation of a single glomerulus in mice was associated with only 2-5 mitral cells but up 150 interneurons, including some dopaminergic ones (Braubach et al., 2018). It would be

difficult to confirm if the TH+ interneurons present in the zebrafish olfactory bulb have a similar function to those in rodents without an investigation of the types of dopamine receptors on the mitral cells. The different morphologies noted in the bulb may be indicative of different functions. Multipolar cells may facilitate crosstalk or lateral inhibition between similar odours or facilitate depression of signals across larger regions, like lateral versus medial.

In conclusion, this study presented a detailed characterization of TH+ cells in the zebrafish brain throughout development. These findings provide a solid basis for the further investigation of the function of these interneurons and how they compare with similar cells in mammals and other animals.

Figure 2: Overview of adult olfactory bulb in a SAGFF(LF)27A;GFP fish stained with anti-TH. (A) Cells (red) were found throughout the bulb and puncta were largely obscuring cell bodies and neurites making analysis difficult. At this point the lateral glomeruli (green) cover the entire lateral side of the bulb. The medial dorsal glomeruli were still visible on the medial side of the bulb. (B) The number of cells is more than triple that of a 28 dpf bulb, now containing 913 (±14.0) TH+ cells. The number of cells in each quadrant has equalized considerably with 29.6%, 26.0%, 25.0% and 19.4% of the cells in the Al, AM, PL and PM quadrants, respectively. This was the most even distribution out of all the developmental stages. (C) The division between the left and right bulbs (dashed line) was crowded with cells and puncta but most cells were clearly on a particular side. (D) The olfactory bulb (OB) was almost continuous with the medial olfactory tract (MOT) at this point, with the division between the two difficult to discern (dashed line). (E) An overview of the olfactory bulbs and forebrain clearly showed the continuity of the medial side of the bulb and the MOT. TH+ cells could be seen lining the tract all the way back into the forebrain (dashed line denotes division between left and right bulbs/FB).
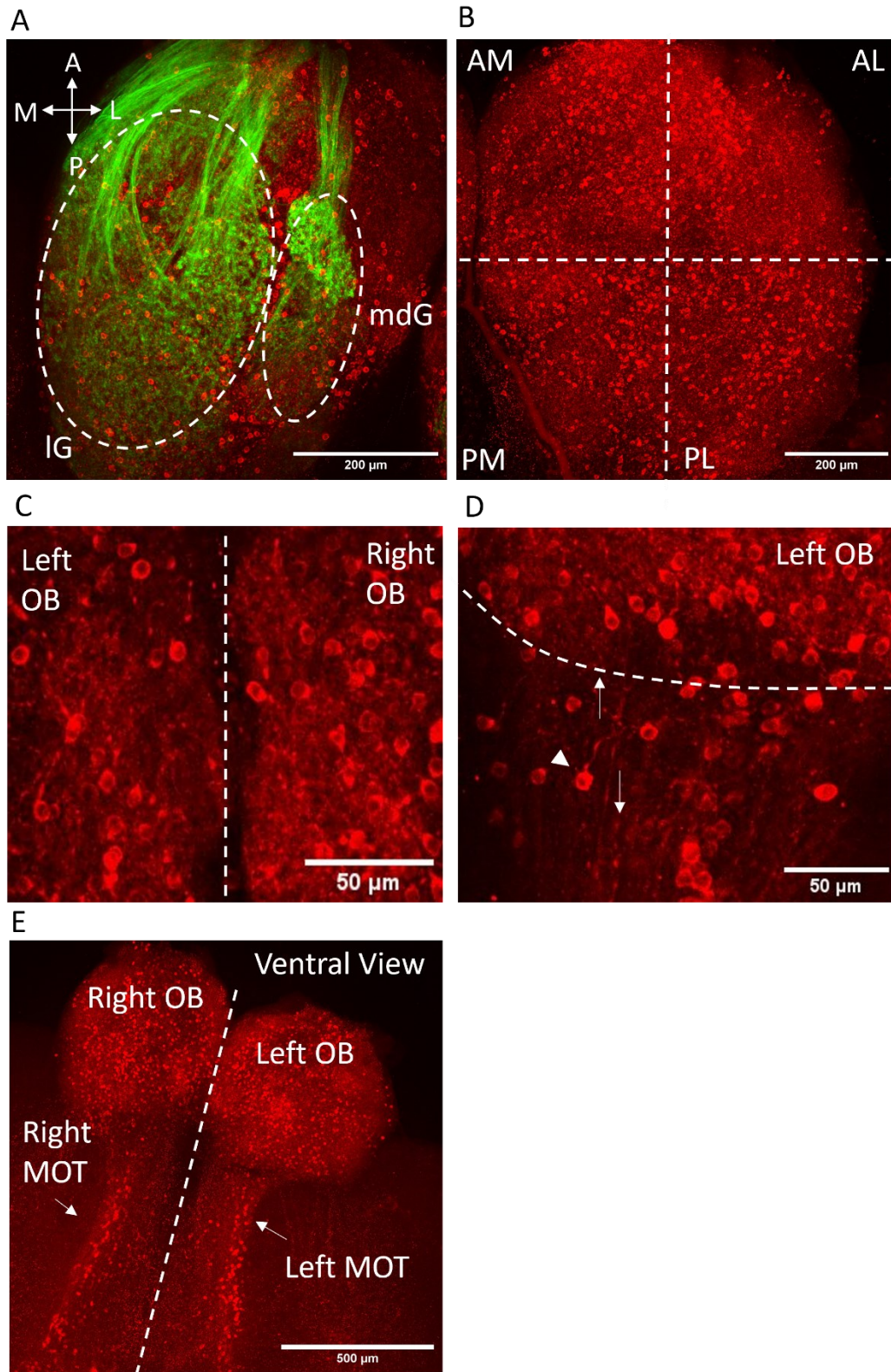
Figure 2: Overview of adult olfactory bulb in a SAGFF(LF)27A;GFP fish stained with anti-TH.

Figure 3: High magnification view of a medial-dorsal glomerulus in an AB fish stained with anti-TH and anti-KLH. (A) The TH+ cells associated with this glomerulus were near the perimeter. There were TH+ cells that were not contained within a glomerulus (white triangle) and extra-glomerular puncta (white square) which may indicate synapses with other olfactory cells. (B) The spherical morphology of the glomeruli was very clear in magnified images and nerve endings were visible within. (C) The two associated cells (white triangles) were located near the perimeter of the glomerulus while the puncta were distributed throughout the glomerulus.
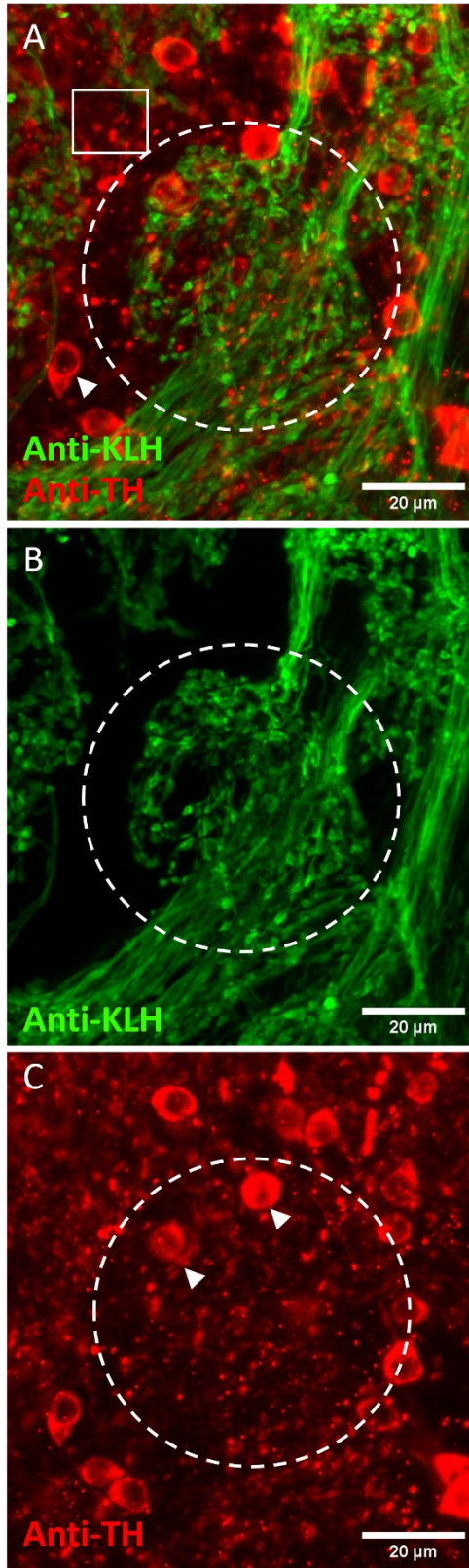
Figure 3: Close-up view of a medial-dorsal glomerulus in an AB fish stained with anti-TH and anti-KLH

Figure 4: Analysis of cell number and location by age of fish. (A) Mean number of cells

per bulb for each age of fish. The number of cells increases more than six-fold from 7

dpf and 28 dpf. The adults were deliberately not included due to the massive difference

in scale. N=10 each age. Error bars = ± S.E.M. (B) Percentage of total cells in each bulb

separated by quadrant at each age. The AL quadrant possessed the smallest percentage

of cells throughout development but did increase as the fish aged. The AM quadrant

grew the largest from 7-28 dpf, while the PL and PM quadrants decreased. The adult

bulbs had the most even distribution of cells. N=10 each age. Error bars = ± S.E.M.
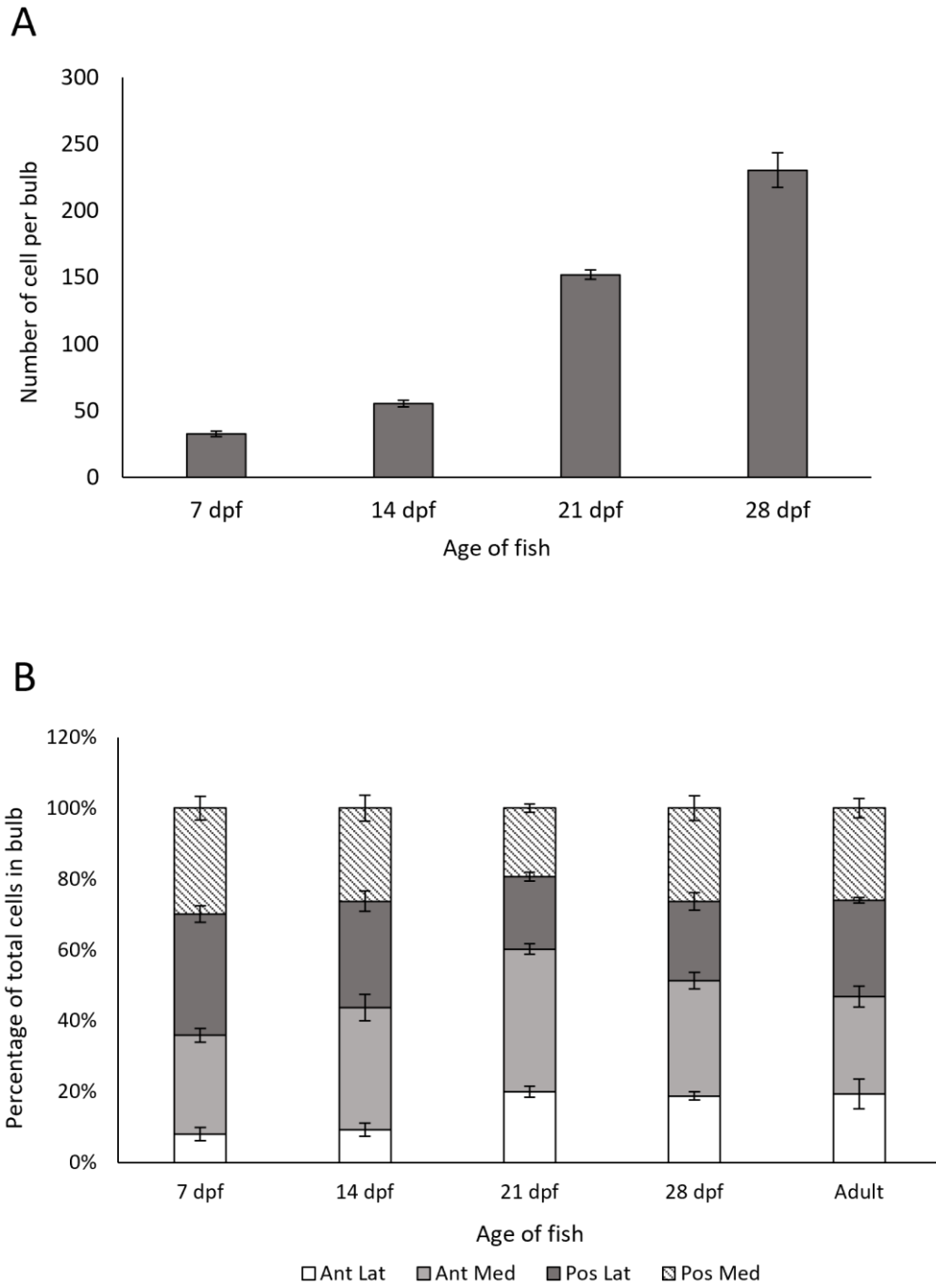
Figure 4: Analysis of cell number and location by age of fish.

Figure 5: Analysis of neurites length and origin based on region. (A) Mean length of neurites (in μm) per age. Neurite length increases with age starting at 13.1 μm and ending at 67.0 μm in adults. However, length almost doubles between the 28 dpf and adult fish, from 38.6 μm to 67.0 μm. N=10 each age. Error bars = ± S.E.M. (B) Percentage of neurites originating in each region (lateral and medial) at each age. Generally, at each age there are more neurites originating from the medial region versus lateral at each age (ANOVA; p<0.05) and a post-hoc analysis revealed significant differences at 7 – 21 dpf (Post-hoc t-test; p<0.05).
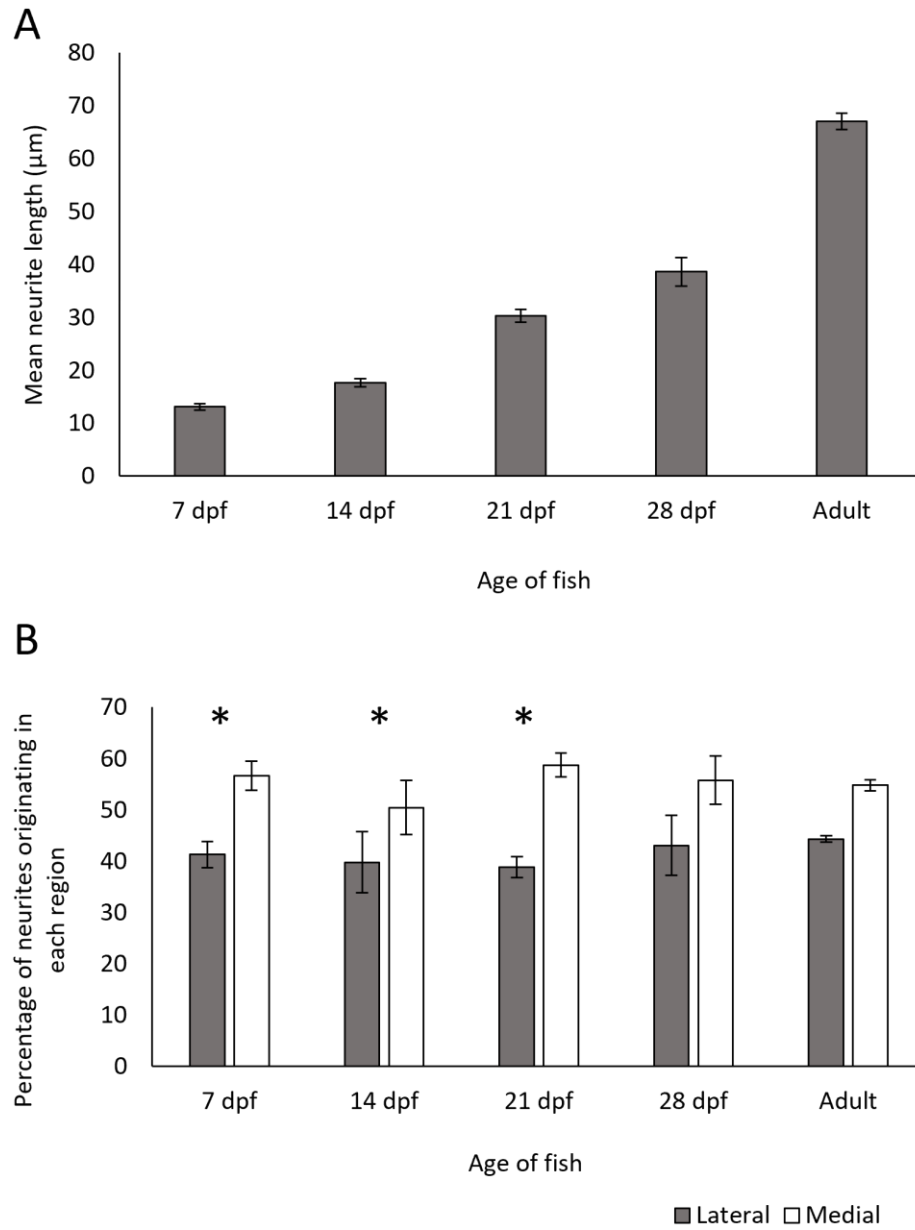
Figure 5: Analysis of neurites length and origin based on region.

Figure 6: Mean neurite length by region at each age. (A) Comparing mean neurite length of the anterior and posterior regions. There was a significant effect of age (ANOVA, $p<0.05$) and region (ANOVA, $p<0.05$) but not interaction effects (ANOVA, $p>0.05$). Pairwise comparisons noted a significant difference between anterior and posterior length at 14 and 21 dpf. (B) Comparing mean neurite length of the lateral and medial regions. There was a significant effect of age (ANOVA, $p<0.05$) but not region (ANOVA, $p>0.05$) and no interaction effect (ANOVA, $p>0.05$). (Error bars = S.E.M.)
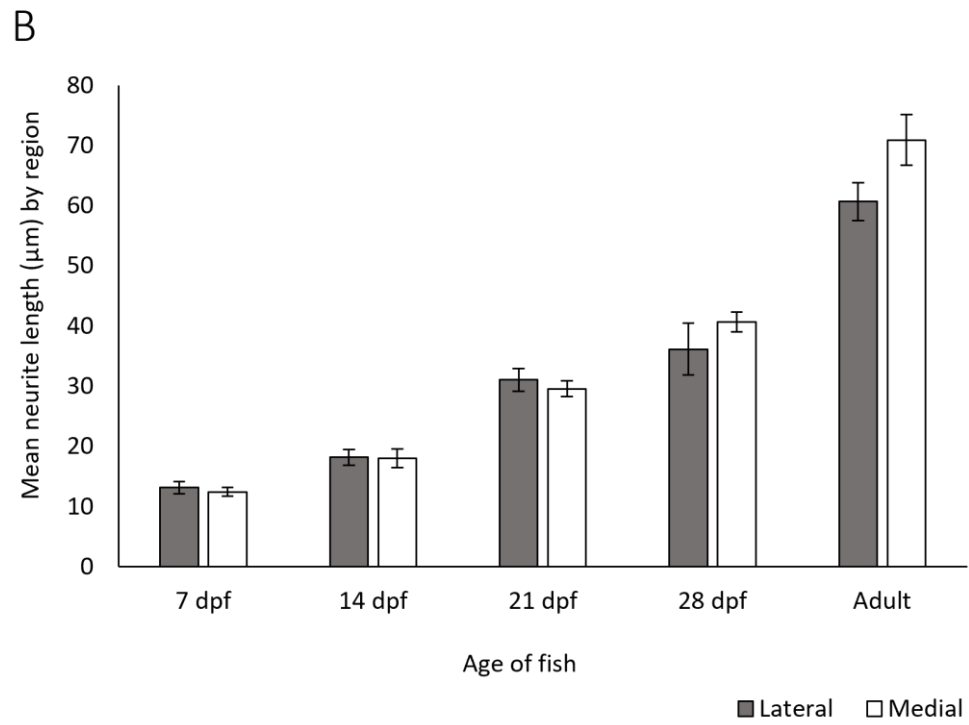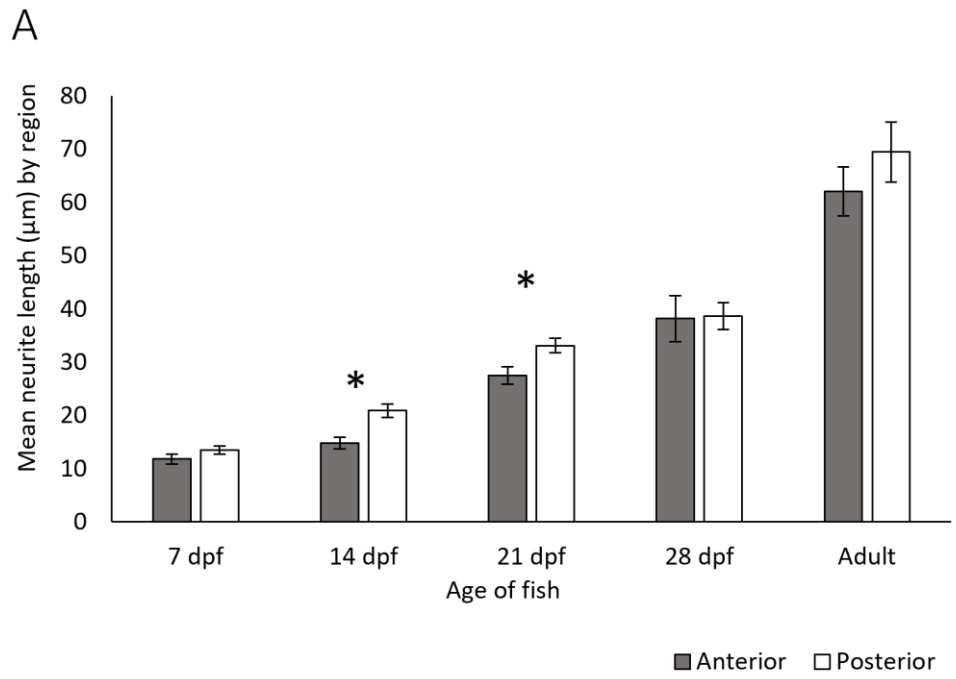
Figure 6: **Mean neurite length by region at each age.**

Figure 7: Overview of the right olfactory bulb of an adult AB fish, stained with anti-TH and anti-GABA. (A) Overview of an adult olfactory bulb stained with anti-TH and (B) anti-GABA. Very few GABA+ cells were identified; less than 50 per bulb. They were located in small clusters near the posterior of the bulb (dashed circles). (C & D) While these cells possessed the same size and soma morphology as the TH+ cells (white triangles), no neurites were noted and there was (E) no doubled labelling of cells with both anti-TH and anti-GABA (white triangles).
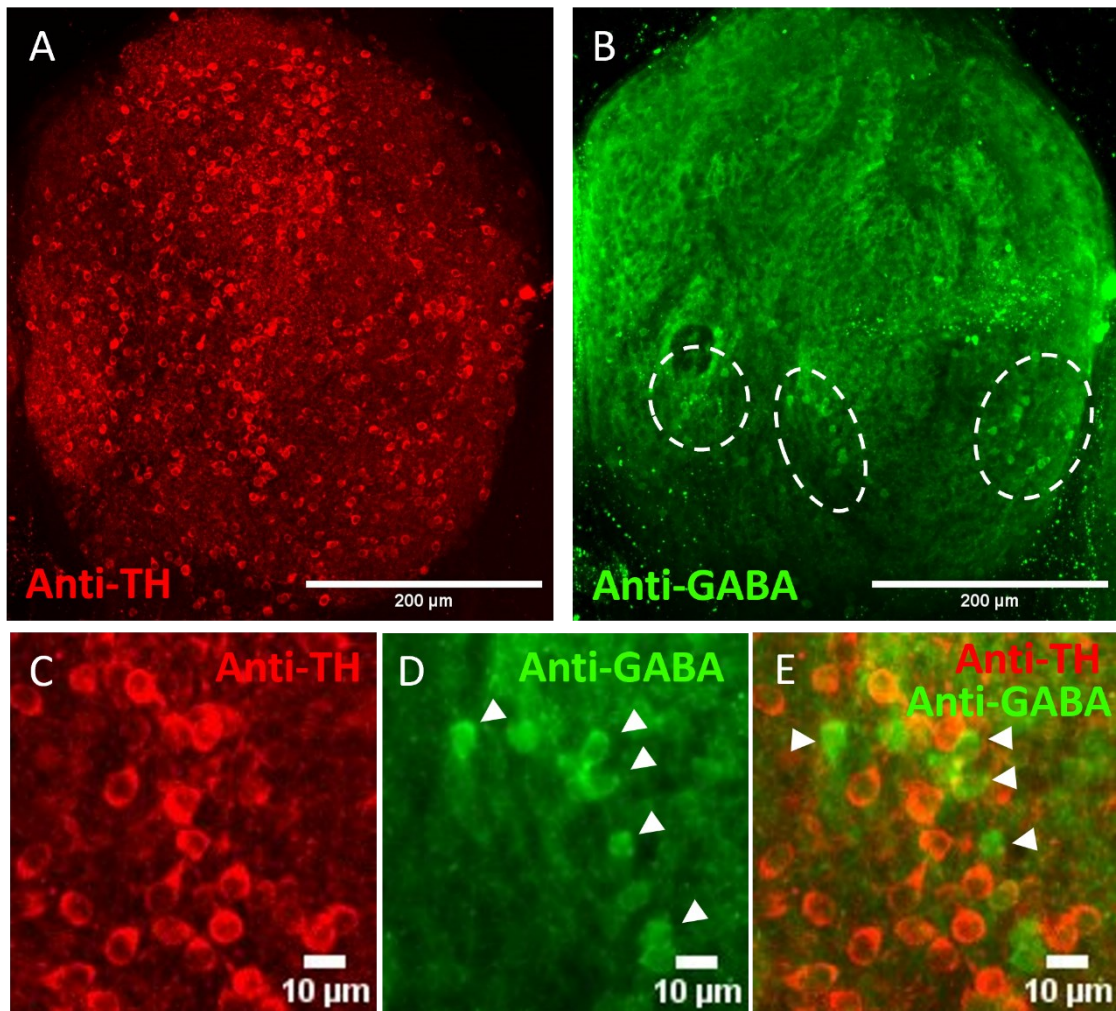
Figure 7: Overview of the right olfactory bulb of an adult AB fish, stained with anti-TH and anti-GABA.

Figure 8: Overview of the olfactory system at 7 dpf in a SAGFF(LF)27A;GFP zebrafish.

The left olfactory rosette (top left) and the developing lateral glomeruli expressed GFP.

The bulbs possessed only a few TH+ cells, which were mostly found towards the medial

posterior region. Most of the visible puncta were located anteriorly and laterally in the

bulb. The divisions between forebrain and bulb were clearly delineated as was the

separation between left and right bulbs. A rudimentary medial olfactory tract (MOT)

was beginning to appear.
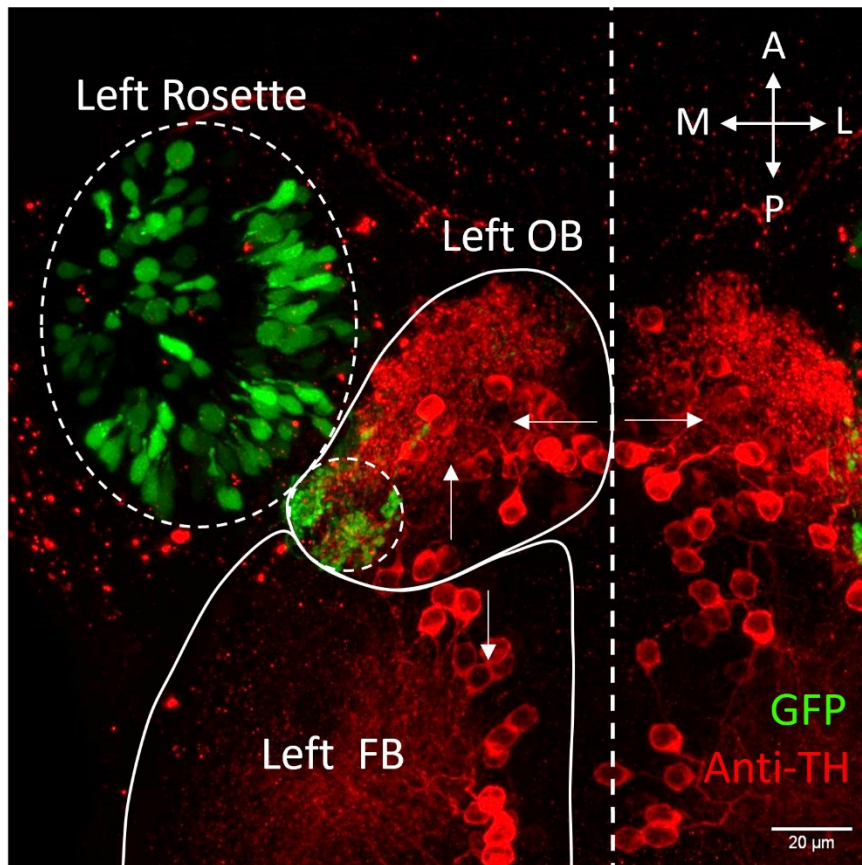
Figure 8: Overview of the olfactory system at 7 dpf in a SAGFF(LF)27A;GFP zebrafish.

Figure 9: High magnification views of the midline division between left and right bulbs in two 7 dpf AB fish stained with anti-TH. The division between the bulbs was easily discerned as neurites of these cells were clearly visible and distinctly innervated only the ipsilateral bulb. The bulbs are not identical as seen in panels A and B, but the cells were generally innervating in the same directions.
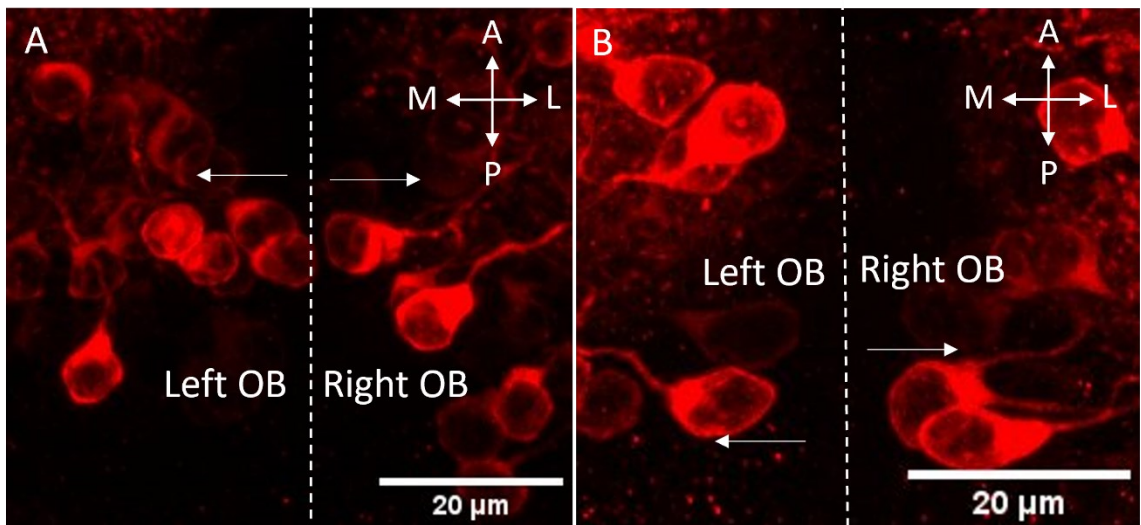
Figure 9: High magnification views of the midline division between left and right bulbs in two 7 dpf AB fish stained with anti-TH.

Figure 10: High magnification views of the olfactory bulb (OB) and forebrain (FB) division in a 7 dpf SAGFF(LF)27A;GFP fish. The posteromedial cells in each bulb appeared to be continuous with those underlying the medial olfactory tract running through the forebrain, but again cells could be easily categorized as being present in the bulb or in the forebrain because their neurites clearly projected either anteriorly or posteriorly, respectively. Again, each bulb is not identical but the cells generally project to the same area.
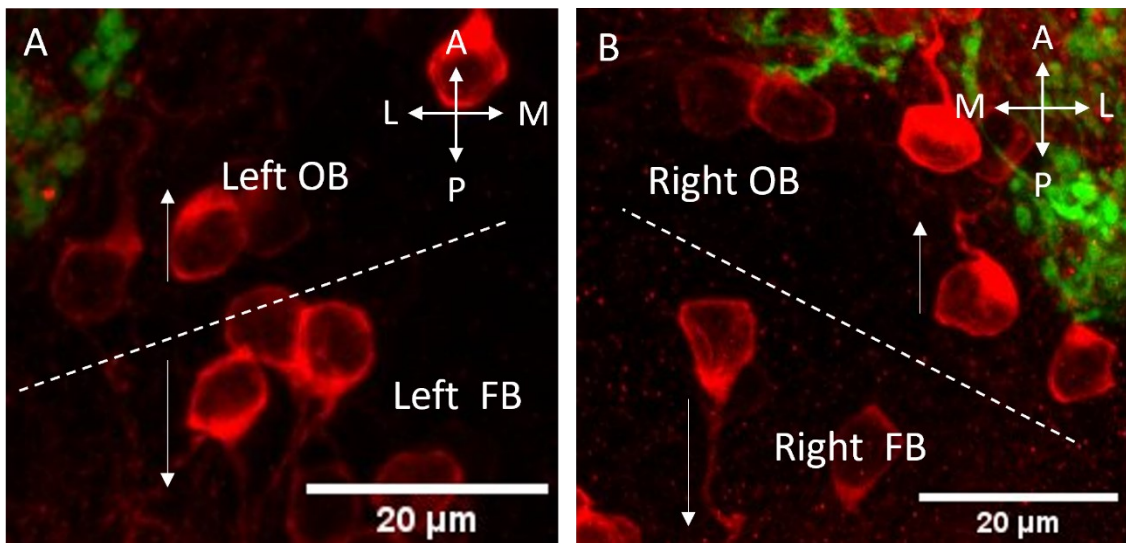
Figure 10: High magnification views of the olfactory bulb (OB) and forebrain (FB) division in a 7 dpf SAGFF(LF)27A;GFP fish.

Figure 11: An overview of the left olfactory bulb of an AB 7 dpf fish stained with anti-TH. The bulb was divided into four quadrants for analysis, those being: Anterior Lateral (AL), Anterior Medial (AM), Posterior Lateral (PL) and Posterior Medial (PM). At this stage, most of the TH+ cells were located in the PM quadrant with the fewest in AL. The two anterior quadrants also contained numerous small puncta, believed to be synapse. The staining was too consistent to be considered artifacts. An expanded view of the AL quadrant showed the puncta in greater detail (arrows).
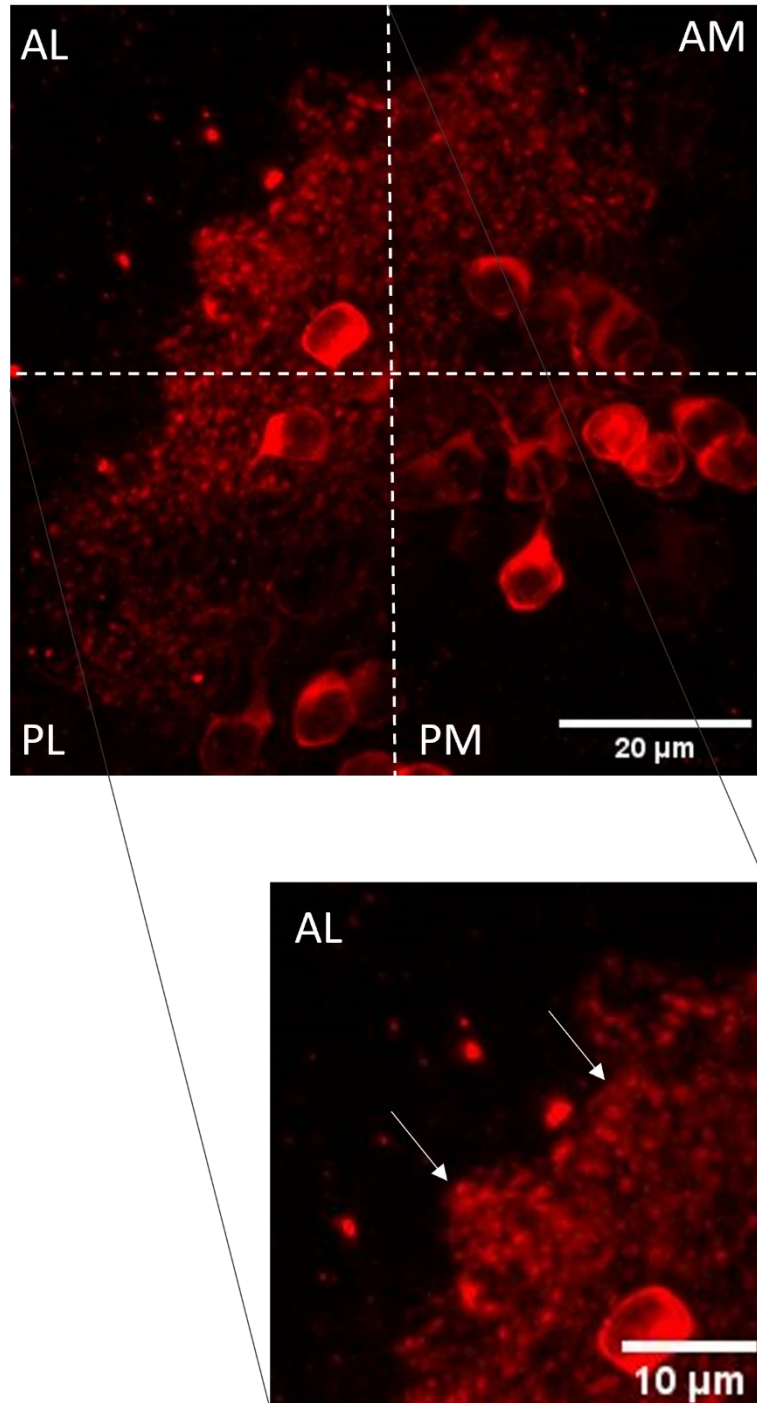
Figure 11: An overview of the left olfactory bulb of an AB 7 dpf fish stained with anti-TH.

Figure 12: High magnification view of the right bulb of a SAGFF(LF)27A;GFP 7 dpf fish stained with anti-TH. The olfactory rosette was clearly visible in the top right. The developing lateral (lG) glomeruli were clustered along the lateral edge, while the medial-dorsal glomeruli (mdG) were located mid-bulb on the medial side. There were several TH+ cells (white triangles) in close proximity to these glomeruli although it was difficult to discern if they directly innervated those glomeruli.
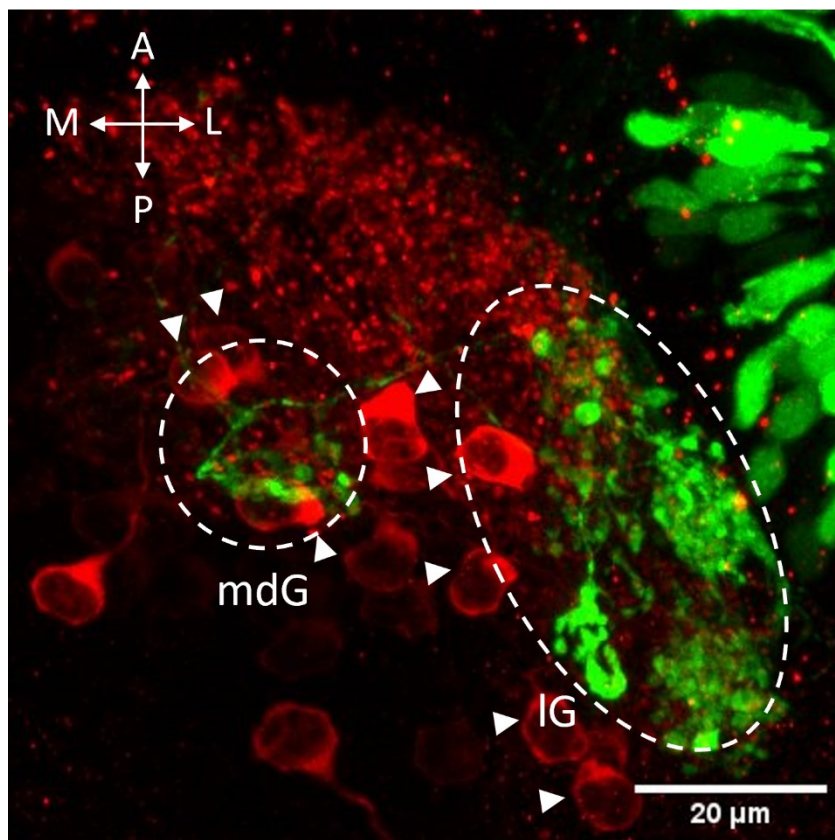
Figure 12: High magnification view of the right bulb of a SAGFF(LF)27A;GFP 7 dpf fish stained with anti-TH.

Figure 13: Overview of the right olfactory bulb of a 14 dpf AB fish, stained with anti-TH. By 14 dpf, the number of TH+ cells doubled, with most cells still located in the medial region of the bulb but with more now present towards the posterior regions. The percentage of cell bodies found in each quadrant largely remained the same with the AM quadrant increasing slightly to 32.0% while the percentage of cell bodies found in the PL and PM quadrants were 27.8% and 24.4%, respectively. The AL quadrant contained 8.8% of the cells, with again most of the puncta were found in this quadrant.
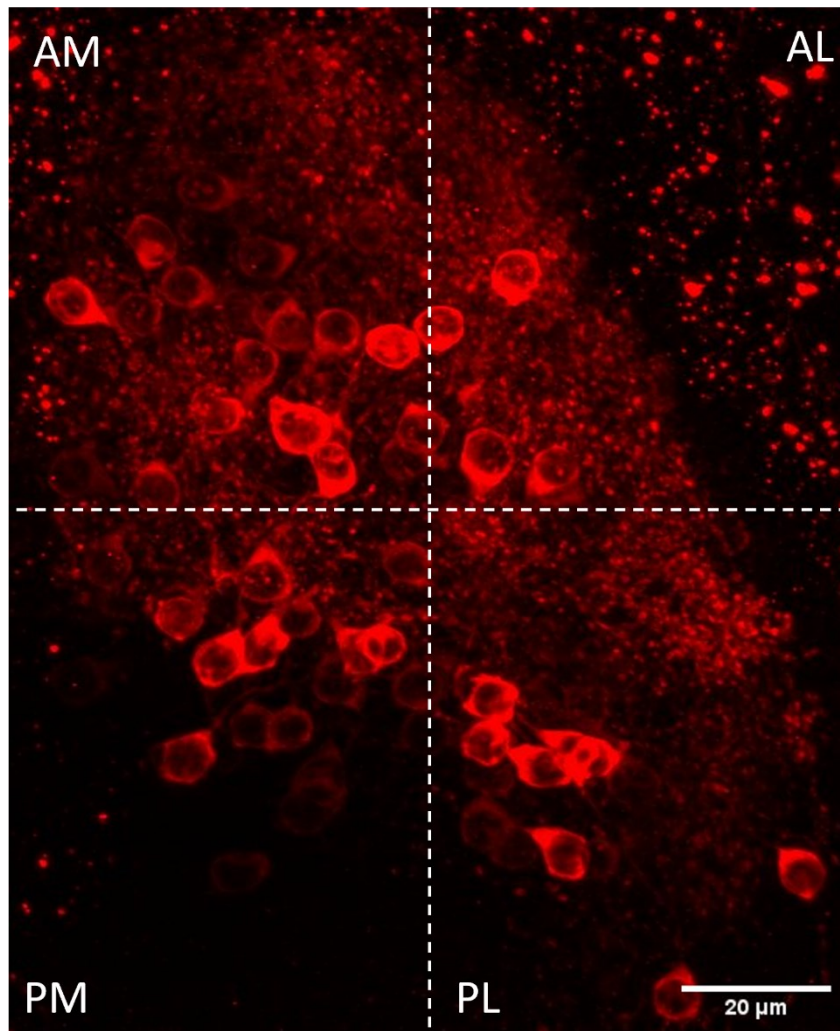
Figure 13: Overview of the right olfactory bulb of a 14 dpf AB fish, stained with anti-TH.

Figure 14: High magnification view of the division between the left olfactory bulb and left forebrain on a 14 dpf fish stained with anti-TH. The division between OB and forebrain was becoming increasingly populated by cell bodies and neurites. Despite the increase in cell bodies, most neurites could still be traced back to the appropriate side (OB or Forebrain).
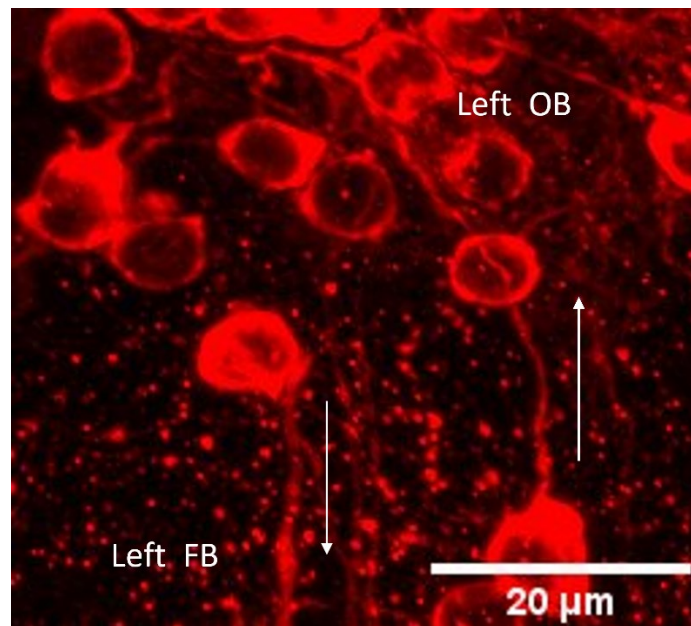
Figure 14: High magnification view of the division between the left olfactory bulb and left forebrain on a 14 dpf fish stained with anti-TH.

Figure 15: Overview of the right bulb of a 14 dpf SAGFF(LF)27A;GFP fish stained with anti-TH. Approximately 10 TH+ cells had somas or neurites within one cell length of the lateral protoglomeruli (lG) of the larvae. The medial protoglomeruli (mdG) possessed ~15 TH+ cells that somas or neurites within one cell length of the cluster. While again, it was difficult to determine if the cells were directly innervating these glomeruli, in the case of the mdG, the cells did appear to develop in close proximity.
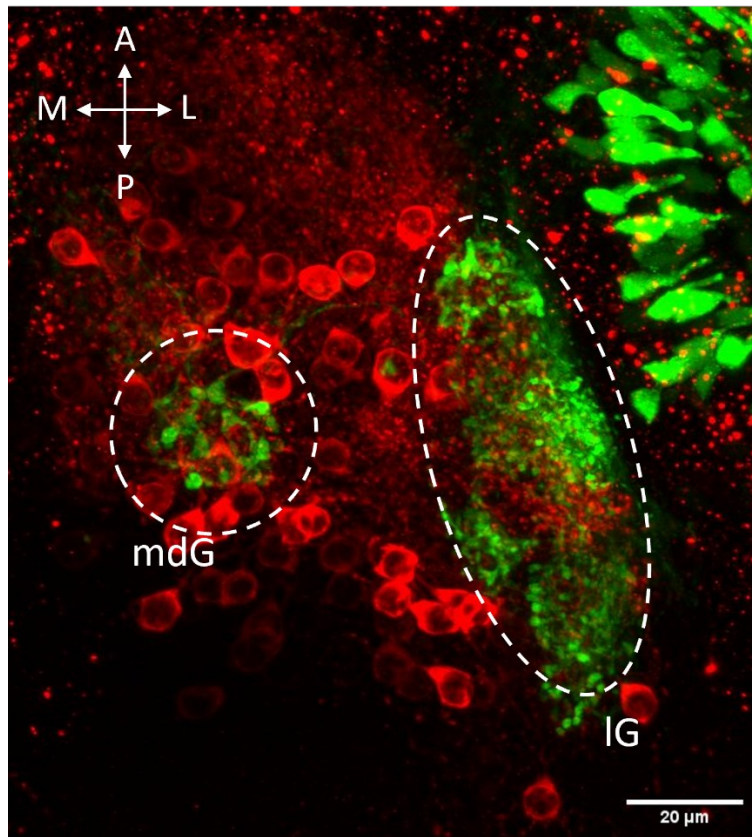
Figure 15: Overview of the right bulb of a 14 dpf SAGFF(LF)27A;GFP fish stained with anti-TH.

Figure 16: Overview of the left olfactory bulb of a 21 dpf fish stained with anti-TH. At 21 dpf, the cells were now filling out from the medial-posterior to the lateral-anterior portion of the OB. The lateral and anterior edges still only possessed few cells and seemed to be mostly populated by puncta, possibly synapses of TH+ cells and glomeruli, as discussed previously. As in the 14 dpf fish, the division between the left and right bulbs was clearly defined, however the OB/forebrain border became harder to discern due to the increased number of cells and puncta.
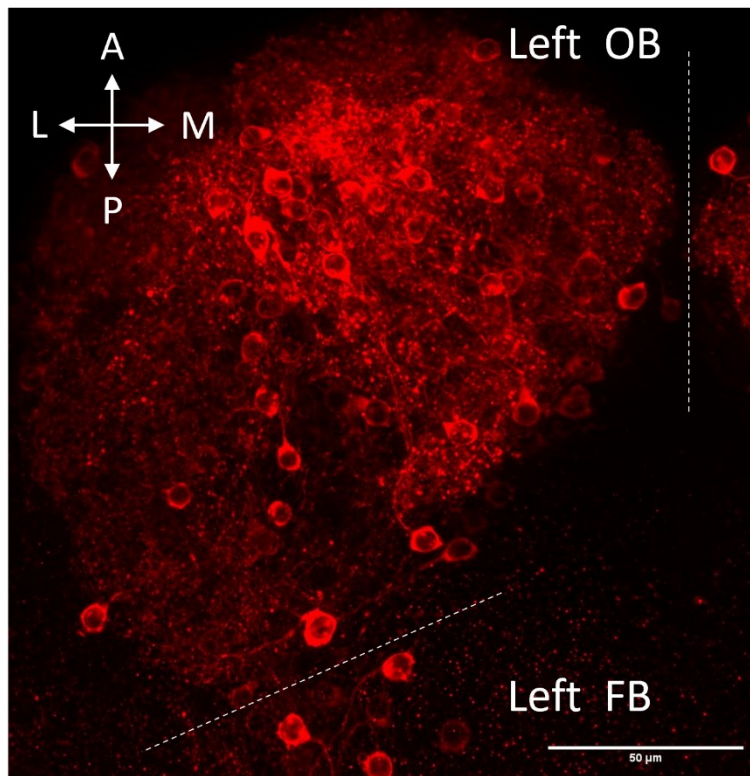
Figure 16: Overview of the left olfactory bulb of a 21 dpf fish stained with anti-TH.

Figure 17: High magnification views of branched unipolar cells in 21 dpf AB fish stained with anti-TH. (A & B) Around the OB/forebrain border, cells with a single branch in the neurite within one cell body length begin to appear. Typically, only 1 or 2 of these cells (white triangles) per bulb were identified and usually one branch (white arrows) projected anteriorly into the bulb, while the other projected posteriorly into the forebrain. Presumably these cells are involved in communication between the olfactory bulb and forebrain.
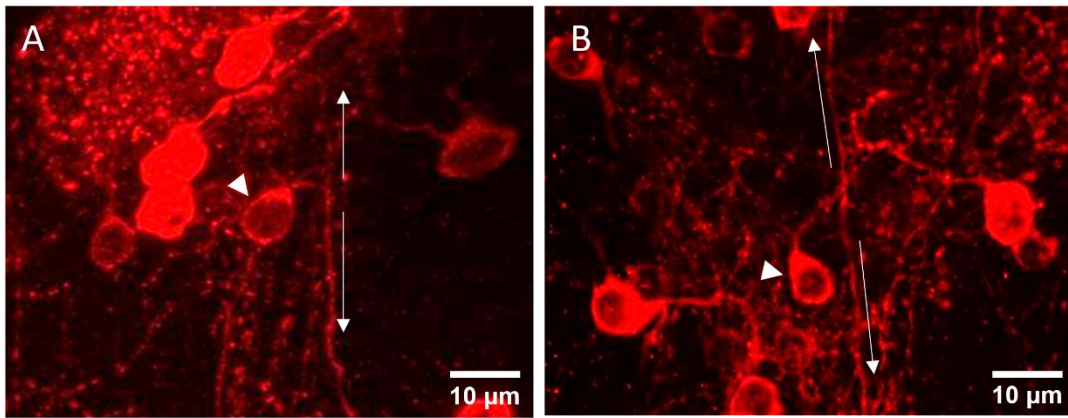
Figure 17: High magnification views of branched unipolar cells in 21 dpf AB fish stained with anti-TH.

Figure 18: High magnification views of multipolar cells in 21 dpf AB fish stained with anti-TH. (A & B) A few bipolar cells are found within the bulbs at this age, mostly in the medial region multipolar cells. These cells (white triangles) had comparatively long neurites (white arrows) and possibly project between regions of the bulb. (B) In a few bulbs a single tri-polar cell (white triangle) with three distinct neurites (white arrows) was noted although never in precisely the same spot but usually in the same general region.
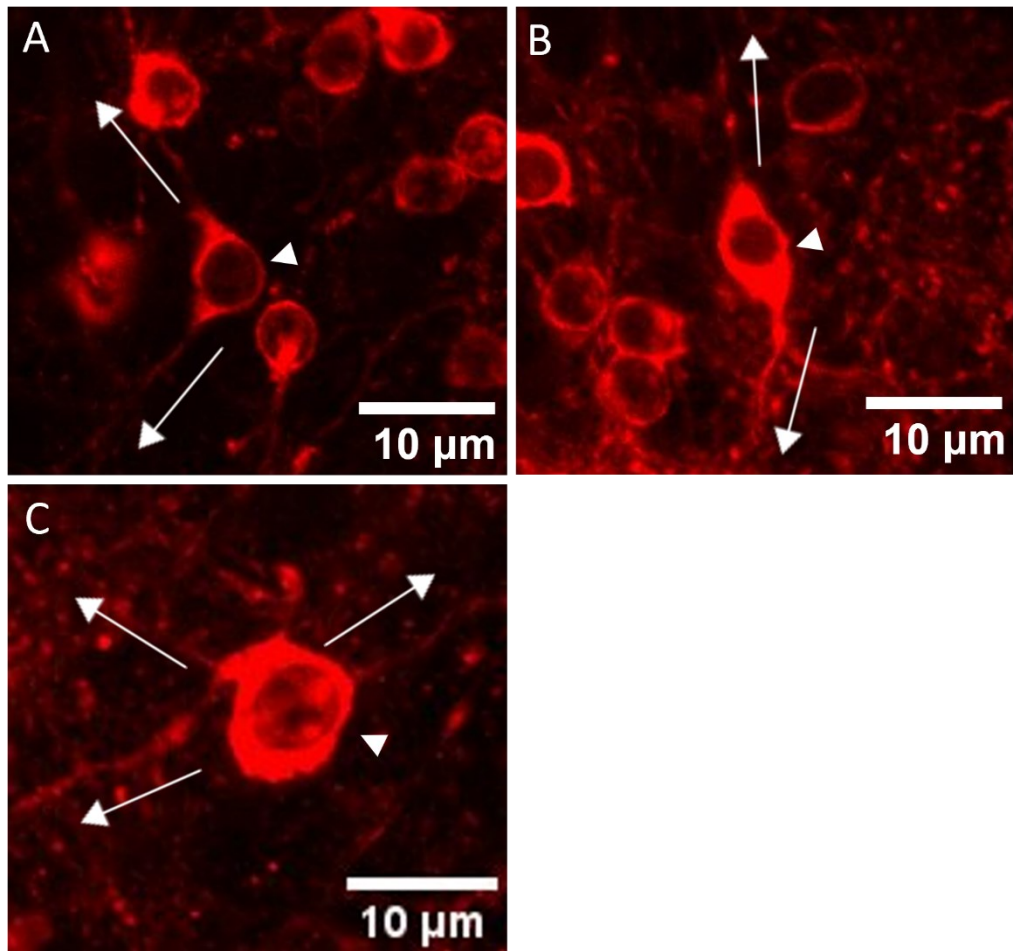
Figure 18: High magnification views of multipolar cells in 21 dpf AB fish stained with anti-TH.

Figure 19: Overview of the right olfactory bulb of a 28 dpf AB fish stained with anti-TH.

(A) The TH cells continued to fill out the anterior and lateral areas of the bulb and cells were now clearly visible along the lateral edges of the OB. The puncta were now present in the posterior and medial regions of the bulb. (B) As with the 21 DPF fish, the division between left and right bulbs was clear, however it became increasingly difficult to differentiate between the OB and the medial olfactory tract in the forebrain as cells developed in that area. (C) At this stage, one multipolar cell was observed crossing between the left and right olfactory bulbs. It was not present in every bulb.
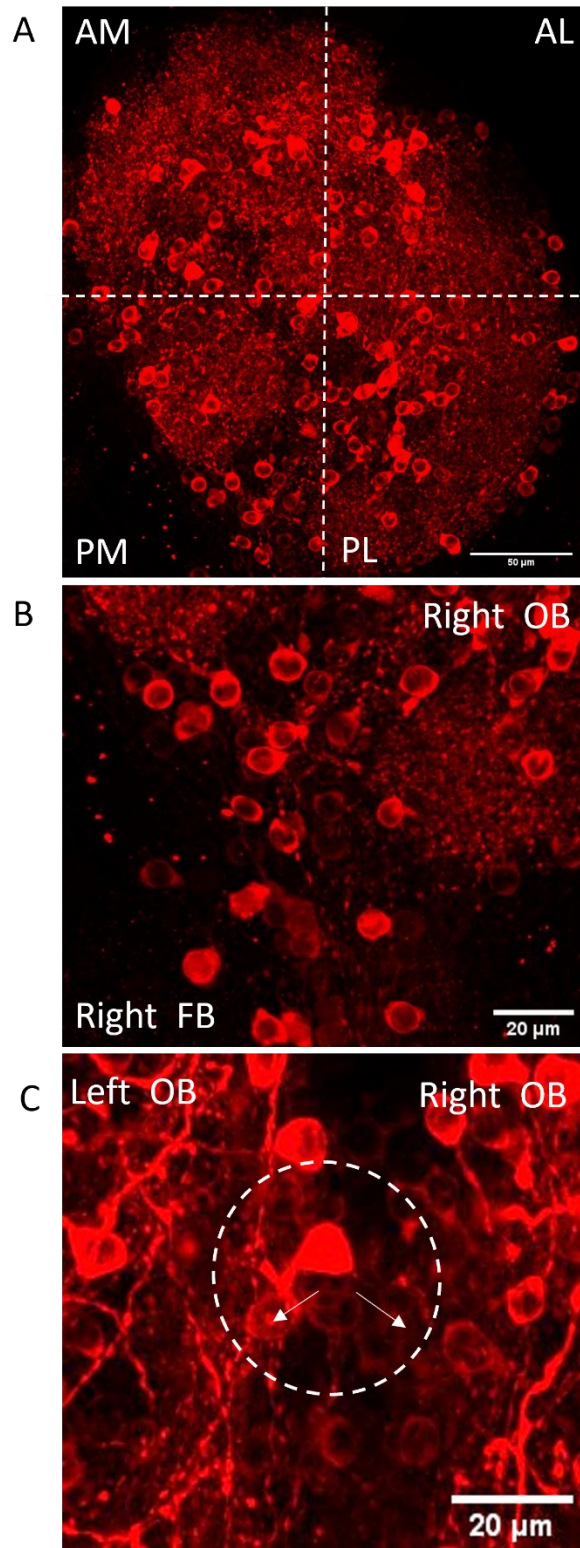
Figure 19: Overview of the right olfactory bulb of a 28 dpf AB fish stained with anti-TH.

Chapter 3: An Appetitive Olfactory Learning Paradigm For Zebrafish In

Their Home Tank

3.1 Introduction

Olfaction plays numerous essential roles in the lives of fish, as of most animals (Doty, 1976; Stoddart, 1980). In particular, it is used for feeding, social interactions, predator avoidance and navigation (Hara, 1994; Zielinski and Hara, 2006). Perhaps one of the best-known and most impressive examples of such an olfactorily mediated behaviour is the extraordinary use of odour cues by salmon to navigate back to their home streams for spawning (Hasler et al., 1978). However, the olfactory processes that fish use are increasingly disrupted by environmental pollution, such as contamination from heavy metals (Scott and Sloman, 2004; Calvo-Ochoa and Byrd-Jacobs, 2019). These pollutants have been shown to disrupt their olfactory system and therefore threaten wild fish populations, thus prompting new lines of research into the roles of olfaction in the lives and survival of fish (Ward et al., 2008; Tierney et al., 2011).

In addition to the ecological relevance of studying fish olfaction, teleosts have become popular biomedical model organisms in recent years for understanding the anatomical and physiological substrates of olfaction (Langheinrich, 2003; Linney et al., 2004). This rise to popularity is largely due to the relative simplicity of the fish olfactory system when compared to other research organisms; for instance, zebrafish have an olfactory bulb that is organized similarly to that of mammals, but with far fewer glomeruli (Braubach et al., 2012; Mombaerts, 2006; Potter et al., 2001). This relative simplicity facilitates research into how the olfactory system codes and processes information and how the system develops both embryonically and into adulthood (Baier & Korsching, 1994; Braubach et al., 2013). Zebrafish also possess a well-documented

83

behavioural repertoire that makes them ideal candidates for studying responses of fish

to odours (Moretz et al., 2007; Spence et al., 2008; Kalueff et al., 2013). Accordingly,

innate responses of zebrafish to olfactory stimuli, such as feeding cues and various

pheromones, have now been well documented (Lipton and Rosenberg, 1994;

Jesuthasan and Mathuru, 2008; Koide et al., 2009). In addition to exhibiting innate

responses to chemical cues, zebrafish can also learn to modify their behavioural

responses to odours (Harden et al., 2006). For example, Braubach et al. (2009)

demonstrated that pairing amino acids or a previously neutral odourant (phenylethyl

alcohol, PEA) with food presentations resulted in rapid and reliable learning. At the end

of training, zebrafish showed increased appetitive swimming behaviour when presented

with the conditioned odourant alone, and largely restricted their swimming to the

immediate area of food reward. In a follow-up study, Braubach et al. (2011) modified

the paradigm for groups of fish, thus increasing the efficiency of training and testing fish

for their responses to olfactory cues and suggesting the possibility of adapting the

paradigm for high-throughput screening. However, olfactory conditioning paradigms are

inherently challenging because the temporal and spatial distributions of odourants are

much more difficult to control than auditory or visual stimuli that can be presented

directly to the fish with almost instantaneous onset and offset. In addition, olfactory

paradigms that utilize multiple pairings require large volumes of water to eliminate

odourants between trials. Braubach et al. (2009) used a flow rate of 360 L/tank/hour

through a relatively large tank to train a single fish. A more recent study by Namekawa

et al. (2018) demonstrated that zebrafish could also learn olfactory cues in smaller tanks

with less flow, however, these studies employed specialized tanks that were unfamiliar to the fish, thereby necessitating prolonged acclimation periods for optimisation (dos Santos et al., 2020).

In this chapter, I describe adaptations of the auditory and visual learning paradigms presented in Doyle et al. (2017) to use a salient olfactory cue (PEA) as the conditioned stimulus (CS). The procedure entailed moving the entirety of the tank assembly, in which fish are routinely maintained, to the test area. This greatly reduced handling stress and, in turn, reduced acclimation times. In addition, the small, 3 L tanks greatly reduced the water requirements and flow rates. I thus demonstrate an efficient and cost-effective appetitive olfactory conditioning paradigm with reasonable water requirements and minimal stress impact on the fish.

3.2 Materials & Methods

3.2.1 Animals

Zebrafish of the AB strain were obtained from the Zebrafish Core Facility, Faculty of Medicine, Dalhousie University, Halifax, NS, Canada. Beginning at least two days prior to experimentation, animals were housed as mixed-sex groups of five in 3 L tanks (Pentair Aquatic Eco-Systems, Apopkoka, FL, USA). All fish were raised and maintained in these tanks, and thus were familiar with their physical properties (i.e., blue lid and baffle at the back, sloped front, consistent water inlet and food delivery through holes in the front of the lid twice each day). Zebrafish were kept on a 14:10 hour light:dark cycle in treated, reverse osmosis water (28°C, pH 7.3 and salinity at 0.20 PSU) with an average flow of 13-14 L per hour per tank. All experiments were conducted in accordance with the Canadian Council on Animal Care standards and guidelines (Dalhousie Protocol 21-117).

3.2.2 Experimental Apparatus

For conditioning, the home tank for each group of fish was moved to one of four specialized testing arenas. Each arena contained a camera (model C930e, Logitech, Newark, CA, USA) that was aimed at the centre of the long side of the tank. The side of the tank opposite the camera was backlit by an LED work light (Snap-on, Kenosha, WI, USA) to provide contrast for the video recording and facilitate tracking. White, nylon schuss fabric (Fabricville, Montreal, QC, CAN) was used to diffuse the LED backlighting and provide a uniform white background. In addition, white corrugated plastic signboard (Home Depot, Marietta, GA, USA) was used to separate each of the four

testing arenas, and a white curtain shielded the entire experiment from outside visual interference in the testing room. Each arena also contained an outlet that removed facility-treated water during experimentation (See 3.2.3 Water delivery).

An automatic feeder, 3D-printed of polylactic acid (PLA) and controlled by an Arduino Uno microprocessor (Sommerville, MA, USA), was placed over an existing hole in the lid of each tank using double-sided foam tape for sound isolation (Fig. 20). Food was dispensed using a stepper motor and a 5 mm steel drill bit (Lee Valley, Ottawa, ON, USA) that served as an auger to dispense approximately one to three pieces of food at a time (Golden Pearl 500-800 Micron; Brine Shrimp Direct, Ogden UT, USA). Programs ("sketches") were created in Arduino software (Arduino, 2014) to control delivery of the odourant (conditioned stimulus; CS) and dispensing of the food reward (unconditioned stimulus; UCS; see Supplemental Material for Arduino sketches). A white PLA divider was placed at the level of the water, 8 cm behind the front of the tank, to keep the dispensed food floating in a restricted area near the feeder.

Odourant (see below for concentration and volume of phenylethyl alcohol, PEA) was delivered using a syringe pump (Model 2040, KD Scientific, Holliston, MA, USA) adapted to hold four 60 mL syringes (Becton Dickinson, Franklin Lakes, NJ, USA). Each syringe was connected to polyethylene tubing (PE No. 160, Becton Dickinson) using an 18-gauge needle (Becton Dickinson). Each tube was placed through a hole in the lid adjacent to the water inflow, near the front of the tank, ensuring that the end of the tube rested just above, but not in contact with, the water surface. A small LED light, to

87

indicate odourant delivery, was partially wrapped in black heat shrink tubing and adhered to the lid so that it was visible to the camera but not to the fish.

3.2.3 Water Delivery

Water for general fish maintenance and experimental purposes was provided by the larger Zebrafish Core Facility of the Dalhousie Faculty of Medicine, as part of its routine, 10% replacement per day. During training, the water was discarded after it flowed through the experimental tanks and was contaminated by the odourant. At night, the system was switched to a recirculating operation to conserve water.

3.2.4 Conditioning

Tanks (experimental n=23, control n=23) of five fish were deprived of food for two days prior to the beginning of training to increase responses to UCS. Conditioning consisted of 12 trials during daylight hours on each of four consecutive days, for a total of 48 trials. Inter-trial intervals ranged from 40-60 minutes and were determined by a pseudorandom time generator (Random Time Generator, http://www.random.org). Each trial was performed by introducing the PEA odourant (CS) to the tank. The automatic feeder presented the food reward 15 seconds after the beginning of odourant delivery. In trials with control fish, the UCS (food) did not immediately follow the CS but was, instead, administered at the midpoint of the inter-stimulus interval, except for the last trial in which it was administered at a time 15-34 minutes later as determined by the random time generator. Of the four tanks run simultaneously, two were designated as experimental and two as control, and their placement in each arena

was changed periodically throughout the experiment to ensure that there was no consistent effect of tank position.

PEA was used for the odourant because it has previously been reported to be a neutral stimulus for zebrafish (Braubach et al., 2009; Harden et al., 2006). During each of the 48 sessions, 1.5 mL of 2.0×10^{-4} M PEA was delivered to the tank over a period of seven seconds. In preliminary experiments, 1.5 mL of food dye (McCormick & Co., Hunt Valley, MD, USA) was injected into the tanks through the odourant delivery system (See Supp. Video 1) to assess the dispersion of stimuli. After injection, a single bolus of dye was visible for about 15 s and then broke into concentrated swirls. The concentrated swirls were observable for approximately 120 s before what appeared to be homogeneous dispersion throughout the tank. During the dye experiment, all fish in the tank appeared to encounter the concentrated dye within about 15 s. Thus, if PEA odourant dispersed similarly to the dye, each fish would be expected to encounter an area of concentrated odourant before the food was presented. After full dispersion in the tank, the concentration of PEA was calculated to be 1×10^{-7} M, which is below the reported threshold for detection for zebrafish (Harden et al., 2006). The continuous water inflow further diluted the odourant during the inter-trial period (See Fig. 21 for dilution curve).

3.2.5 Water-Only Trial

To evaluate whether the fish were responding specifically to the PEA and not to turbulence from the odourant delivery, each tank of fish was exposed to a water-only trial on the morning after the last training trial. Instead of odourant, 1.5 mL of

89

conditioned system water was delivered to the tank using the same delivery method, but with separate syringes and tubing. The responses of fish were recorded, and behaviour analyzed using the same method as employed for the training videos. After 48 training sessions and the water-only trial, the feeders, indicator lights and odourant dispensing tubes were removed from the lid and the tanks were then returned to the racks on which they were routinely maintained, until animals were tested for memory retention.

3.2.6 Memory Probe Trials

Probe trials to test memory retention were conducted seven days after training. Each tank of five previously trained fish was gently moved from the maintenance rack back to an observation arena and switched to the flow-through water system at least one hour before testing. The feeders, indicator lights and odourant tubes were placed back on the lids of the tanks. Fish were exposed to the PEA odourant without the food reward, and their behaviour recorded to test whether they retained a conditioned association between the CS and the UCS.

3.2.7 Data Collection And Analysis

Experiments were video recorded in colour at a resolution of 1280 x 720 pixels. Surveillance software (iSpy, http://www.ispyconnect.com) permitted the recording of time-stamped video files from cameras in all four arenas simultaneously. Video clips were recorded at 6 frames/second for 30 seconds covering the 15 seconds immediately before exposure to the olfactory CS and the 15 second period during presentation of the

CS. Food, the UCS, was dispensed 15 seconds after the CS presentation, i.e.,

immediately after termination of the video recording (see timeline in Fig. 20C).

The behaviours of groups of fish during training and during the water only and memory-

probe trials were analysed using a program developed in Matlab (MathWorks, Natick,

MA, USA) (Wyeth et al., 2011) but recreated in ImageJ (National Institute of Health,

Bethesda, MD, USA; https://imagej.nih.gov/ij /) as described below. Specifically, the

stationary background (average of all the frames in the video) was subtracted from each

individual frame, and the resultant image was then converted to a binary image (white

fish on a black background). The natively installed "Analyze Particles" plug-in for ImageJ

was used to establish the mean position (horizontal and vertical coordinates of the

centroid) for the group of fish for each frame.

It was noted in Doyle et al. (2017) that different stimuli (i.e., light or sound) may

have different latency periods between presentation and response of the fish. To

examine when the fish were responding to the olfactory cue, the position of the

centroid of the positions of all of the pixels occupied by fish in each frame was averaged

across all (23) experimental tanks for Trial 48, the last of the training trials. The fish

showed a spike in response to the stimulus from the 20th second to the 30th second of

the video, suggesting that there is a latency of approximately five seconds, meaning that

it took about five seconds before the fish began to respond to the odourant. Therefore,

the period 5-15 seconds after presentation of PEA CS was chosen for analysis. Using this

information, various aspects of fish behaviour were examined with three different

measures.

The first measure was similar to that employed by Braubach et al. (2009) and evaluated changes in the proportion of time that the fish (represented by their positional centroid) spent in each quadrant of the tank (see Fig. 20A). For each video frame, the centroid of the subject group of fish was located relative to the quadrants of the tank. The number of frames spent in each quadrant was tallied for selected intervals before and after presentation of odourant. The interval of interest included 60 frames, spanning 5-15 seconds after odourant delivery. A baseline interval included 90 frames, spanning 15 seconds immediately preceding delivery of the odourant. The percentage of frames in each quadrant was calculated for each interval, and the differences in percentages between the intervals was calculated, such that a positive value signified that the fish spent more time in a particular quadrant after odourant delivery than before delivery.

The second measure was similar to that employed by Doyle et al. (2017) and more directly evaluated movements of the positional centroids toward the site where the food was dispensed. The X and Y coordinates of the centroid for each group of fish were first calculated for each video frame with the origin of the axes at the top left corner of the tank, near the food source. The mean position was next calculated for each tank during the 15 seconds immediately before presentation of the CS. Those values were then subtracted from the mean coordinates that were similarly calculated for the centroid in each tank during the 5-15 seconds after presentation of the CS. Changes in positions of the fish were then calculated as a single value using the

Pythagorean Theorem $\sqrt{(\Delta X^2 + \Delta Y^2)}$ with scores correspond to net movements of the groups of fish towards the food source.

During the experiments, it was noted that fish not only changed their positions in the tank during presentation of the odourant, but they also increased their swimming velocity and darting behaviour (See Supp. Video 2). Similar observations were made by Braubach et al. (2009) who noted increased numbers of turns after presentation of a conditioned odourant. The third measure aimed to quantify this behaviour by examining the jittering movements of the group centroids from frame to frame. I measured the total absolute distance (regardless of direction) travelled by the centroid of each fish group in the 15 sec (60 frames) before the odourant delivery and in 5-15 sec after odourant delivery, consistent with the timeframe used for the other two measures. In each instance, the distance travelled was divided by the time interval to give a measure of speed of the centroid (in cm/sec) moving within the video frame. That value was then subtracted to give the difference in centroid speed before versus during odourant presentation, thus reflecting general changes in fish activity.

Statistical analyses of all these measures were performed as described here. Two-way repeated measures ANOVA were performed for the acquisition periods, with post-hoc pairwise comparisons using a Bonferroni correction in SPSS 28 (IBM, Armonk, NY, USA). Simple comparisons of two means, such as the retention, water trial and satiation trials, were analysed using a Student's t-test.

3.3 Results

When presented with PEA on the first day of training, both experimental and

control groups moved towards the area where the CS was dispensed as evidenced by an

increase of about 15-20% more time spent in the top left quadrant of the tank (Q1)

during odourant delivery compared to the period **before** odourant delivery (Fig. 20).

This initial response subsequently decreased over the first two days; but on Day 3 of

training, the two groups began to diverge, with the experimental animals once again

spending more time in Q1 (Fig. 22). The control group showed no similar increase but

rather continued to decline slightly in the time spent in Q1. To better demonstrate this

divergence, Figure 23 shows the control values subtracted from the experimental

values, with the difference between groups becoming greater after Trial 25. This

separation of groups continued, culminating in nearly a 20% difference between

experimental and control groups by the end of Day 4 (ANOVA; $p < 0.05$; Post-hoc t-test;

$p < 0.05$). Figure 24 shows that, by the end of training, the increased time spent by the

experimental fish in Q1 occurred at the expense of time spent in all three other

quadrants (Q2-4; ANOVA; $p < 0.05$; Post-hoc t-test; $p < 0.05$); however, the control fish

showed no such pattern. We interpret the divergence between groups that happened

on Days 3 and 4 to be the result of the experimental group forming a learned

association between the conditioned stimulus and the food reward and therefore

spending more time in Q1 during odourant delivery in anticipation of a food reward; in

contrast, no such association formed in the control group. Statistical analysis revealed a

94

significant interaction between conditioning and training trials (ANOVA, p<0.05) in the time spent in Q1.

To gain further insights into the behaviour of the fish during conditioning, I examined other measures such as the net movement toward the feeding area, regardless of quadrant boundaries, before and after the beginning of odourant delivery (Fig. 25). The results of this analysis support the quadrant findings, showing the initial attraction of both groups to the site of stimulus presentation, the subsequent reduction in this attraction and the final divergence of the experimental and controls groups starting on Day 3 of training, specifically Trial 34 (Post-hoc t-test, p<0.05).

In response to the odourant, the conditioned fish also appeared to exhibit an increase in general activity (See Supp. Video 2). To quantify this behaviour, speed of the movement of the centroid was calculated over the observation period (Fig. 26). Like the previous analyses, both groups initially show an increased value upon odorant presentation, moving more after stimulus presentation than before. However, groups diverged beginning on Day 2 and remained separate throughout Day 4, with the experimental group increasing and the control group maintaining the centroid speed. Thus, in addition to moving towards the food and spending more time in Q1, the experimental fish also exhibit increased swimming activity. Although both of the latter two measures of behaviour are consistent with the experimental fish forming an association between PEA and the presentation of food by the end of the fourth day of training, the quadrant analysis demonstrated the clearest divergence when graphed and was therefore used exclusively in subsequent experiments.

The initial attraction of both the experimental and control groups to PEA was unexpected, as previous experiments indicated that PEA was a neutral stimulus. One possible factor contributing to the observed response could have been that fish in both groups were starved for two days prior to the conditioning experiment. Therefore, to further investigate the nature of the initial movement of all fish to Q1 upon presentation of PEA, an additional experiment was conducted. One group of fish was starved for two days, as had been the fish in the experiment described above. The second group of fish was fed twice daily over this time, according to the routine maintenance procedures, up to 30 min before experimentation. Results indicated that the starved fish responded similarly to the fish on the beginning of Day 1 of training with a 15-20% increase in time spent in Q1, while the non-starved fish showed little or no such increase (t-test: $p<0.05$, Fig. 27A). This suggests that food motivation played a major role in initial attraction to PEA during training.

To test whether fish were responding to the PEA itself and not simply to turbulence caused by odourant administration, both the experimental and control groups were exposed to a puff of water alone on the morning after training finished on the fourth day. The experimental group spent significantly less time in Q1 then they did on the last trial of training (Fig. 27B & Fig. 22; t-test: $p<0.05$). Also, there was no significant difference in the scores of the experimental and control groups in response to the water puff only (t-test: $p>0.05$, Fig. 27B). This finding supports the hypothesis that the experimental group learned an association between the PEA odour and subsequent food delivery. These conclusions are congruent with the results of Braubach et al. (2009)

in which fish that were rendered anosmic by occluding their nares did not exhibit an association between PEA and a food cue, indicating that fish were mainly using the odour as the CS. However, it should be noted that both the experimental and control groups did spend 4-12% more time in Q1 following the water puffs only, thus also suggesting a small innate attraction of the fish to mild turbulence that might signal a potential food source.

Finally, Braubach et al. (2009) showed that fish retained the learned association between PEA and the food reward for two days after the end of training; I extended this time frame and examined whether the association between the olfactory stimulus and the food reward was retained seven days post-training. Groups of experimental and control fish were tested for their responses to the olfactory stimulus alone with probe trials one week after training, with both groups starved for 24 hours before. The experimental and control groups both spent more time in Q1, with values similar to the beginning of Day 1, and differences between the groups were not statistically significant (Fig. 27C; t-test, $p>0.05$). Thus, I cannot conclude that the fish retained an association at seven days.

3.4 Discussion

The present chapter demonstrates that adult zebrafish can be trained to respond to olfactory cues in their home tanks while being supplied with the same quantities of water used for their routine maintenance. Initially, both experimental and control groups responded to the novel odourant, PEA, with their mean positions (as represented by their centroids) moving toward and into the region of the tank where the stimulus was presented (Quadrant 1, Q1) and increasing their general activity. This initial response was not anticipated given the previous literature reporting that PEA elicits neither attractive nor repulsive innate responses (Harden et al., 2006; Braubach et al., 2009; Tierney, 2011; Morin et al., 2013). Further investigation indicated that this apparent attraction of naïve fish was dependent upon a high level of food motivation, as starved fish showed a heightened response while non-starved fish showed little attraction (Fig. 27A). I suggest that both the initial attraction and its subsequent decline over the first two days of testing were the results of interactions of stimulus novelty, potential signalling of a new food source and changing levels of satiation as the initially starved fish were fed during training. Further research is warranted given the frequent use of PEA as an odourant in research on teleost olfaction (Harden et al., 2006; Braubach et al., 2009; Morin et al., 2013). In addition, although the fish appeared to respond primarily to PEA as an olfactory stimulus (Fig. 22), subjects presented with only a non-scented water puff still showed a small positive response (Fig.27B). Thus, a component of the initial response may be attributed to the turbulence caused by odourant delivery. Surface feeding zebrafish (Lucore and Connaughton, 2021) appear to

have an innate response to water turbulence such as that which accompanied odourant

delivery, and this response may further explain why control fish still exhibited slightly

elevated scores even late into training (Figs. 22, 25, 26).

Regardless of the reason for the initial behaviours after PEA delivery, the

responses of all fish waned over the first two days of training. By Day 3, however, the

two groups began to diverge from each other with the experiment group increasing its

movement into or toward Q1 and increasing its general activity (Figs. 22, 25, 26). By

contrast, the control group continued to spend less time in Q1 and showed a decrease

in general activity. This divergence between the groups is best demonstrated in Fig. 23,

which shows the differences in responses between the experimental and control fish

over the 4-day training period and indicated that the fish began to associate the CS and

UCS around the end of Day 2 or beginning of Day 3.

A wide range of acquisition rates have been reported for conditioning in

zebrafish. Studies with aversive stimuli, such as strong water turbulence or electric

shocks, have required one to 40 pairings presented over one to five days (Xu et al.,

2007; Blank et al., 2009; Agetsuma et al., 2012; Morin et al., 2013). Previous appetitive

paradigms, on the other hand, required 20 to 400 trials for up to eight days (Colwill et

al., 2005; Braubach et al., 2009; Shiba et al., 2009; Sison and Gerlai, 2011; Mueller and

Neuhauss, 2012; Chacon and Luchiari, 2014; Buatois et al., 2024). Thus, acquisition rates

appear to vary widely between paradigms and sensory modalities; and fish, in general,

seem to take longer to form appetitive associations compared to aversive associations.

However, the present results and those of Doyle et al. (2017) and Buatois et al. (2023)

suggest that under less stressful conditions, such as when training in familiar environments, fish can form appetitive associations relatively quickly. Fish trained with a visual paradigm, similar to that used in the present olfactory study, began to exhibit an association with a food reward by the 7th to 10th pairings on the first day of training and an auditory paradigm showed learning by the 5th pairing (Doyle et al., 2017). The longer acquisition time for the olfactory paradigm used here may be attributed to several reasons, including the relatively imprecise temporal characteristics of PEA presentation, in comparison to both auditory and visual stimuli with almost instantaneous onsets and offsets. As seen in the dye trial (See Supp. Video 1), each fish in the group initially encountered concentrated swirls of odourant at slightly different times and concentrations. Also, comparison of acquisition rates between modalities can be problematic because the intensities of the conditioned stimuli are inherently different. Several studies have been conducted to examine the effect of stimulus intensity on the reaction of zebrafish (Carvan et al., 2004; Bilotta et al., 2005; Wolman et al., 2011; Avdesh et al., 2012). Ideally, the intensities of the different stimuli should be chosen to fall within the detection range known for zebrafish but without evoking startle responses. In the case of the olfactory stimulus used here, I also had to factor in the time required for the odourant to fall below the effective threshold and I therefore sought to minimize its concentration. Thus, although the fish were exposed to PEA at a concentration above their detection threshold, it is possible that the stimulus was not as salient as those in the other modalities.

An additional point to consider is that each sensory system may have a different neural substrate for learning. Most of the current studies on zebrafish, and fish in general, examine brain regions associated with learning generally and not with learning specific to a sensory stimulus (Rodríguez et al., 2002; Portavella et al., 2004; Salas et al., 2006; Mueller and Wullimann, 2009; Broglio et al., 2010; Mueller et al., 2011; Northcutt, 2011). It is unknown to what degree various types of learning utilize different areas of the zebrafish brain or different neural mechanisms. Consequently, it is also unknown if associations via one sensory modality are inherently easier for zebrafish to acquire than via another modality.

In contrast to the numerous reports of acquisition of learned associations by zebrafish, memory retention is not often examined. Results from Braubach et al. (2009) indicated that fish could recall an olfactory association for at least 48 hours and Doyle et al. (2017) and Alamdari et al. (2018) also noted a 48-hour retention of the association between a food reward and a visual or auditory stimulus. In the present study, the memory probe seven days after training revealed no significant difference in responses of the experimental and control groups and might therefore suggest that the fish lose the association between UCS and CS at two to seven days post-training. However, closer inspection of these results indicate that other factors might have obscured any possible memory retention. Specifically, the scores for the experimental group were similar to those exhibited on the last day of training (Fig.27C & 22), but the scores for the control group were also elevated and were thus reminiscent of values observed at the beginning of the training. The higher level of food motivation with one day of starvation

before the memory probe could, therefore, explain the elevated response, and further studies might be needed to determine the capacity of zebrafish for long term retention of olfactory memories.

The primary goal of the present study was to provide a proof-of-concept demonstrating that home tank learning paradigms could be extended to olfactory conditioning. While that goal was achieved, the paradigm may benefit from further optimization (Doyle et al., 2017; Alamdari et al., 2018; Buatois et al., 2024). For example, not starving the fish before training and memory probe may elicit clearer behavioural responses, without the initial attraction of all fish to PEA. As mentioned above, additional experiments indicated that routine feeding before PEA exposure mostly eliminated the initial reaction (Fig. 27A). However, changing the satiation of the fish may result in lower food motivation and therefore could require changes to the number of trials per day and how much food is dispensed at a time. In fact, further fine tuning of the inter-trial period may result in more efficient learning and therefore more successful retention. Also, minimizing the turbulence created by the odourant delivery could reduce the increases in the scores for both groups after the stimulus delivery. As stated, zebrafish are sensitive to surface vibrations that may indicate the presence of food; therefore, the fish may have an innate response to water disturbances (Hara, 1994; Lucore and Connaughton, 2021). Future experiments could reduce the turbulence by increasing odourant concentration while decreasing the volume delivered to the tank. Another possibility would be to introduce the odourant directly into the water inlet so

the turbulence is masked by the inflow, although this may change the diffusion of the odourant in the tank, so further investigation is needed.

There are also various tracking options available to use in conjunction with this paradigm that might result in much better measures of learning. The software used in this project is open source and therefore extremely cost-effective, but it lacks the sophisticated tracking ability of more expensive, proprietary software. For instance, it cannot automatically track the movements of individual fish but instead relies on measurements of the mean position for the group of fish in each frame. More advanced software may provide greater insight into the fish behaviour, leading to earlier detection of acquisition and longer retention times.

One of the largest challenges of an olfactory paradigm is the large water requirement. The present experiments were performed in a large zebrafish facility by saving the daily outflow from routine replacement of 10% of its water in a reservoir for use in these experiments. Further modification of the olfactory conditioning paradigm to recirculate more of the water would make this behavioral method even more sustainable. As discussed above, the olfactory paradigm described here uses 13-14 L of water per tank per hour; approximately 1000 L were required to train one group of fish to criterion over four days. This is a substantial improvement over the method of Braubach et al. (2009) which used 360 litres per tank per hour (thus approximately 16 000 L to train a single fish to criterion over five days) but is still a large water requirement and may restrict the number of tanks that can be used in the paradigm at any one time. The present olfactory paradigm used a flow-through system to ensure no

contamination of the main water supply; however, this precaution was extremely

conservative. The PEA added to the tanks was already diluted below threshold by the

time it was homogeneously diffused in the individual tanks. The concentration of PEA

was therefore negligible upon dilution into the entire volume of water in the whole

recirculation system. Furthermore, treating the outflow to break down or absorb the

odourant could allow reconditioned water to be recirculated into the experimental

water supply without significant odourant contamination. In addition, this experiment

only used PEA, but other odourants may prove more effective for zebrafish

conditioning. For example, amino acids as employed by Braubach et al (2009) for

olfactory conditioning could be easily used with a recirculation system because they will

degrade in any system with bio-filtration (Barker, 1981).

Apart from optimizing this olfactory paradigm for adult zebrafish, another future

goal might be to adapt it for use with juveniles. Their small size makes them ideal for

adaption to a high-throughput paradigm and, in fact, many disease models almost

exclusively use young zebrafish, so having a function paradigm for juveniles would be

beneficial (Sager et al., 2010; Nellore and Nandita, 2015; Doyle and Croll, 2022). I have

already determined that fish 49 days post-fertilisation (dpf) can successfully learn to

associate a frequency modulated auditory tone sweep with food reward in a similar

paradigm by the 10th to 13th pairing, and they can retain the association for at least two

days (Doyle et al., 2017). Merovitch (2016) showed that 30 dpf fish began to show an

association between the 8th and 10th pairing and retained the association for at least 2

days after training. It will be of interest to determine whether the olfactory paradigm can be adapted for use on such juvenile fish.

In conclusion, this paper presented a feasible olfactory-based appetitive conditioning paradigm for zebrafish which demonstrated learning after three to four days of training. The cost-effectiveness and relatively low water requirements make this set-up easily scalable for high-throughput screenings and other applications. Having an efficient olfactory learning paradigm will also facilitate investigations into the effects of olfactory disruption. This is becoming more important with the increase in environmental pollution in aquatic habitats and the detrimental effects on the ability of fish to navigate using olfactory cues. Olfactory disruption is also a symptom of some neurodegenerative diseases, like Parkinson's Disease. This paradigm would be useful to assess the effects of therapeutics in rescuing olfaction. In all, this paradigm has great potential as an easily accessible tool for evaluating the ability of fish to learn using an olfactory stimulus.

Figure 20: Diagram of behavioural apparatus for olfactory conditioning in home tanks.

Panels A and B illustrate representative positions of experimental fish before and during the presentation of conditioned stimulus, respectively. In (A), the approximate mean position of the group of fish (centroid; *) is near the center of the tank. Water flow enters via a tube on the top left of the tank and exits on the right. In (B), the centroid is in Quadrant 1 (Q1), where the odour (phenylethyl alcohol; PEA) is first dispensed via tube. A red LED indicated to the camera when the odourant was being delivered. Then, 15 seconds later, food was dispensed by the automatic feeder located above the tank. A plastic baffle keeps the food contained in Q1. In (C), a timeline of a single trial is presented. The video starts and 15 seconds of behaviour is recorded. Then, the odour is dispensed as indicated to the camera with the LED light. After 30 total seconds the video ends and then the experimental fish are fed, while control fish are fed at a later time in between trials.

(A) Baffle, H₂O, Feeder, LED, Centroid, H₂O Out

(B) Odour, H₂O, Food port, Q1, Q2, Q3, Q4, H₂O Out

(C) Video Starts — 0 s; Odour Dispensed LED On — 15 s; Video Ends, then Food Dispensed — 30 s
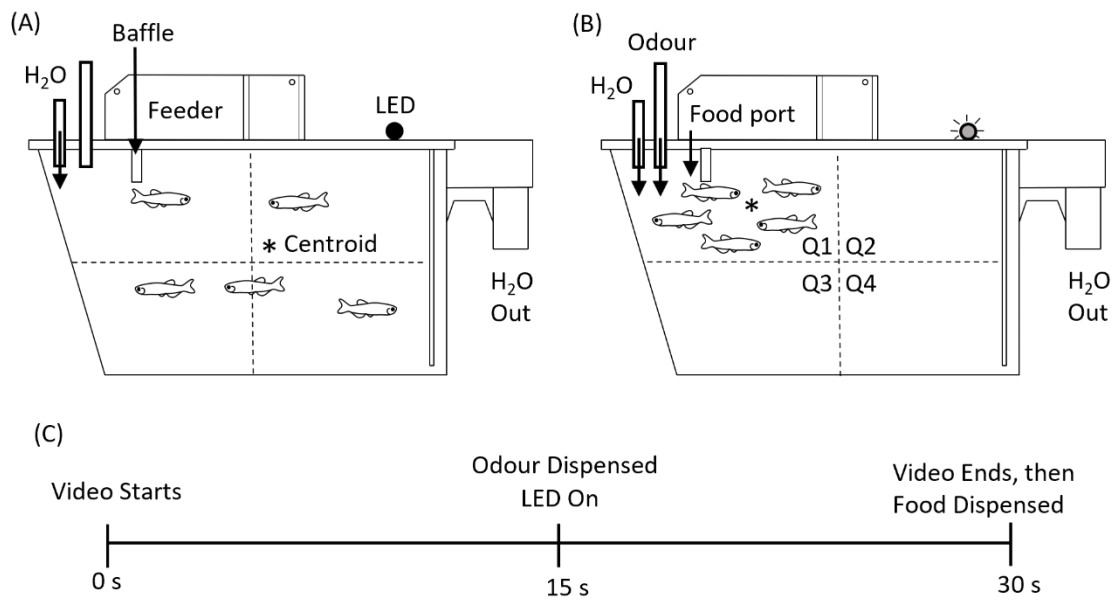
Figure 20: Diagram of behavioural apparatus for olfactory conditioning in home tanks.

Figure 21: Theoretical calculation of odourant dilution after delivery to the tank based on water flow. Assuming the solution remains well-mixed, the form of the differential equation is: $C(t) = C_i e^{(-t/T)}$

Concentration (C) as a function of time (t) is equal to initial concentration (C_i) times Euler's number (e) to the power of negative time over a time constant (T).

Known: $C_i = 1.05 * 10^{-7}$ M $V = 3$ L $Q = -14$ L/hr

Initial rate of solute loss is: $Q * C_o = -14$ L/hr $* 1.05*10^{-7}$ M $= -1.47 * 10^{-6}$ mol/hr

Such that the initial rate of change of concentration is:

$Q * C_o / V = -1.47 *10^{-6}$ mol/hr $/ 3L = -4.9*10^{-7}$ M/hr

This is equal to $C'(0)$, or dC/dt at t=0, where dC/dt may be found using calculus:

$dC/dt = -C_o/T e^{(-t/T)}$

Such that:

$C'(0) = -C_o/T = -4.9*10^{-7}$ M/hr

$T = 1.05*10^{-7} / 4.9*10^{-7}$ M/hr $= 0.2143$ hr

OR

$T = 12.86$ minutes

The equation ($C=e^{(-t/12.86)}$; c =amount odourant remaining; t=time) assumed the odourant is homogenously distributed in the tank, which occurred approximately 2 min after delivery to the tank. The odourant was reduced 90% by 30 min and 99% by 60 min.

Figure 21: Theoretical calculation of odourant dilution after delivery to the tank based on water flow.

Figure 22: Change in percentage of time spent in Q1 (before PEA compared to during PEA exposure) over 48 trials (4 days). Zero indicates no change in percentage of time spent in Q1, near the feeding area. Zebrafish in experimental and control groups initially spent more time in Q1. This response decreased until the end of Day 2 with fish spending less time in Q1 as training progressed. However, starting on Day 3, the experimental group increased time spent in Q1, near the food source, while the control group continued to decrease. By the end of Day 4, there was a significant difference between the two groups (t-test: $p<0.05$). Trials were binned in groups of six (comprising morning and afternoon sessions for each day). N=23. Error bars = ± S.E.M.
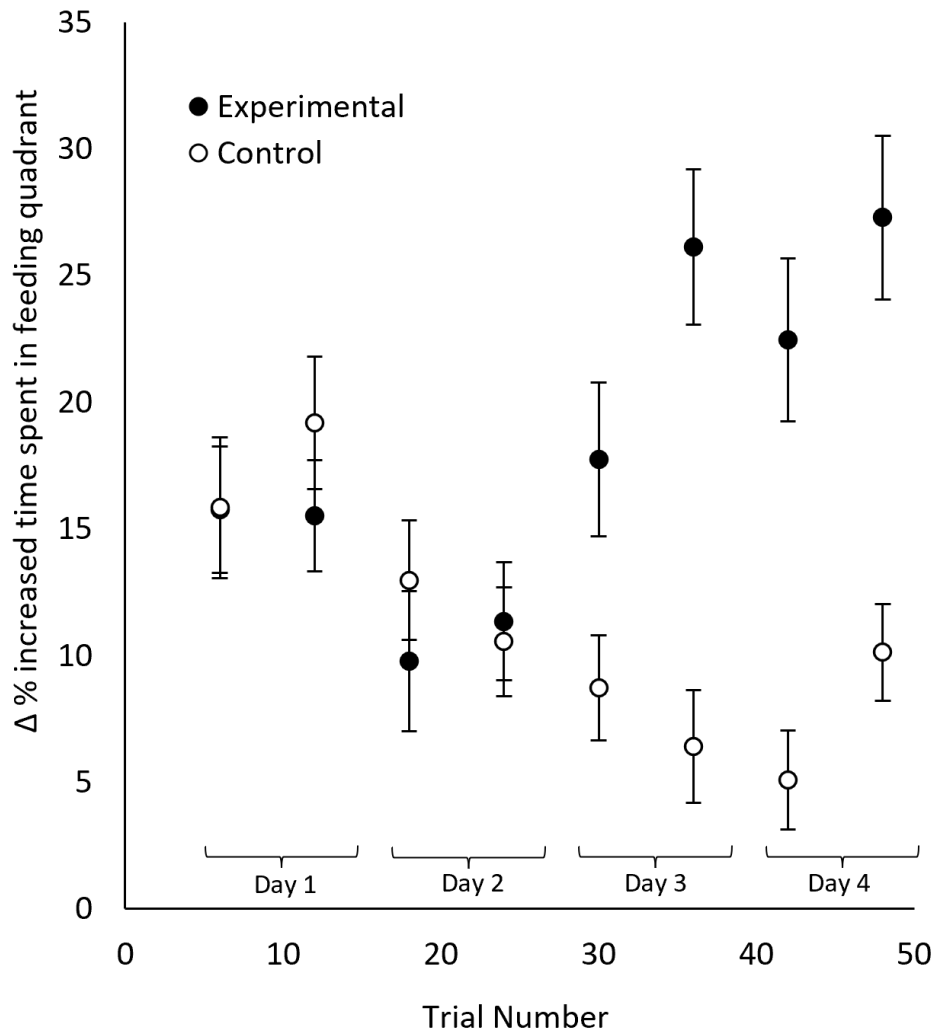
Figure 22: Change in percentage of time spent in Q1 (before PEA compared to during PEA exposure) over 48 trials (4 days).

Figure 23: Change in percentage of time spent in Q1 (before PEA compared to during PEA exposure) over 48 trials (4 days) experimental group minus control group. Zero indicates no change in percentage of time spent in Q1, near the feeding area. The first two days, the difference between the groups was near zero, however over the next two days the difference increased greatly. Trials were binned in groups of six (morning and afternoon of training days). N=23. Error bars = ± S.E.M.
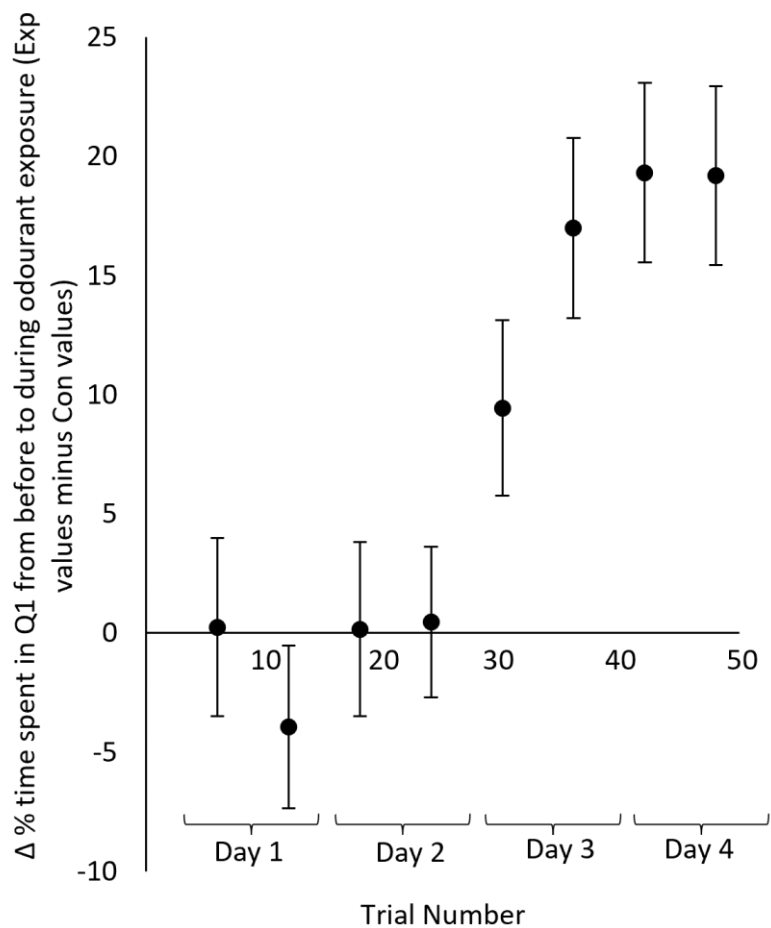
Figure 23: Change in percentage of time spent in Q1 (before PEA compared to during PEA exposure) over 48 trials (4 days) experimental group minus control group.

Figure 24: Change in percentage of time spent in each quadrant (before PEA compared to during PEA exposure) for the last six trials (binned) of training. Zero indicates no change in percentage of time spent in each quadrant. Both groups spent increased time in Q1 during PEA exposure, however the experimental group spent significantly more than the control group in Q1 (ANOVA; $p < 0.05$; Post-hoc t-test; $p < 0.05$). Time spent in most other quadrants decreased, indicating that fish spent more time in Q1 at the expense of all other quadrants. N=23. Error bars = ± S.E.M.
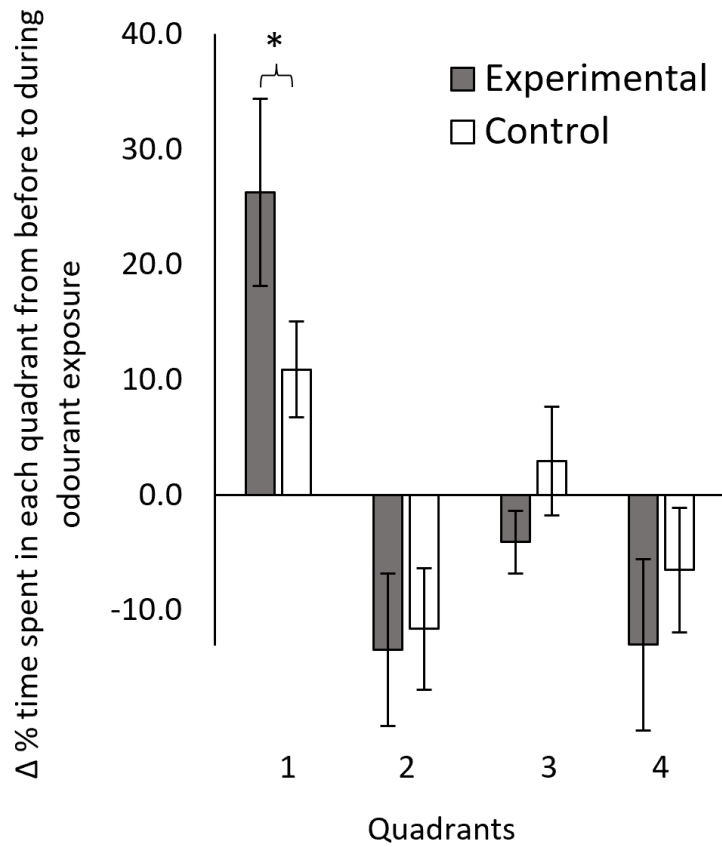
Figure 24: Change in percentage of time spent in each quadrant (before PEA compared to during PEA exposure) for the last six trials (binned) of training.

Figure 25: Movement of zebrafish groups during acquisition of an olfactory appetitive paradigm, regardless of quadrant boundaries. Zero indicates no movement from before to during PEA delivery. Initially, zebrafish in both groups showed movement towards the site of later food delivery from their initial positions when exposed to the olfactory stimulus. This response decreased until the end of Day 2. Zebrafish in the control group showed less movement towards the feeding site in response to the olfactory stimulus as training progressed. However, the experimental group showed increased movement towards the food source. Data points are mean distance from the food source before PEA delivery minus mean distance from the food source during PEA delivery. N=23. Error bars = ± S.E.M.
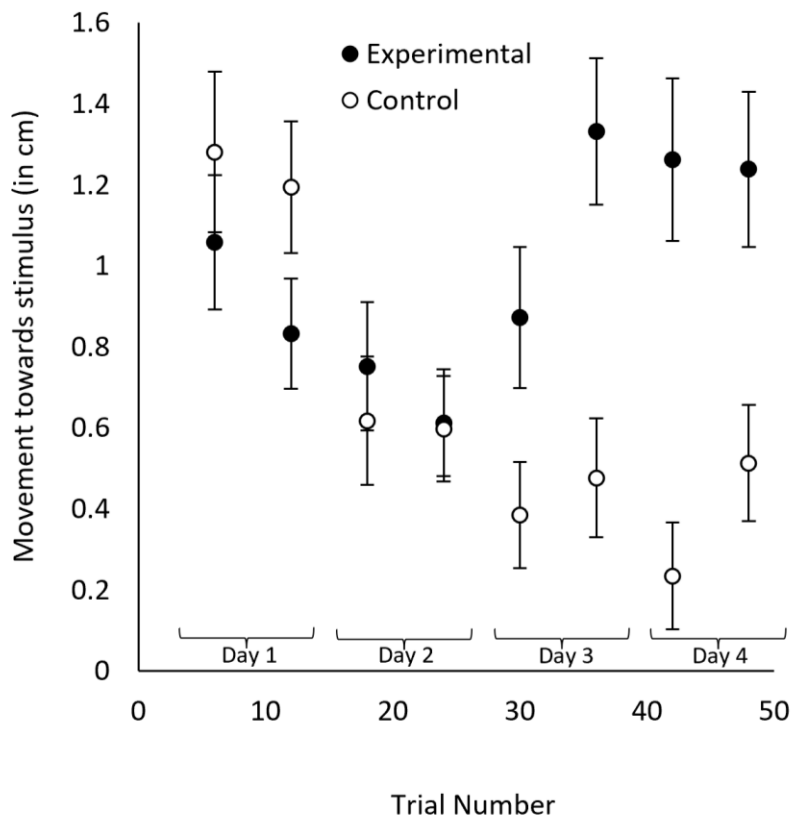
Figure 25: Movement of zebrafish groups during acquisition of an olfactory appetitive paradigm, regardless of quadrant boundaries.

Figure 26: Total distance traversed of zebrafish group (as centroid) with respect to time (speed) during acquisition of an olfactory appetitive paradigm. The centroid of the zebrafish in both groups increased speed when exposed to olfactory stimulus. This response decreased throughout until the end of Day 2. Zebrafish in the control group showed less activity as training progressed. However, the experimental group showed increased activity. Data points represent total distance travelled (by centroid) before PEA delivery minus total distance travelled during PEA delivery. N=23. Error bars = ± S.E.M.
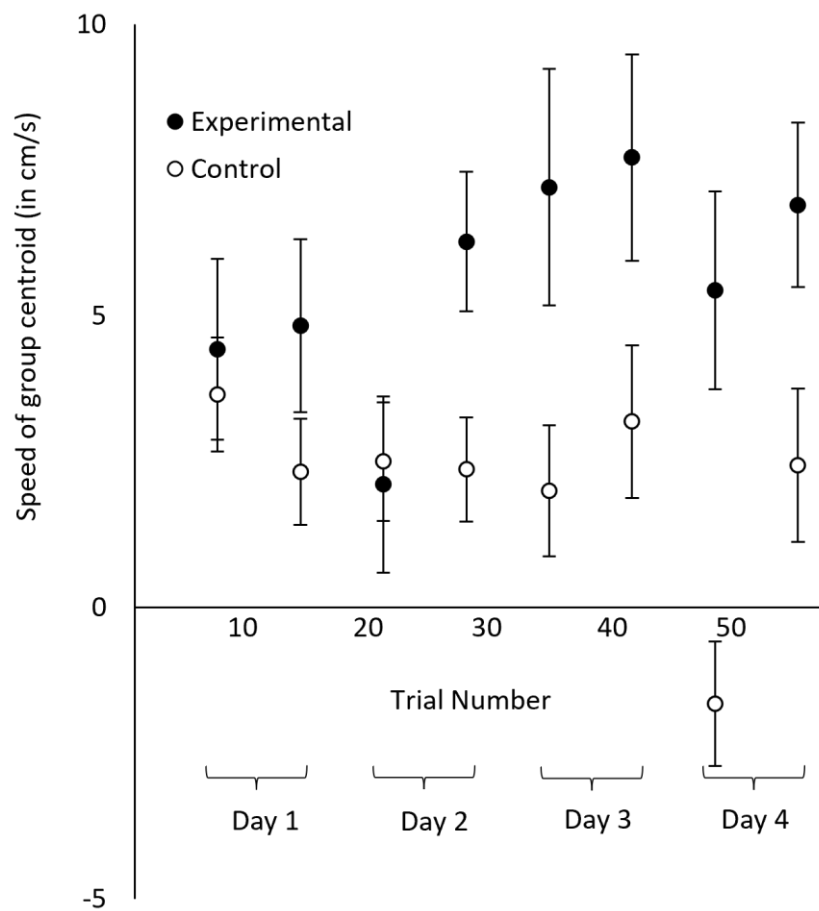
Figure 26: Total distance traversed of zebrafish group (as centroid) with respect to time (speed) during acquisition of an olfactory appetitive paradigm.

Figure 27: (A) Starvation effect on novel PEA response. Change in percentage of time spent in Q1 from (before PEA compared to during PEA exposure) of starved vs non-starved zebrafish in response to novel PEA exposure. Starved (48 hours) fish spent significantly more time in Q1 near the feeding area than non-starved fish (fed immediately before experiment; N=37). **(B) Response to water puff post-training.** Change in percentage of time spent in Q1 (before water puff compared to during water puff) for experimental and control fish. The water puff trial showed no significant response by either the control or experimental fish N=23. **(C) Memory retention seven days post-training.** Change in percentage of time spent in Q1 from (before PEA compared to during PEA exposure) for retention trial at 7 days post training. There was no significant difference between time spent in Q1 between the experimental and control groups. N=12. [Zero indicates no change in percentage of time spent in Q1, near the feeding area. Error bars = ± S.E.M.]
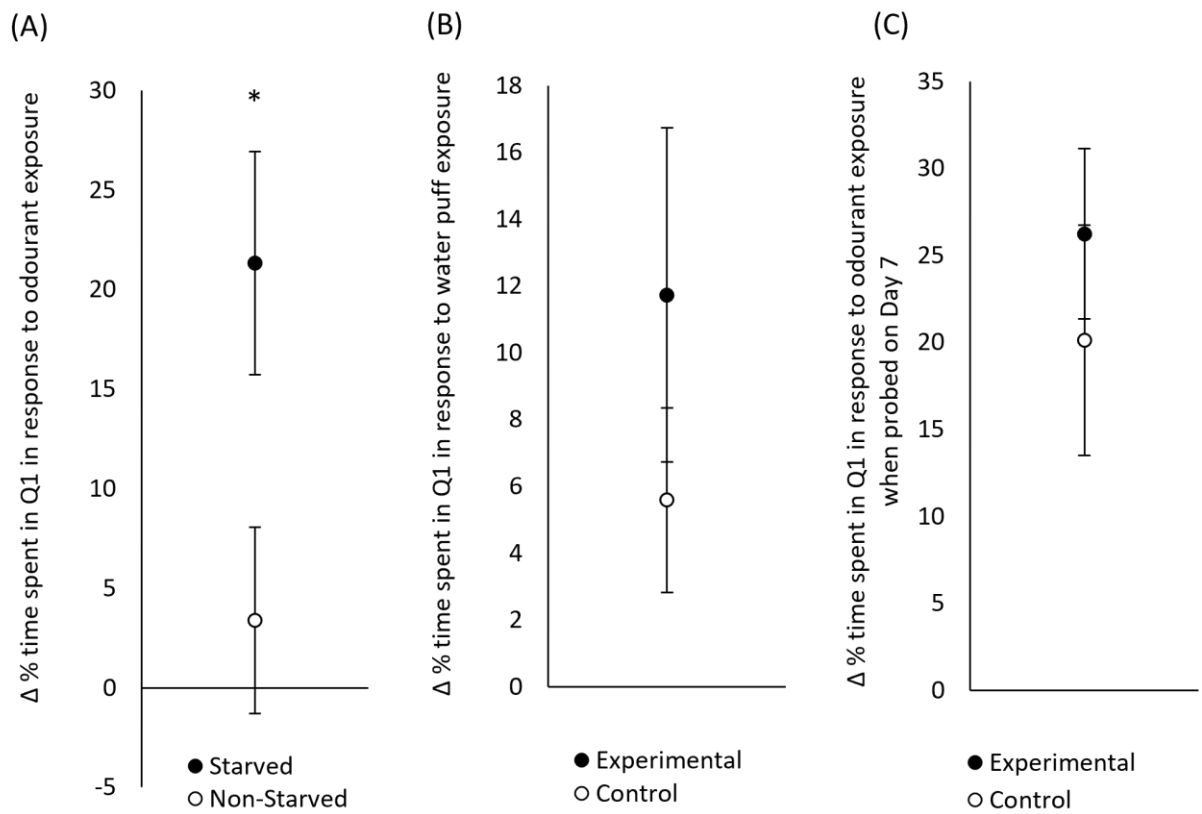
Figure 27: (A) Starvation effect on novel PEA response. (B) Response to water puff post-training. (C) Memory retention seven days post-training.

Chapter 4: Environmental Exposure Of The Olfactory System To

Manganese

4.1 Introduction

As discussed in Chapter 1, disruption of the olfactory system can be severely detrimental to the survival of animals, as most depend on it for appetitive and social behaviours. Only separated from the environment by a thin mucosal layer, olfactory sensory neurons (OSNs) and therefore the rest of the olfactory system are particularly sensitive to external pathogens and chemicals (Calderon-Garciduenas et al., 1998; Gobba, 2006). Environmental pollution results in chemical exposure to the olfactory system through various sources including air pollution from exhaust fumes and industrial manufacturing but also contamination of water and food due to run-off from farms, mining operations and other industries (Voulvoulis and Georges, 2015). Heavy metals are particularly problematic because they are almost impossible to remove from the environment and can also accumulate in both plants and animals (Wang et al., 2018a). Manganese is a prevalent pollutant due to its wide variety of industrial applications (Wu et al., 2022).

Manganese is considered an essential trace element, used as a cofactor for several enzymes and therefore indirectly involved in various processes such as bone formation, blood clotting, immune response, etc. (Takeda, 2003). While naturally found in small amounts in the brain and body, manganese can become toxic in excessive amounts (Calne et al., 1994). Chronic exposure to high amounts of manganese can occur from various sources. The most direct context is occupationally for humans, through industries that utilize manganese, like mining, welding and alloy production, to name a few (Clarke and Upson, 2017). The most reported route for exposure is via inhalation,

which incidentally causes the most serious side effects (Santamaria and Sulsky, 2010).

Several studies examining longitudinal effects in miners have presented disturbing

results. South African manganese miners exhibited chronic parkinsonian symptoms

which worsened with the length of time spent in the mine (Racette et al., 2022). Chinese

manganese miners showed general cognitive impairment and olfactory dysfunction

(Rolle-McFarland et al., 2019).

In addition to direct-contact workers, many people are exposed outside of

industrial occupations. The areas surrounding these operations often have

contamination of the soil, water and air (Chen et al., 2016). Children who were raised

near manganese mines exhibited a range of negative health effect including reduced

intellectual function, skeletal deformities and high concentrations of manganese in the

blood and hair (Riojas-Rodríguez et al., 2010; Duka et al., 2011; Bjørklund et al., 2017).

People living near (<1 km) a manganese processing plant demonstrated impaired

olfactory function, performing poorly on threshold, discrimination and identification

tasks (Guarneros et al., 2013). Contaminated groundwater can even affect communities

far away from manganese-related industries. School children raised on tap water with

elevated manganese levels showed significantly lower IQ than their counterparts

(Bouchard et al., 2011). Manganese also forms part of the compound

methylcyclopentadienyl manganese tricarbonyl (MMT), an additive in unleaded gasoline

which also contributes to environment pollution (Lynam et al., 1999). Given the serious

and wide-ranging effects of manganese exposure, it is important to investigate the

mechanisms by which it causes deficits.

The dysfunction caused by manganese exposure has been linked to the death of dopaminergic neurons in the brain, although the mechanism by which this occurs is not fully understood (Zimmermann Prado Rodrigues et al., 2019). Fish have been a common target for investigating the effects of pollutants on the olfactory system (Ward et al., 2008; Tierney et al., 2010; Olsén, 2011, 2015) and zebrafish, in particular, have become popular for toxicological research due to their widespread use as a medical model (MacDonald et al., 2016; Volz et al., 2020; Takesono et al., 2023). Many manganese-exposure studies are performed in zebrafish, usually as either a toxicity model or a Parkinson's model (Altenhofen et al., 2017; Fasano et al., 2021). Although olfaction is often not the focus of these papers, a few have addressed it briefly. Bath applications are the preferred methods of exposure as manganese is readily transported up the olfactory nerve into the olfactory bulb and then can cross synapses and migrate to other areas of the brain (Sunderman, 2001; Tjälve and Tallkvist, 2003). A 2022 study examined the general effects of manganese in zebrafish and its uses as a model of induced parkinsonism (Nadig et al., 2022). A 21-day exposure to 2.0 mM manganese caused numerous deficiencies but there was no noted decrease in tyrosine hydroxylase (TH; rate limiting enzyme in the dopamine pathway) immunoreactive cells in the fore- and mid-brain. This contradicts the findings of Z. P. Rodrigues et al., (2020) which found a decrease in these cells in the ventral telencephalon following both acute and chronic manganese exposures. Neither study examined the olfactory bulbs specifically; therefore, it is possible the majority of TH immunoreactive neurons lost were restricted to that area or not at all. More examination is needed to establish precisely how

manganese exposure affects the dopaminergic neurons in the olfactory bulb. Some

studies also examined behavioural changes in response to exposure. A chronic 30-day

exposure caused an increase in anxiogenic behaviours in an open tank test, namely more

time spent on the bottom (Zimmermann Prado Rodrigues et al., 2020). The 2022 study

also noted increased anxiety-like behaviours and reduced locomotion (Nadig et al.,

2022). Those researchers also noted a decreased preference for two amino acids, which

possibly indicates olfactory dysfunction. Further assessment is required to determine

the effect of manganese exposure on olfactory behaviour.

This chapter aims to further the investigation into the role of the dopaminergic

cells in the olfactory bulb by examining what happens when the animal is exposed to

environmental manganese. A thorough catalogue of the normal anatomy of these

neurons in the zebrafish olfactory bulb (See Chapter 2) was created and possible

functions were discussed. Then in Chapter 3, advances in methods for examining

olfactory behaviour were explored. Now, the methods from both chapters will be

employed to examine the effects of the heavy metal, manganese, on the dopaminergic

neurons in the bulb. Using similar metrics from Chapter 2, the changes in cell number,

location and distribution were noted. Differences in neurite length, direction and

whether cells innervate locally or across regions were again investigated. Although the

full learning paradigm from Chapter 3 was not employed, the experimental set-up was

used to perform odour exposures on the manganese-exposed zebrafish. This included

the video recording and analysis procedure developed for the home tanks in which these

fish were tested. It was determined that manganese negatively affects normal behaviour

towards attractive odours but perhaps not aversive ones. It is probable that the 50%

reduction in TH+ cells in the olfactory bulb was responsible for this deficit. However, it

was unclear if these results were solely due to the disruption in the TH+ cells of the bulb,

as the OSNs showed major disorder as well.

4.2 Materials & Methods

4.2.1 Animals

Adult, AB-strain zebrafish between 2.5 – 3.0 cm in length were obtained from the Zebrafish Core Facility, Faculty of Medicine, Dalhousie University, Halifax, NS, Canada. Fish were kept on a 14:10 hour light:dark cycle in treated, reverse osmosis water (28°C, pH 7.3 and salinity at 0.20 PSU). All experiments were conducted in accordance with the Canadian Council on Animal Care standards and guidelines (Dalhousie Protocol 21-117).

4.2.2 Exposure

The manganese exposure procedure largely expanded on the work of Altenhofen et al. (2017), with some modifications. Groups of five zebrafish were placed in breeding tanks (Pentair Aquatic Eco-Systems, Apopkoka, FL, USA) containing 1.5 mM of $MnCl_2$ (Sigma-Aldrich, Oakville, ON, CAN) dissolved in charcoal filtered, municipal water treated with 600 mg Instant Ocean (United Pet Group, Blacksburg, VA, USA) and 26.4 mg sodium bicarbonate (Pentair Aquatic Eco-Systems, Apopkoka, FL, USA) per litre for ten days. This was the highest dose used by Altenhofen et al. (2017). The solution was changed every 24 hours and tanks were maintained at 25.0 °C. Fish were fed daily with Golden Pearl 500 – 800 μm fish food (Brine Shrimp Direct, Ogden, UT, USA). After the ten-day exposure, the fish were moved to new tanks containing only charcoal filtered, conditioned water (but without $MnCl_2$) for 24 hours before behavioural testing and eventual sacrifice for histological examination. Control fish were treated in the same manner except only charcoal filtered water was used throughout.

4.2.3 Facility Controls

To account for any possible effects of being maintained in relatively stagnant water during drug exposures, fish taken from the university zebrafish facility were also tested. Fish were moved from their facility tank to the testing apparatus and permitted a one-hour acclimation period.

4.2.4 Behavioural Testing

After exposure to $MnCl_2$ or control procedures, fish underwent behavioural testing using the apparatus described in Chapter 3. The 3 L tank for each group of five fish was moved to one of four specialized observation arenas. Each arena contained a camera (model C930e, Logitech, Newark, CA, USA) that was centred on the long side of the tank. The side of the tank opposite the camera was backlit by an LED work light (Snap-on, Kenosha, WI, USA) to provide contrast for the video recording and facilitate tracking. White, nylon schuss fabric (Fabricville, Montreal, QC, CAN) was used to diffuse the LED backlighting and provide a uniform white background. In addition, white corrugated plastic signboard (Home Depot, Marietta, GA, USA) was used to separate each of the four testing arenas and a white curtain shielded the entire experiment from outside visual interference in the testing room. Each arena also contained an inlet providing each tank with an average flow of 13-14 L per hour and an outlet to drain facility-treated water during experimentation.

Groups of five experimental or five control fish were acclimated to the testing tanks for one hour prior to experimentation. Then, one minute of spontaneous behaviour was recorded before the administration of the odourant. After that, fish

underwent four odour exposures with a 30 min washout between each. The optimal

washout was determined using the dilution curve in Chapter 3 (Fig. 21). The first two

exposures were to 250 µL and then 500 µL of an amino acid solution known to be

attractive to zebrafish (Braubach et al., 2011). It consisted of alanine, histidine, lysine,

methionine, phenylalanine, tryptophan and valine, each at 0.0167M (Sigma-Aldrich, St.

Louis, MO, USA; for further details see Braubach et al., 2013). The last two exposures

were to cadaverine, a repulsive chemical found in decaying tissue, which elicits aversive

behaviour in fish (Hussain et al., 2013; Dieris et al., 2017; Godoy et al., 2020). The fish

were then exposed to 20 µL and 60 µL doses of a 95% cadaverine (Sigma-Aldrich, St.

Louis, MO, USA). The 60 µL dose was similar to the dose used by Godoy et al. (2020).

Due to the small size of the tank used in this study and consequently the inability of the

fish to distance themselves from the odour, both the 20 µL and 60 µL doses were mixed

in 1 mL of tank water before delivery to the tank. This method of delivery reduced the

initial startle response the fish experienced when they physically contacted the texture

of the pure cadaverine.

4.2.5 Data Collection And Analysis

The behaviour of the fish was video recorded in colour at a resolution of 1280 x

720 pixels. Surveillance software (iSpy, http://www.ispyconnect.com) permitted the

recording of time-stamped video files from cameras in all four arenas simultaneously.

Video clips were recorded at 6 frames/second for one min immediately before exposure

to the odourant and four min thereafter. The videos were analysed using a program

developed in Matlab (MathWorks, Natick, MA, USA) (Wyeth et al., 2011) but recreated in

ImageJ (National Institute of Health, Bethesda, MD, USA; https://imagej.nih.gov/ij /) as described below. Specifically, the stationary background (average of all the frames in the video) was subtracted from each individual frame, and the resultant image was then converted to a binary image (white fish on a black background). The natively installed "Analyze Particles" plug-in for ImageJ was used to establish the mean position (horizontal and vertical coordinates of the centroid) for the group of fish for each frame.

4.2.6 Dissection and Tissue Preparation

Immediately after behavioural testing, zebrafish were sacrificed by immersion in cold water (<4°C) for 10 minutes, as described in Chapter 2 (Chen et al., 2014; Wallace et al., 2018). The whole brains were removed immediately and then fixed overnight in 4% paraformaldehyde (PFA; Electron Microscopy Sciences, Hartfield, PA, USA) dissolved in phosphate-buffered saline (PBS: 100 mM Na_2HPO_4, 140 mM NaCl, pH 7.4) at 4 °C. After fixation, the brains were subjected to four 20 min washes in PBS before being placed in blocking solution (PBS-Block; 0.25% Triton X-100, 2% dimethyl sulfoxide, 1% bovine serum albumin, 1% normal donkey serum and 1% normal goat serum in PBS; ingredients from Sigma-Aldrich, St. Louis, MO, USA) for 24 hours at 4°C. The samples were again washed for four times at 20 min each before application of antibodies.

4.2.7 Immunocytochemistry

The primary antibodies used in this study are listed in Table 4. To label the tyrosine hydroxylase (TH) immunoreactive interneurons I used antibodies raised against TH, the rate-limiting enzyme in the dopamine pathway. For more details on why these antibodies were employed, see Chapter 2. To label the axons of the OSNs and their

terminals in the glomeruli, a rabbit polyclonal antibody raised against keyhole limpet

hemocyanin (KLH) was employed. The antibody has been used previously in teleosts

because it labels an unknown epitope in or on OSN axons of fish (Riddle and Oakley,

1992; Starcevic and Zielinski, 1997; Fuller et al., 2006; Gayoso et al., 2011; Braubach et

al., 2012).

Table 4: List of Primary Antibodies

Antibody	Antigen/Host	Source
Anti-keyhole-limpet-hemocyanin (KLH) (1:100 dilution)	keyhole limpet hemocyanin/rabbit	Sigma-Aldrich H0892 (St. Louis, MO, USA)
Anti-tyrosine-hydroxylase (TH) (1:200 dilution)	TH purified from rat PC12 cells LNC1 clone/ mouse	Immunostar 22941 (Hudson, WI, USA)

Brains were double labelled with anti-KLH rabbit polyclonal antibody and anti-TH

mouse monoclonal antibody, both diluted 1:200 in PBS blocking solution (Table 4).

Specimens were incubated in primary antibodies for two days at 4°C with gentle

agitation on a rocker. After incubation in the primary antibodies, the samples were

washed in PBS (4x 20 min) as described before. Samples were then placed in a solution

of secondary antibodies diluted 1:200 in PBS-Block for two days at 4 °C. Secondary

antibodies were donkey anti-rabbit and donkey anti-mouse conjugated to either Alexa

Fluor 488 or Alexa Fluor 555 (Table 5).

Table 5: List of Secondary Antibodies

Antibody	Source
Donkey anti-Rabbit IgG (H+L) Highly Cross-Adsorbed Secondary Antibody, Alexa Fluor™ 488	Invitrogen (Waltham, MA, USA)
Donkey anti-Mouse IgG (H+L) Highly Cross-Adsorbed Secondary Antibody, Alexa Fluor™ 555	Invitrogen (Waltham, MA, USA)

After incubation in antibodies, samples were again washed (4x 20 min) in PBS and then immersed in CUBIC clearing/mounting agent for 24 hours before mounting (Susaki et al., 2014, 2015). Brains were separated between the fore- and mid-brain division and mounted separately in the clearing solution dorsal side down on glass slides. Small dots of silicon grease (Dow-Corning, Midland, MI, USA) were applied to the four corners of an 18 mm x 18 mm glass coverslip before it was placed over the specimen. The coverslips were then sealed to the slide with nail polish and viewed with a confocal microscope.

4.2.8 Imaging

Specimens were viewed either with a Zeiss LSM 710 or LSM 880 laser scanning confocal microscope (Carl Zeiss, Thornwood, NY, USA). Whole olfactory bulbs were initially imaged using either a 10x or 20x objective, and the final magnification was adjusted using digital zoom until the bulb filled the field of view. Optical sections were obtained at the "optimal" intervals (0.5 µm – 3.5 µm) suggested by the acquisition software, Zen (Carl Zeiss, Thornwood, NY, USA). Higher magnification images were then obtained using 25x or 40x oil immersion lenses depending on the thickness of the sample. Image stacks were imported into ImageJ (National Institute of Health, Bethesda, MD, USA; https://imagej.nih.gov/ij/) for further analysis.

4.2.9 Analysis

Low power images were used for general cell counts and noting prominent neurites. Cell counts were performed using the "Cell Counter" function in ImageJ, which enabled the tagging of the cell bodies in each optical section while advancing through

133

the image stack and outputting the X, Y and Z coordinates of each cell. The tag was placed in the middle of each cell's nucleus and denoted it as the "centre" of the cell body. The images were converted to maximum intensity projections to provide a view of the entire olfactory bulb, enabling division into anterior medial, anterior lateral, posterior medial and posterior lateral quadrants. X and Y coordinates bounding each of the quadrants were recorded in an Excel spreadsheet containing a macro that sorted all the cell locations coordinates into the appropriate quadrants.

The higher power images were then examined to determine the number of neurites per bulb and the location of the cell body. The "Simple Neurite Tracer" plug-in in ImageJ then allowed the tracing of cell neurites and yielded the starting and ending coordinates of each path. Due to the density of cells, only clearly visible neurites that exited the cell body in a narrow tapering of the soma were traced, as not to be confused with neurites running beneath cells. Using these data, I catalogued the number of neurites per cell and whether visible branching occurred. Neurite coordinates were logged into another spreadsheet, which determined the quadrant that each of the neurites started and ended within, therefore providing information on where the cells were projecting.

Statistical analyses of all these measures were performed as described. A one-way ANOVA was used to compare the mean baseline positions, with post-hoc pairwise comparisons using a Bonferroni correction in SPSS 28 (IBM, Armonk, NY, USA). For the odour exposures a two-way mixed ANOVA with repeated measures was employed along with post-hoc pairwise comparisons using a Bonferroni correction. A two-way ANOVA

was performed for the neurite analysis. Simple comparisons of two means were

analysed using a Student's t-test.

4.3 Results

4.3.1 Baseline Behaviour

During the experimentation, it was observed that both the manganese-exposed (Mn) and exposure-control fish appeared to demonstrate reduced movement and startle responses. It was hypothesized that the exposure conditions of keeping fish in small volumes of stagnant water according to (Altenhofen et al. (2017) alone may have influenced the zebrafish behaviour. To investigate the possible confounding variables of the exposure process, fish directly from the zebrafish facility, which were referred to as "facility-controls", were also tested. The baseline behaviour of all groups was, therefore, first evaluated in the behavioural apparatus. The experimental and both control groups maintained similar group mean horizontal (X) positions near the middle of the tank (ANOVA, $p > 0.05$; Fig. 28A), however there was a significant difference between the average mean vertical (Y) position of the three groups (ANOVA, $p < 0.05$; Fig. 28B). Further analysis showed that while the Mn-exposed and exposure-controls were not significantly different from each other (Pairwise; $p > 0.05$), they were both significantly lower in the tank than the facility-controls (Post-hoc t-test; both $p < 0.05$), which is typically a sign of stress possibly due to the exposure process (Cachat et al., 2010). The facility-controls maintained a baseline Y position near the middle of the tank, which was consistent with typical zebrafish behaviour when sufficiently acclimated to a tank (See Chapter 3; Blaser & Rosemberg, 2012; Doyle et al., 2017).

4.3.2 Responses To Amino Acids

When the horizontal responses of fish to amino acids were examined, there was a significant effect of condition (ANOVA; $p < 0.05$) but no effect of dose or interaction effect between the two measures (ANOVAs; $p > 0.05$). When presented with the low dose of amino acids, the facility-controls showed movement (2.56 cm) towards the odour on the left side of the tank (Fig. 29A), and this movement was even larger (3.09 cm) with the higher dose. As mentioned in Chapter 2, fish tend to move toward the area where the attractive stimulus is presented (left side). Exposure-controls showed a similar but slightly diminished horizontal response moving only 1.04 cm and 2.10 cm towards the odour with the low and high dose, respectively. In contrast to the positive responses of both control groups, the Mn-exposed fish showed almost no leftward movement (0.03 cm) and that measurement showed almost no increase (0.50 cm) when the dose was increased. At the higher dose, the Mn-exposed fish were significantly lower than the facility-controls (Post-hoc t-test; $p < 0.05$).

When vertical movement was examined (Fig. 29B), there was no effect of condition, dose, or any interaction between the two (ANOVAs; $p > 0.05$). The facility-controls showed no net movement in either direction (0.23 cm), remaining unchanged with the increase in dosage concentration (0.06 cm). The fish did not move towards the surface but instead had an average position in the center of the tank; however, the standard error of this mean was quite high, which may have indicated an increase in activity. The exposure-controls were similar to the facility-controls, showing little movement with both the low (0.19 cm) and high (0.60 cm) doses. With the low dose, the

Mn-exposed fish moved towards the bottom of the tank (1.19 cm), away from the attractive stimulus, which had been expected to elicit appetitive responses in these surface feeding fish. When the dosage of amino acid mixture was increased, the Mn-exposed fish showed an even larger movement (1.98 cm) towards the bottom of the tank away from the stimulus. In summary, in response to amino acid exposure, the Mn-treated fish showed severely reduced horizontal responses when compared with the controls and demonstrated inappropriate vertical responses by dropping to the bottom of the tank, which was opposite of the expected behaviour.

4.3.3 Responses To Cadaverine

Exposure to the aversive odour cadaverine produced conflicting results. With respect to the horizontal movement, there was no effect of condition, dose, or any interaction between the two (Fig. 30A; ANOVAs; $p > 0.05$). The facility controls showed slight movement (0.91 cm) towards the left when exposed to the low dose of cadaverine with a large standard of error and increasing the dosage caused the facility controls to move to the right, away from the odour (0.58 cm). Like the facility-controls, the low dose exposure-controls showed movement towards the left side of the tank (1.69 cm), but when the dosage increased the left movement decreased (0.98 cm). When the experimental fish were exposed to low dose cadaverine, they showed no net horizontal movement in either direction (0.21 cm) and when the dosage was increased, there was still no net horizontal movement (0.37 cm); however, standard error increased which may have indicated increased activity.

In terms of vertical movement (Fig. 30B), there was a significant effect of condition, dose and a significant interaction effect between condition and dose (ANOVAs; p<0.05). The facility-controls showed movement towards the bottom of the tank (2.44 cm) when exposed to the low dose, and this increased with the dose (3.93 cm). Like the facility-controls, the exposure-controls moved towards the bottom of the tank when exposed to the low dose (2.83 cm), but the movement decreased significantly when the dose increased (0.91 cm; Post-hoc t-test; p<0.05). This unusual effect may have been due to freezing behaviour or because this group was already near the bottom of the tank and could sink no further. The Mn-treated fish also showed movement towards the bottom of the tank with the low dose (1.97 cm) and like the exposure-controls exhibited a reduced response with the increased dose (1.38 cm). At the higher dose, the facility-controls demonstrated significantly more downward movement in the tank than the exposure-controls (Post-hoc t-test; p<0.05) and the Mn-exposed fish (Post-hoc t-test; p<0.05). In general, all groups showed movement towards the bottom of the tank, and this reaction was consistent with a known stress response in zebrafish; sinking in the water column (Cachat et al., 2010). In conclusion, all groups exhibited conflicting horizontal movement, but Mn-treated fish showed an appropriate, but blunted, vertical response to cadaverine.

4.3.4 Tyrosine Hydroxylase

For the immunohistochemistry results, only the exposure-controls were reported here as there were no detectable differences in the images, cell counts or neurite analysis when compared to the adult fish from Chapter 2. Exposure-controls possessed 1019 ±93.5 cells compared to adult fish in Chapter 2 that had 913 ±14. Neurite length

was also very similar, 64.4 ±2.58 μm (exposure-controls) compared to 67.0 ±1.49 μm (adult fish).

The anti-TH stained the brains from Mn-treated fish without issue and the bulb morphology initially appeared normal but upon closer examination, a large reduction in the number of TH+ cells was noted (Fig. 31A). The Mn-treated olfactory bulbs showed an all-over depletion of TH+ cells not specific to one area of the bulb, while exposure-control fish exhibited normal bulb anatomy with TH+ cells in abundance (Fig. 31B). In a higher magnification image, the lower density of TH+ cells was evident in the Mn-treated olfactory bulbs (Fig. 31C). Cells were clearer and less crowded, therefore making them easier to quantify. In contrast, the control bulb had more numerous, densely packed cells (Fig. 31D). When quantified, a significant 50% decrease from 1020 cells to 552 cells was observed between the exposure-control bulbs and the Mn bulbs (Fig. 32A; t-test; $p<0.05$). The depletion seemed to be evenly distributed between the four quadrants: anterior lateral (AL), anterior medial (AM), posterior lateral (PL) and posterior medial (PM); however, post-hoc analysis revealed significant differences in the AM and PL quadrants (Post-hoc t-test; $p<0.05$) (Fig. 32B). Further analysis showed a significant decrease in the length of neurites in the anterior and posterior region (Fig. 32C; ANOVA; $p<0.05$) between the experimental and controls; however, there were no differences between the anterior and posterior regions themselves (ANOVA; $p>0.05$). There were similar differences with the lateral and medial regions as well, a significant effect of condition (Fig. 32D; ANOVA; $p<0.05$) but no difference between lateral and medial specifically (ANOVA; $p>0.05$). To summarise, there was a general overall decrease of

neurite length, not specific to a region. As discussed in the introduction, Mn is readily

transported up the olfactory nerve to the nose, thus it is possible the behavioural

changes in the fish, including locomotor deficits, could be caused by the depletion of

TH+ cells further back in the brain. Therefore, a population of TH+ cells in the posterior

forebrain was characterized to determine if the long-term exposure affected other brain

regions. When compared to the exposure-control brains (Fig. 33A), these TH+ cells in

Mn-exposure brains appeared unaffected (Fig. 33B). After quantification, there was no

statistical difference between the number of cells in the posterior population in the

control and experimental conditions (Fig. 33C; t-test; $p<0.05$).

4.3.5 Keyhole Limpet Hemocyanin

Exposure-control brains stained with anti-KLH displayed normal staining with all

regions clearly visible, innervation with smooth bundled OSNs and properly formed

glomeruli (Fig.34A; See Chapter 2 for detailed description of normal anatomy). Axons of

OSNs were bundled and smooth, curving from the olfactory nerve around the outside of

the olfactory bulb before separating and ending in glomeruli (Fig. 34A$_I$). Glomeruli were

well defined and round; and the synapses of the OSNs were visible within (Fig. 34A$_{II}$). All

eight of the bulbs exhibited normal anatomy. Conversely, the brains of the Mn-exposed

fish showed major disruptions in OSN organization. An earlier short-term (four-day) Mn-

exposure showed moderate defasciculation of the OSN axons and disruption of the

glomeruli in the bulb (Fig. 34B). In general, the axons of the OSNs were no longer

smooth and bundled (Fig. 34B$_I$). Instead, most axons were unbundled, or the bundles

gave the impression of being wavy and frayed. Glomeruli, when present, were no longer

round, with most of the fine nerve endings of the OSNs not visible, giving a sparse appearance (Fig. 34B$_{II}$). It was difficult to determine at this stage whether the number of OSN axons decreased. Contradictorily, they appeared more numerous at this stage, probably due to the unbundling. Some of the samples possessed normal bundling near the olfactory nerve, but this was only observed in two of the six bulbs. In fish exposed to Mn for ten-days, the OSN axons from the nares were largely missing and poorly stained. Fluorescence was dim and glomeruli were largely absent, therefore identifying particular ones was not possible (Fig. 34C). It appeared that degradation of the OSNs increased with exposure. At this stage, there were almost no discernable OSN axons, and any that were present showed major disorganization (Fig. 34C$_I$). Most bulbs possessed no discernable glomeruli; instead, there were often sporadic bright blebs that may indicate the remnants of glomeruli. In fact, only one of eight bulbs possessed anything resembling a glomerulus, and it was misshapen and unidentifiable (Fig. 34C$_{II}$). Some bulbs had limited staining around the olfactory nerve but no traceable OSNs or recognizable glomeruli (Fig. 35A-D). Instead, they possessed the aforementioned small blebs of bright staining which may have indicated the former location of glomeruli. In some bulbs, these blebs were larger and brighter (Fig. 35E), and in one bulb gave the appearance of a misshapen glomeruli (Fig. 35F). Few bulbs showed defasciculated OSNs which were mostly very faint (Fig. 35E); however, one bulb was much brighter (Fig. 35F).

4.4 Discussion

4.4.1 Behaviour

Amino acids have been used extensively as an attractive odourant for zebrafish in novel exposure tests and learning paradigms, and it has been noted that fish exposed to amino acids generally move towards the odour while exhibiting appetitive behaviour (Friedrich and Korsching, 1998; Lindsay and Vogt, 2004; Li et al., 2007; Braubach et al., 2013). Therefore, it was expected that a normal, unaffected fish would move towards the top left-hand corner of the tank where an amino acid mixture was being delivered and where food was normally presented. One unique characteristic of this experiment was that it occurs in a standard 3 L facility-style tank for the dual purposes of convenience and stress reduction through decreased handling. Because most other learning paradigms occur in larger, often custom tanks, it was reasonable to infer that behaviour towards to odourants would differ slightly from other studies. Therefore, as a new paradigm, both horizontal and vertical measures were examined for each odourant. Both the exposure- and facility- control groups moved laterally towards the amino acids but showed no net movement in the vertical direction, possibly because they were continuously moving in the vertical plane of the tank, averaging in the middle. The manganese (Mn)-exposed fish, on the other hand, showed no lateral movement and moved inappropriately to the bottom of the tank, away from the amino acid mixture. This reaction became stronger when the odourant concentration was increased. Therefore, it was possible that the either the zebrafish were incorrectly identifying the odour as an alarming substance and exhibiting a stress response or that the addition of

any odour would cause a stress response. There is some conflicting evidence on the effects of Mn exposure on anxiety-like behaviour in zebrafish. A chronic 30-day exposure to Mn found that fish spent a larger amount of time in the bottom of the tank, a known anxiogenic behaviour (Zimmermann Prado Rodrigues et al., 2020). However, a four-day Mn exposure noted significant time spent at the top of the tank, which was not indicative of stress (Altenhofen et al., 2017). These contradictions may be due to the differences in concentration and exposure time. The fish in this experiment exhibited more anxiogenic behaviours, spending most of the time near the bottom of the tank (See Fig. 28).

The second odourant used in this experiment, cadaverine, is associated with the putrefaction of animal tissue and known to cause stress response in many animals, including zebrafish (Hussain et al., 2013). When cadaverine was introduced to one end of a tank in a previous study, fish spent more time in the opposite end of the tank (Hussain et al., 2013). Therefore, the fish would be expected to move to the right and down to the bottom of the tank, away from the stressful odour of dead conspecifics. All groups showed movement towards the bottom with exposure to the lower dose of cadaverine, and with the higher dose, the facility controls showed the most movement. The reduced movement of the other two groups was probably due to the initial starting position of these groups. In Figure 28, the Mn and control groups started the 60 µL exposure at a lower position in the tank than the facility controls. Once accounting for the movement downwards during the trial, the fish were at the very bottom of the tank. In contrast, the facility controls started in the middle of the tank and therefore could

travel further down. The horizontal movement of all groups was inconsistent, with large

standard errors. This possibly indicated that the fish are moving erratically at the bottom

of the tank and therefore measuring horizontal measurement may not be a good

indicator for behaviours associated with cadaverine. Most other experiments that

exposed zebrafish to cadaverine were performed in much larger tanks with stagnant

water (Hussain et al., 2013; Godoy et al., 2020). Fish in those experiments could

successfully move away from the odour, while fish in this apparatus would be constantly

immersed in the odour given the small size of the tank and the inflow of water. This may

have contributed to the incongruities in the horizontal movement.

To summarize, the Mn-exposed fish had diminished and inappropriate responses

to amino acids and blunted responses to cadaverine. However, it was difficult to

determine the extent to which the reactions were caused by reduced olfactory

capabilities or due to increased stress caused by the exposure. In addition, given the

smaller sample size in the behavioural experiments (N=10 per group) some of the

behavioural measures did not quite meet significance and may prove significant with a

few more repetitions.

4.4.2 Anatomy

As expected, the Mn-exposure caused a significant reduction of the TH+ cells in

the bulb. Earlier Mn exposure studies either did not examine the olfactory bulb at all or

measured general brain TH levels through western blot. In this experiment, the

reduction of the number of neurons and neurites was relatively equal throughout the

bulb. This would support the idea that Mn the 10-day exposure time was sufficient to

affect the whole olfactory bulb consistently. It was important to confirm that the

behavioural anomalies were not caused by other affected brain regions. Given the

unaffected forebrain population of TH+ cells, this indicated that the Mn preferentially

affected the olfactory bulb and did not have time to deplete TH+ in the posterior

forebrain.

Another interesting development was the disruption of the OSNs of the bulb.

This demonstrated that Mn was also affecting other olfactory cell types in the bulb. The

loss of OSNs was likely a contributing factor to the reduced olfactory behaviour. Given

the apparent near absence of glomeruli, it would be conservative to assume that the fish

would have extreme difficulty processing odours, particularly discriminating between an

attractive odour or a repulsive one. While other Mn exposure experiments in zebrafish

typically did not examine the effects on OSNs, there was research available on other

heavy metals. Environmental exposure to copper caused significant damage to OSNs in

the zebrafish olfactory bulb (Ma et al., 2018). Retraction or loss of axons was noted, in

addition to loss of fluorescent signal intensity. Other studies that examined the effects of

heavy metals on the origin of the OSNs in the olfactory rosette noted substantial

reduction in the number of OSNs (Blechinger et al., 2007; Calvo-Ochoa and Byrd-Jacobs,

2019; Lazzari et al., 2019). How then do the Mn-exposed zebrafish still respond to

odours at all? In the case of the amino acids, gustation may have played a role, as

zebrafish are capable of tasting amino acids (Kotrschal, 2000; Yasuoka and Abe, 2009).

Although Braubach et al., (2009) found that fish rendered anosmic by blocking the nares

demonstrated no appetitive swimming behaviour when exposed to L-alanine and L-

valine, both of which are present in at the same concentration in the amino acid mixture used in this study. Another consideration was the anti-KLH staining itself. The antibody has been used previously in teleosts because it labels an unknown epitope in or on OSN axons of fish (Riddle and Oakley, 1992; Starcevic and Zielinski, 1997; Fuller et al., 2006; Gayoso et al., 2011; Braubach et al., 2012). It was unclear if Mn interfered with the staining of the epitope during a long term exposure. Fish that were subjected to four days of manganese exposure and anti-KLH staining had OSNs that displayed normal fluorescence despite clear degradation. This contrasts with OSNs of fish exposed for ten days, which did not display normal fluorescence. Therefore, even with the almost non-existent staining, enough of the OSNs may still be present to have some olfactory response. However, it was not possible to determine if the deficits in behaviour were due specifically to the loss of TH+ cells or a general degradation of the bulb and OSNs as a result of the prolonged Mn exposure.

In summary, a ten-day Mn exposure did not appear to cause complete anosmia in zebrafish but caused anxiogenic behaviour and reduced the ability of the fish to appropriately respond to both attractive and repulsive odour. The bulb showed depletion in the TH+ cells and disruption of normal OSN morphology. It was to what extent the behavioural responses were caused by TH depletion or due to total disruption of the bulb by Mn.

Figure 28: Average horizontal and vertical position of groups of 10-day MnCl$_2$-treated fish before administration of an amino acid mixture or cadaverine. (A) All groups began each trial roughly in the same position and were not statistically significant from each other (ANOVA; p>0.05). Zero indicates the origin of the odour (left side of the tank) and 21.0cm is the far-right side of the tank. (N=10. Error bars = ± S.E.M.) (B) The MnCl$_2$-treated fish and the exposure controls began each trial near the bottom of the tank, while the facility controls maintained an average position in the middle of the tank and was significantly difference from the other two groups (denoted with *; ANOVA; p<0.05). Zero indicates the bottom of the tank and 13.0 cm is the top of the tank (water's surface). (N=10. Error bars = ± S.E.M.)
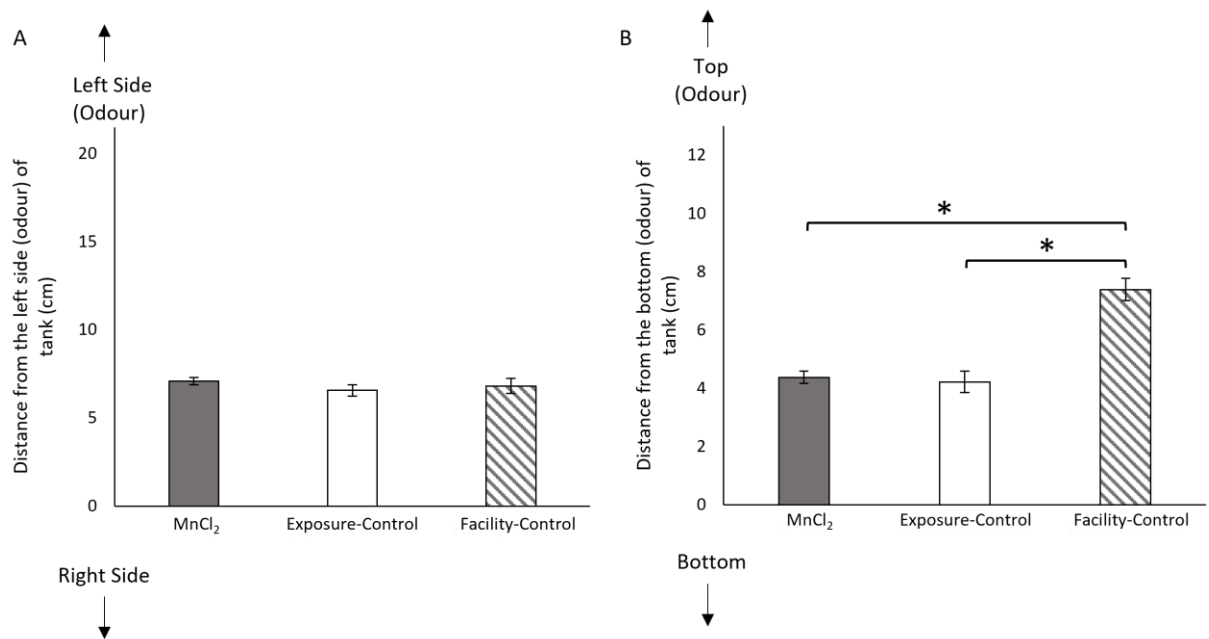
Figure 28: Average horizontal and vertical position of groups of MnCl₂-treated fish before administration of an amino acid mixture or cadaverine.

Figure 29: Horizontal and vertical movement of 10-day MnCl$_2$-treated zebrafish in response to two different concentrations of amino acid mixture. (A) Positive values indicate horizontal movement towards the left side of the tank where the odour was introduced. MnCl$_2$-treated fish showed no response to the low dose amino acid mixture, while the exposure and facility controls exhibited mild and moderate movement towards the left (odour), respectively. Both controls increased their movement in response to the higher concentration of amino acid. The MnCl$_2$-treated fish displayed a very small movement towards the left when the amino acids concentration was increased. There was a significant effect of condition (ANOVA; $p<0.05$) and at the higher dose the MnCl$_2$-treated group was significantly lower than the facility-controls (Post-hoc t-test; $p<0.05$). Data points are mean horizontal distance from the odour source (left) before amino acid delivery minus mean distance from the odour source during amino acid delivery. (B) Positive values indicate vertical movement towards the top of the tank where the odour was introduced. There was no significant effect of condition or dose (ANOVA; $p>0.05$). Both control groups did not show net movement in either direction in response to the lower or higher concentration of amino acids. The MnCl$_2$-treated fish moved away from the odour towards the bottom of the tank and this response increased with the higher concentration of amino acids. Data points are mean vertical distance from the odour source (top) before amino acid delivery minus mean distance from the odour source during amino acid delivery. (N=10. Error bars = ± S.E.M.)
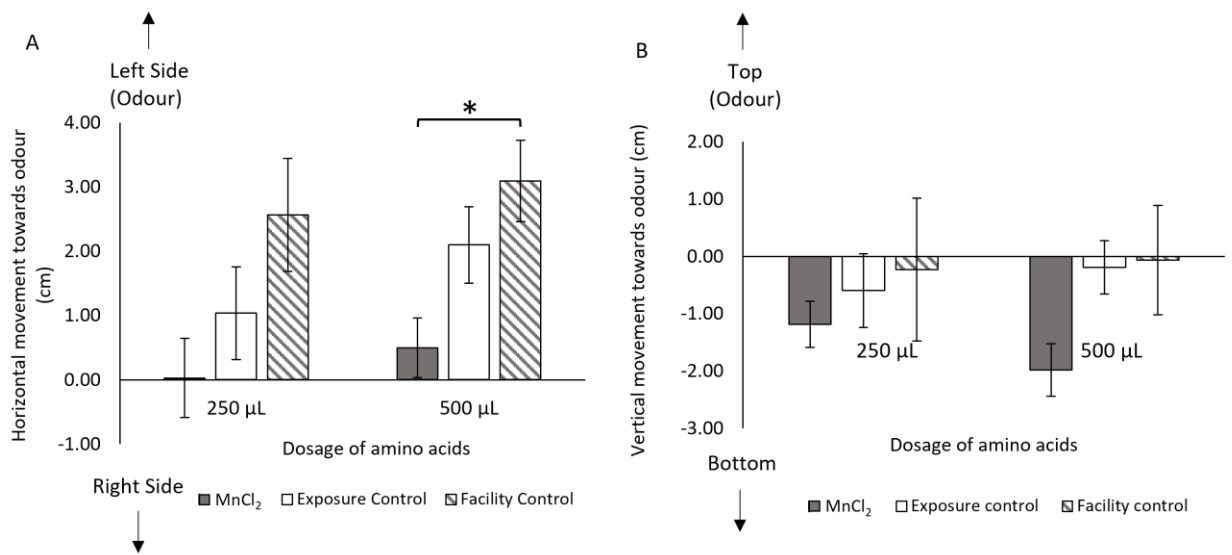
Figure 29: Horizontal and vertical movement of 10-day MnCl₂-treated zebrafish in response to two different concentrations of amino acid mixture.

Figure 30: Horizontal and vertical movement of 10-day MnCl2-treated zebrafish in response to two different concentrations of the aversive odour, cadaverine. (A) Positive values indicate horizontal movement towards the left side of the tank where the odour was introduced. There was no effect of condition, dose, or any interaction between the two (ANOVAs; p>0.05). In response to the lower cadaverine dose, the MnCl$_2$-treated fish and facility controls exhibited no net movement in either direction while the exposure controls moved towards the left side of the tank. When the concentration increased, the MnCl$_2$-treated fish displayed no net movement, while the exposure controls and facility controls moved left and right, respectively. Data points are mean horizontal distance from the odour source (left) before cadaverine delivery minus mean distance from the odour source during cadaverine delivery. (B) Positive values indicate vertical movement towards the top of the tank where the odour was introduced. There was a significant effect of condition and a significant interaction effect between condition and dose (ANOVA; p<0.05). All groups demonstrated similar movement towards the bottom of the tank in response to the lower dose of cadaverine. When the dose increased, the facility fish showed increased movement towards the bottom of the tank. The MnCl$_2$-treated and exposure control fish showed decreased movement and were significantly different from the facility-controls (Post-hoc t-test; p<0.05, *), however, given their lower vertical starting position in the tank, they were at the lowest possible position in the tank. Data points are mean vertical distance from the odour source (top) before cadaverine delivery minus mean distance from the odour source during cadaverine delivery. N=10. Error bars = ± S.E.M
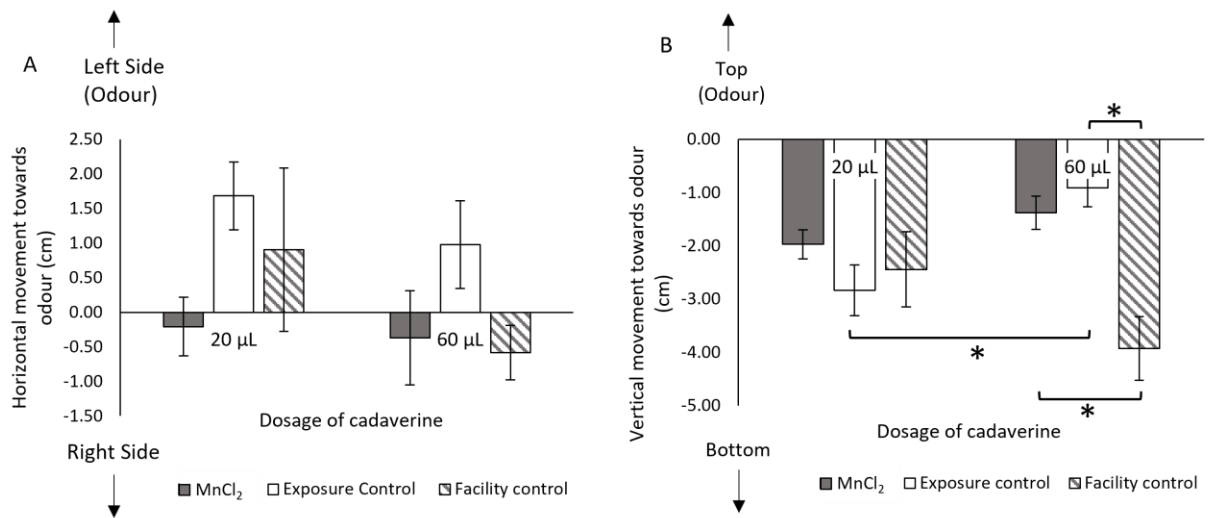
Figure 30: Horizontal and vertical movement of 10-day MnCl2-treated zebrafish in response to two different concentrations of the aversive odour, cadaverine.

Figure 31: Anti-tyrosine hydroxylase (TH) staining of 10-day MnCl$_2$-treated zebrafish olfactory bulbs. (A) The MnCl$_2$-treated olfactory bulbs showed an all-over depletion of TH+ cells not specific to one area of the bulb. (B) Exposure control fish exhibited normal bulb anatomy with TH+ cells in abundance. (C) In a higher magnification image, the lower density of TH+ cells was evident in the MnCl$_2$-treated olfactory bulbs. (D) In contrast, the control bulb had more numerous, densely packed cells.
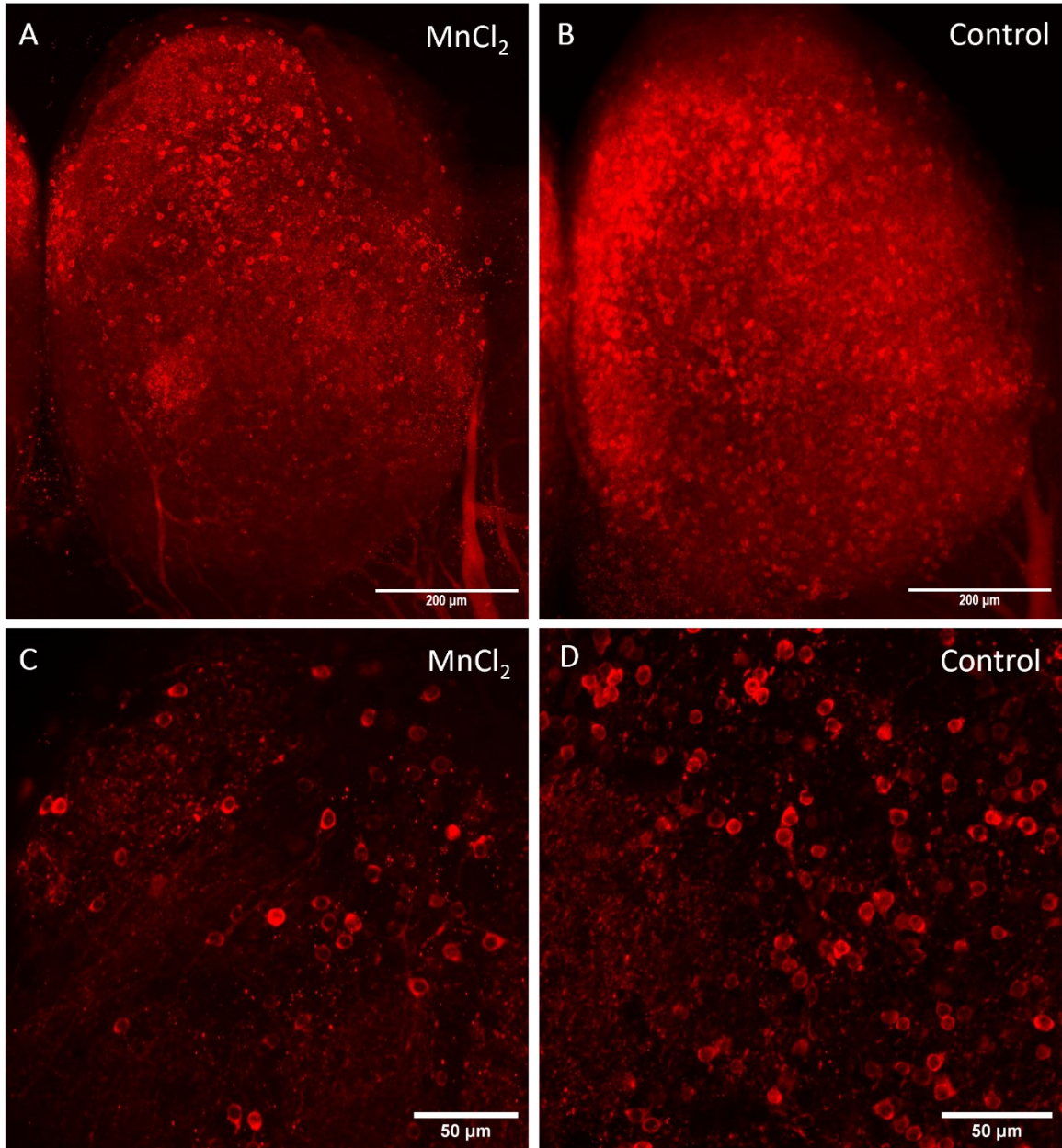
Figure 31: Anti-tyrosine hydroxylase (TH) staining of 10-day MnCl₂-treated zebrafish olfactory bulbs.

Figure 32: Quantification of TH+ cells and neurites in the olfactory bulb (OB) of 10-day MnCl₂-treated versus control zebrafish. (A) MnCl₂-treated OBs had significantly fewer cells than the exposure controls (ANOVA; $p < 0.05$), dropping from 1020 cells to 552 (approx. 50%). (B) The TH+ cells were depleted in all four quadrants: Anterior Lateral (AL), Anterior Medial (AM), Posterior Lateral (PL) and Posterior Medial (PM). There was a significant difference between the MnCl₂-treated fish and the exposure-controls (ANOVA; $p < 0.05$), with a significant decrease noted in the AM and PL quadrants. (C) When the neurites were analysed, there was a significant difference between the neurite lengths in the anterior and posterior regions of the MnCl₂-treated fish and the exposure-controls (ANOVA; $p < 0.05$). Neurite lengths decreased evenly throughout the bulb as there was no difference between the anterior and posterior regions within each condition (ANOVA; $p > 0.05$). (D) There were similar results between the lateral and medial regions. There was a significant difference between the neurite lengths of the MnCl2-treated fish and the exposure-controls (ANOVA; $p < 0.05$), but no difference between the lateral and medial regions within each condition (ANOVA; $p > 0.05$). [N=10. Error bars = ± S.E.M.]
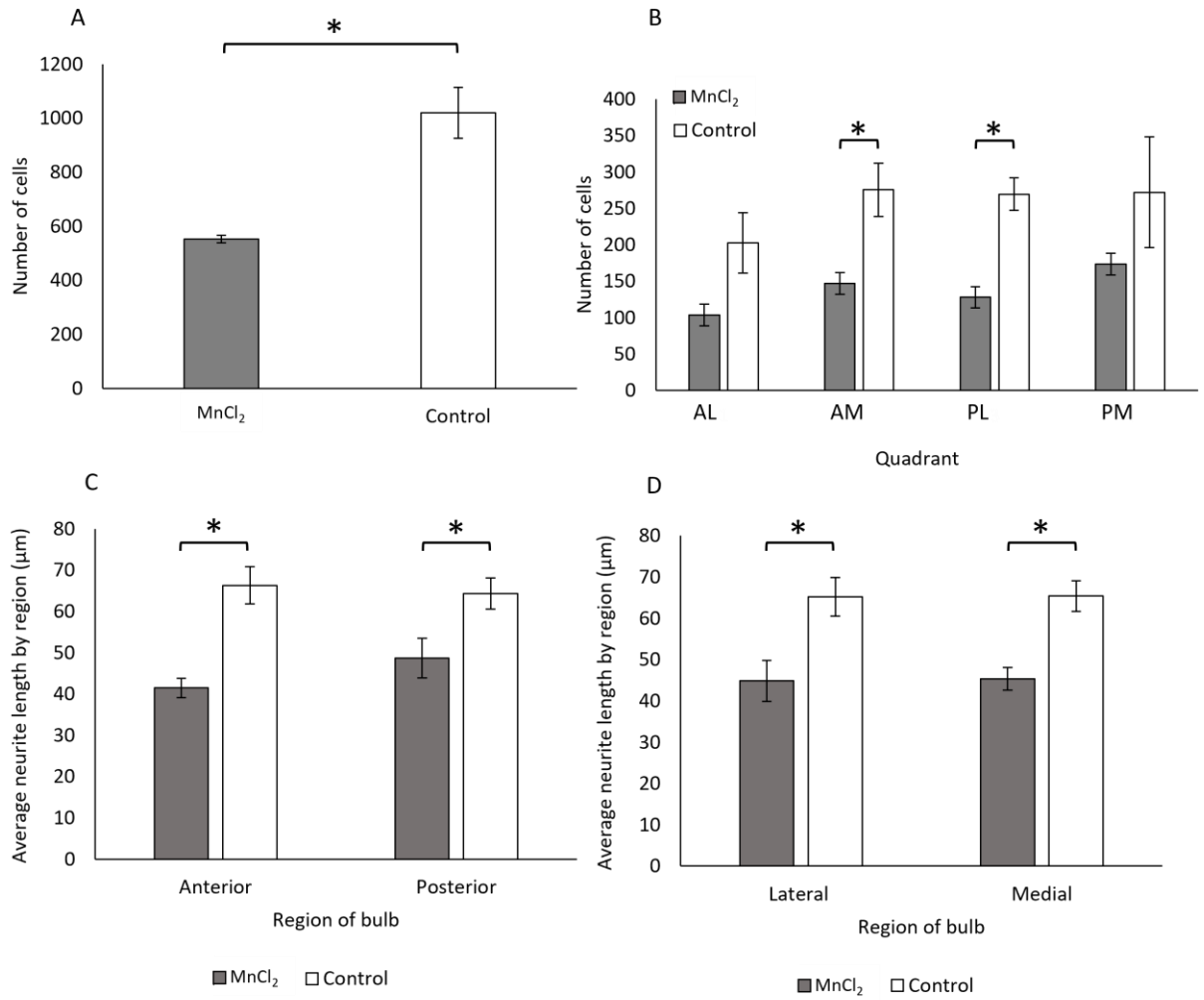
Figure 32: Quantification of TH+ cells and neurites in the olfactory bulb (OB) of 10-day MnCl₂-treated versus control zebrafish.

Figure 33: Examination of TH+ cells in posterior forebrain of 10-day MnCl2-treated versus control zebrafish. (A) The MnCl2-treated forebrain showed no depletion of TH+ cells and was indistinguishable from the (B) forebrain population of the exposure-control fish. (C) When the cells were quantified, there was no significant difference between the experimental and control brains (t-test; p<0.05) [N=6. Error bars = ± S.E.M.]
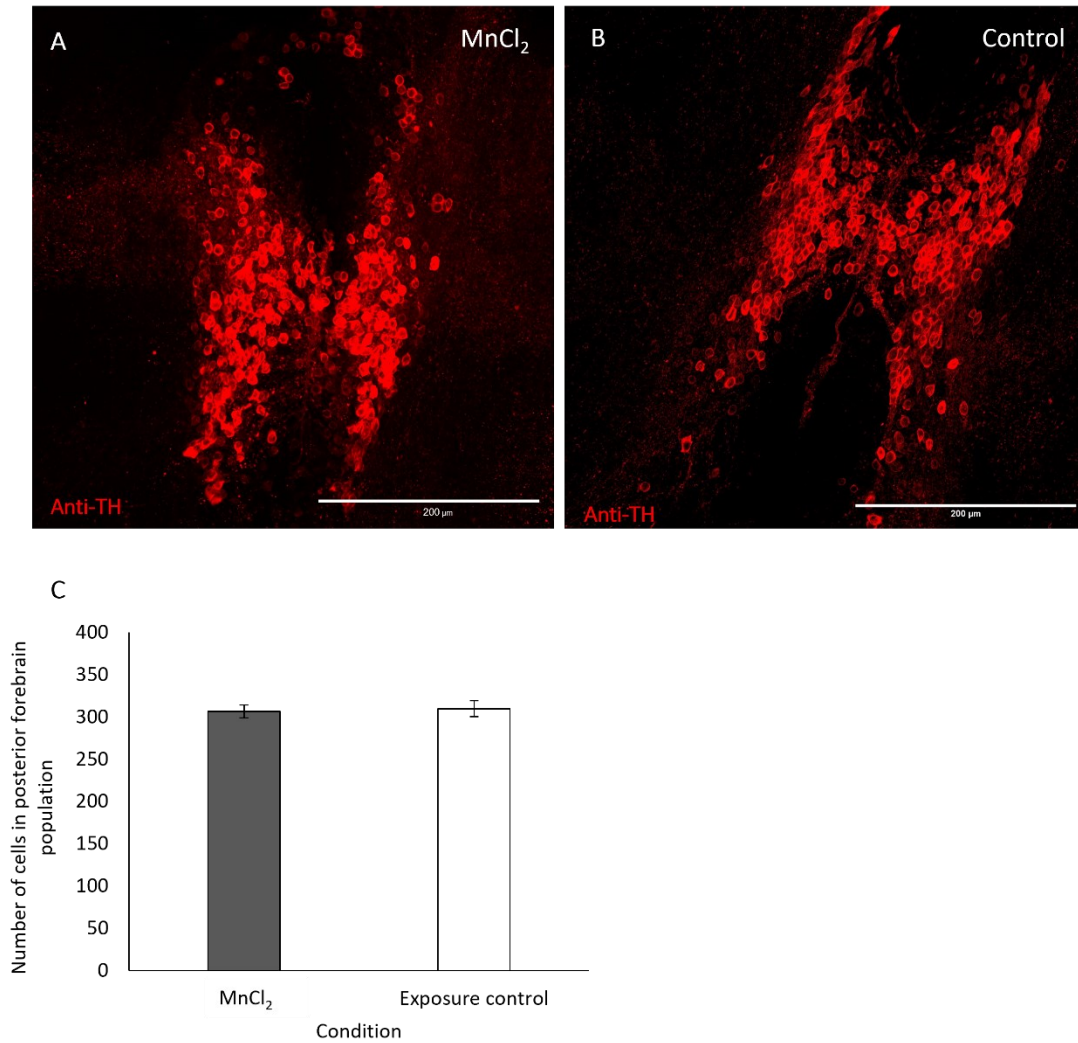
Figure 33: Examination of TH+ cells in posterior forebrain of 10-day MnCl2-treated versus control zebrafish.

Figure 34: Anti-Keyhole Limpet Hemocyanin staining of olfactory sensory neurons (OSNs) in 4-day and 10-day MnCl₂-treated zebrafish olfactory bulbs. (A) Exposure-control brains stained with anti-KLH displayed normal staining with all regions clearly visible, innervation with smooth bundled OSNs and properly formed. (A$_I$) Axons of OSNs were bundled and smooth, curving from the olfactory nerve around the outside of the olfactory bulb before separating and ending in glomeruli. (A$_{II}$) Glomeruli were defined, round and the synapses of the OSNs were visible within. (N=8). (B) An earlier short-term (four-day) MnCl₂-exposure showed moderate defasciculation of the OSN axons and disruption of the glomeruli in the bulb. (B$_I$) In general, the axons of the OSNs were no longer smooth and bundled, but instead were unbundled and gave the impression of being wavy and frayed. (B$_{II}$) Glomeruli, when present, were no longer round, with most of the fine nerve endings of the OSNs not visible, giving a sparse appearance (N=6). (C) In fish exposed to manganese for ten-days, the OSN axons from the nares were largely missing and poorly stained. Fluorescence was dim and glomeruli were largely absent, therefore identifying particular ones was not possible. Therefore, it appeared that degradation of the OSNs increased with exposure. (C$_I$) At this stage there were almost no discernable OSN axons and any that were present showed major disorganization. (C$_I$) Most bulbs possessed no discernable glomeruli, instead there were often sporadic bright blebs that may indicate the remnants of glomeruli.
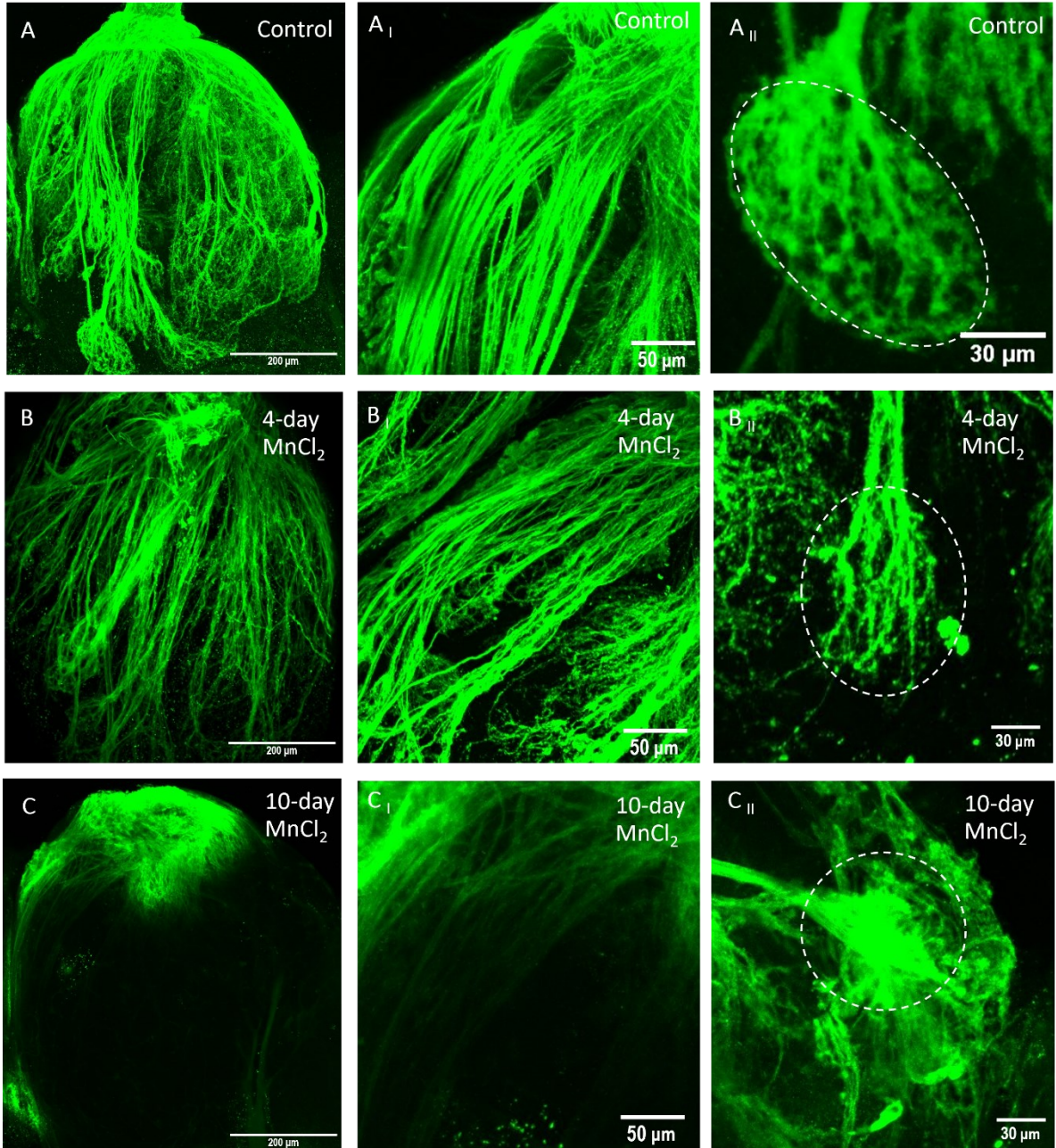
Figure 34: Anti-Keyhole Limpet Hemocyanin staining of olfactory sensory neurons (OSNs) in 4-day and 10-day MnCl₂-treated zebrafish olfactory bulbs.

Figure 35: Anti-Keyhole Limpet Hemocyanin staining of olfactory sensory neurons (OSNs) in 10-day MnCl$_2$-treated zebrafish olfactory bulbs. (A-D) There was no consistency between bulbs in the ten-day exposure. Some bulbs had limited staining around the olfactory nerve but no traceable OSNs or recognizable glomeruli. Instead, they possessed the aforementioned small blebs of bright staining which may have indicated the former location of glomeruli. (E) In some bulbs these blebs were larger and brighter and (F) in one bulb gave the appearance of a misshapen glomeruli. (E) Few bulbs showed defasciculated OSNs which were mostly very faint, however (F) one bulb was much brighter.
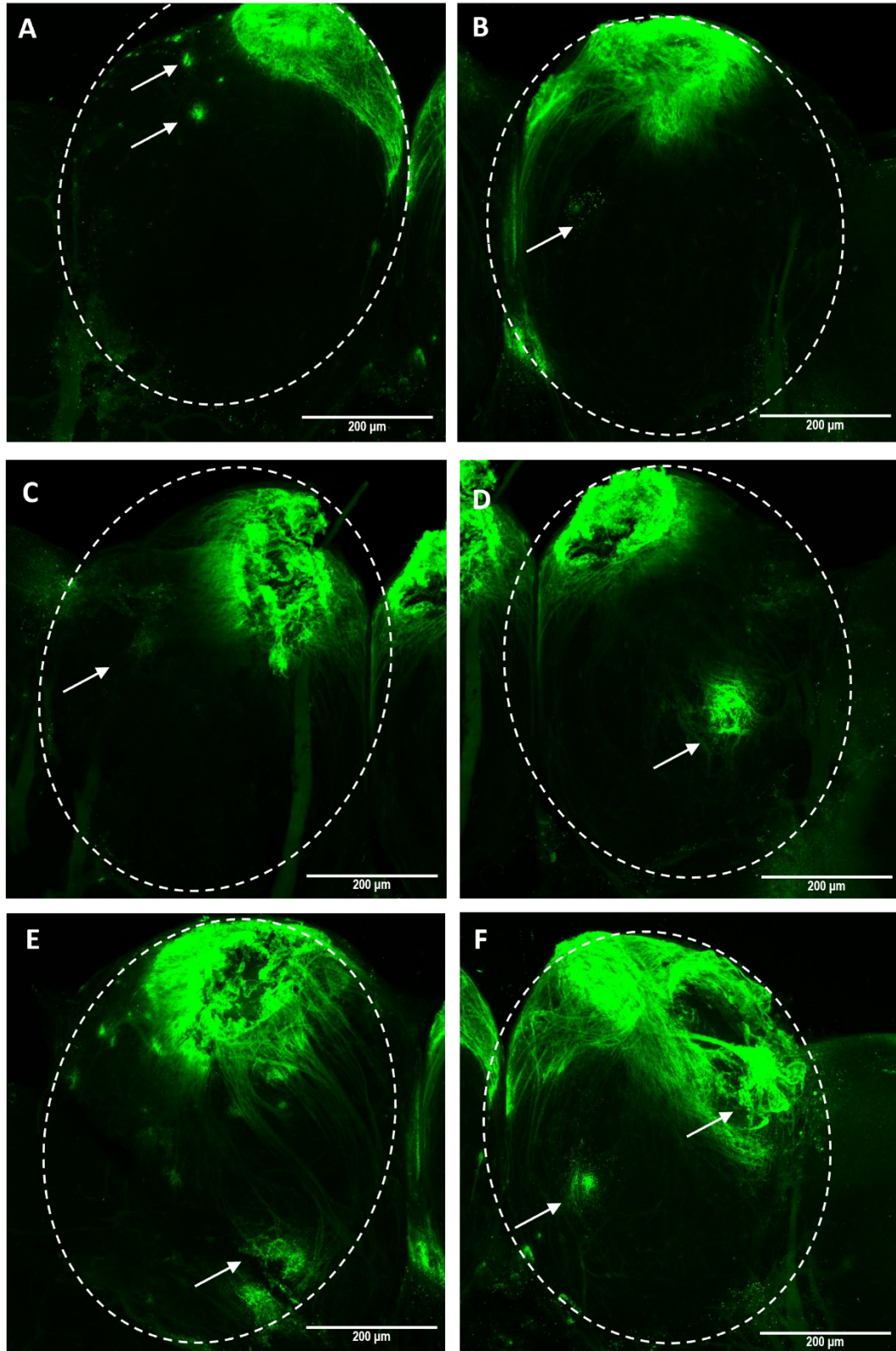
Figure 35: Anti-Keyhole Limpet Hemocyanin staining of olfactory sensory neurons (OSNs) in 10-day MnCl₂-treated zebrafish olfactory bulbs.

Chapter 5: Environmental Exposure Of The Olfactory System To

Metronidazole

5.1 Introduction

As discussed in the previous chapter, it is difficult to specifically target the TH+ interneurons in the olfactory bulb without negatively impacting the olfactory sensory neurons (OSNs). Examining the role of TH+-cells in olfactory behaviour becomes difficult when the loss of other cells may confound the results. Most of the studies involving manganese did not examine the effects of the heavy metal on TH+-cells in the olfactory bulb specifically, let alone the effects on the OSNs. One relatively new ablation technique claims to exclusively target the dopaminergic neurons of zebrafish. This technique is unique in that it employs a combination of genetic and chemical methods to achieve the ablation of dopaminergic cells. The method uses nitroreductase (NTR), a bacterial enzyme derived from *Escherichia coli*, which converts the antibiotic metronidazole (Mtz) into a cytotoxic metabolite (Curado et al., 2008). A transgenic zebrafish line expresses NTR under the control of the dopamine transporter (DAT), in the telencephalon, diencephalon, olfactory bulb and caudal hypothalamus of zebrafish (Godoy et al., 2015). Therefore, Mtz would only be converted into a toxin in those cells where NTR is present. This leads to spatially and temporally specific ablation of targeted cells (Pisharath and Parsons, 2009). Administration of Mtz at 1 dpf resulted in loss of DAT-expressing neurons at 5 dpf in addition to motor impairments. Some motor function was re-established by 7 dpf when there was evidence of new DAT- expressing cells; however, there was still a deficit at 14 dpf. A follow-up study in adult transgenic zebrafish found that a 24-hr exposure to Mtz resulted in significant loss of dopaminergic neurons in the olfactory bulb and a decrease in the ability to smell the death-associated odour

cadaverine (Godoy et al., 2020). Although both experiments used transgenic fish for specific ablation of cells, they did not address the effects of only Mtz on the dopaminergic neurons in wild-type fish. In addition, neither of these papers addressed the possible effects of the treatment on other cells in the bulb, like the OSNs.

I have already examined in detail the effects of manganese exposure on the bulb and the effects on olfactory behaviour. I now aim to specifically investigate the effects of Mtz on TH immunoreactive neurons in wild-type fish but also on the OSNs. Using similar metrics from Chapters 2 and 4, I note changes in cell number, location and distribution. I again investigate differences in neurite length, direction and whether cells innervate locally or across regions. I also examine behavioural changes caused by the treatment on fish exposed to an attractive stimulus, amino acid mixture, and an aversive stimulus, cadaverine.

5.2 Materials & Methods

5.2.1 Animals

Adult, AB-strain zebrafish between 2.5 – 3.0 cm in length were obtained from the Zebrafish Core Facility, Faculty of Medicine, Dalhousie University, Halifax, NS, Canada. Fish were kept on a 14:10 hour light:dark cycle in treated, reverse osmosis water (28°C, pH 7.3 and salinity at 0.20 PSU) with an average flow of 13-14 L per hour per tank. All experiments were conducted in accordance with the Canadian Council on Animal Care standards and guidelines (Dalhousie Protocol 21-117).

5.2.2 Exposure

The metronidazole (Mtz) exposure procedure was based largely on the work of Godoy et al. (2020), with some modifications. Groups of five zebrafish were placed in breeding tanks (Pentair Aquatic Eco-Systems, Apopkoka, FL, USA) containing 10 mM of Mtz (Sigma-Aldrich, St. Louis, MO, USA) dissolved in 0.2% DMSO and 1 L of charcoal filtered water for 24-hrs in complete darkness, as the solution was light sensitive (Godoy et al., 2015). After the 24-hr exposure the fish were moved to an intermediate tank to rinse off any remaining Mtz before being transferred to an 8 L tank containing fresh water until the seventh day after exposure. Water was recirculated using a Tetra® Whisper IQ Power Aquarium Filter with charcoal media (PetSmart, Phoenix, AZ, USA) and maintained at 25.0 °C. Control fish were treated in the same manner except only DMSO was added to the charcoal filtered water.

5.2.3 Behavioural Testing

After exposure to Mtz or control procedures, fish underwent behavioural testing using the apparatus described in Chapter 3 and employing the same odourant exposure protocol outlined in Chapter 4. Groups of five experimental or five control fish were acclimated to the testing tanks for one hour prior to experimentation. Then, one minute of spontaneous behaviour was recorded before the administration of the odourant. After that, fish underwent four odour exposures with a 30 min washout between each. The optimal washout was determined using the dilution curve in Chapter 3 (Fig. 21). The first two exposures were to 250 µL and 500 µL of an amino acid solution known to be attractive to zebrafish (Braubach et al., 2011). It consisted of alanine, histidine, lysine, methionine, phenylalanine, tryptophan and valine, each at 0.0167M (Sigma-Aldrich, St. Louis, MO, USA; for further details see Braubach et al., 2013). The last two exposures were to cadaverine, a repulsive chemical found in decaying tissue, which elicits aversive behaviour in fish (Hussain et al., 2013; Dieris et al., 2017; Godoy et al., 2020). The fish were then exposed to 20 µL and 60 µL doses of a 95% cadaverine (Sigma-Aldrich, St. Louis, MO, USA). The 60 µL dose was similar to the dose used by Godoy et al. (2020). Due to the small size of the tank used in this study and consequently the inability of the fish to distance themselves from the odour, both the 20 µL and 60 µL doses were mixed in 1 mL of tank water before delivery to the tank. This method of delivery reduced the initial startle response the fish experienced when they physically contacted the texture of the pure cadaverine.

5.2.4 Data Collection And Analysis

The behaviour of the fish was video recorded in colour at a resolution of 1280 x 720 pixels. Surveillance software (iSpy, http://www.ispyconnect.com) permitted the recording of time-stamped video files from cameras in all four arenas simultaneously. Video clips were recorded at 6 frames/second for one minute immediately before exposure to the odourant and 4 min after. The videos were analyzed using the procedure described in Chapter 4 to establish mean position for the group of fish in each frame.

5.2.5 Dissection and Tissue Preparation

Immediately after behavioural testing, zebrafish were sacrificed by immersion in cold water (<4°C) for 10 minutes, as described in Chapter 2 (Chen et al., 2014; Wallace et al., 2018). The whole brains were removed immediately and then fixed overnight in 4% paraformaldehyde (PFA; Electron Microscopy Sciences, Hartfield, PA, USA) dissolved in phosphate-buffered saline (PBS: 100 mM Na_2HPO_4, 140 mM NaCl, pH 7.4) at 4 °C. After fixation, the brains were subjected to four 20 min washes in PBS before being placed in blocking solution (PBS-Block; 0.25% Triton X-100, 2% DMSO, 1% bovine serum albumin, 1% normal donkey serum and 1% normal goat serum in PBS; ingredients from Sigma-Aldrich) for 24-hrs at 4°C. The samples were again washed for four times at 20 min each before application of antibodies.

5.2.6 Immunocytochemistry

Primary antibodies were used in this study as listed in Table 6. For background on the use of each antibody see Chapter 2. To label the TH immunoreactive interneurons I used an antibody raised against tyrosine hydroxylase (TH), the rate-limiting enzyme in

the dopamine pathway. To label the terminals of the OSNs in the glomeruli, a rabbit

polyclonal antibody raised against keyhole limpet hemocyanin (KLH) was employed. The

antibody has been used previously in teleosts because it labels an unknown epitope in

or on OSN axons of fish (Riddle and Oakley, 1992; Starcevic and Zielinski, 1997; Fuller et

al., 2006; Gayoso et al., 2011; Braubach et al., 2012).

Table 6: List of Primary Antibodies

Antibody	Antigen/Host	Source
Anti-keyhole-limpet-hemocyanin (KLH) (1:100 dilution)	keyhole limpet hemocyanin/rabbit	Sigma-Aldrich H0892 (St. Louis, MO, USA)
Anti-tyrosine-hydroxylase (TH) (1:200 dilution)	TH purified from rat PC12 cells LNC1 clone/ mouse	Immunostar 22941 (Hudson, WI, USA)

Brains were double-labelled with anti-KLH rabbit polyclonal antibody and anti-TH

mouse monoclonal antibody, both diluted 1:200 in PBS blocking solution. Specimens

were incubated in primary antibodies for two days at 4 °C with gentle agitation on a

rocker. After incubation in the primary antibodies, the samples were washed in PBS (4x

20 min) as described before. Samples were then placed in a solution of secondary

antibodies diluted 1:200 in PBS-Block for two days at 4 °C. Secondary antibodies were

donkey anti-rabbit and donkey anti-mouse conjugated to either Alexa Fluor 488 or Alexa

Fluor 555 (Table 7).

Table 7: List of Secondary Antibodies

Antibody	Source
Donkey anti-Rabbit IgG (H+L) Highly Cross-Adsorbed Secondary Antibody, Alexa Fluor™ 488	Invitrogen (Waltham, MA, USA)
Donkey anti-Mouse IgG (H+L) Highly Cross-Adsorbed Secondary Antibody, Alexa Fluor™ 555	Invitrogen (Waltham, MA, USA)

After incubation in antibodies, samples were again washed (4x 20 min) in PBS and then immersed in CUBIC clearing/mounting agent for 24-hrs before mounting (Susaki et al., 2014, 2015). Brains were separated between the fore- and mid-brain division and mounted separately in the clearing solution dorsal side down on glass slides. Small dots of silicon grease (Dow-Corning, Midland, MI, USA) were applied to the four corners of an 18 mm x 18 mm glass coverslip before it was placed over the specimen. The coverslips were then sealed to the slide with nail polish and viewed with a confocal microscope.

5.2.7 Imaging

Specimens were viewed either with a Zeiss LSM 710 or LSM 880 laser scanning confocal microscope (Carl Zeiss, Thornwood, NY, USA). Whole olfactory bulbs were initially imaged using either a 10x or 20x objective and the final magnification was adjusted using digital zoom until the bulb filled the field of view. Optical sections were obtained at the "optimal" intervals (0.5 μm – 3.5 μm) suggested by the acquisition software, Zen (Carl Zeiss, Thornwood, NY, USA). Higher magnification images were then obtained using 25x or 40x oil immersion lenses depending on the thickness of the sample. Image stacks were imported into ImageJ (National Institute of Health, Bethesda, MD, USA; https://imagej.nih.gov/ij/) for further analysis.

5.2.8 Analysis

Low power images were used for general cell counts and noting prominent neurites. Cell counts were performed using the "Cell Counter" function in ImageJ, an Excel macro to sort cell coordinates into quadrants, as described in Chapter 4. The

higher power images were then examined to determine the number of neurites per bulb

and the location of the cell bodies. The "Simple Neurite Tracer" plug-in in ImageJ to yield

the starting and ending coordinates of each neurite path and to catalogue the number of

neurites per cell and the presence of branching, as described in Chapter 4.

Statistical analyses of all these measures were performed as described. A one-

way ANOVA was used to compare the mean baseline positions, with post-hoc pairwise

comparisons using a Bonferroni correction in SPSS 28 (IBM, Armonk, NY, USA). For the

odour exposures a two-way mixed ANOVA with repeated measures was employed along

with post-hoc pairwise comparisons using a Bonferroni correction. A two-way ANOVA

was performed for the neurite analysis. Simple comparisons of two means were

analysed using a Student's t-test.

5.3 Results

5.3.1 Baseline Behaviour

Before the behavioural analysis, the fish were examined in the exposure tanks for normal activity. While the experimental fish showed slightly reduced swimming behaviour, the controls behaved normally. Therefore, no facility controls were utilized in this experiment. The Mtz-treated and control groups maintained similar group mean horizontal (X) positions near the middle of the tank (ANOVA, p>0.05; Fig. 36A), however there was a significant difference between the average mean vertical (Y) position of the two groups (ANOVA, p<0.05; Fig. 36B), as seen with the manganese fish in Chapter 4.

5.3.2 Responses To Amino Acids

In terms of horizontal movement, there was a significant effect of condition (ANOVA; p<0.05) but no effect of dose or any interaction effect between treatment and dose (ANOVAs; P>0.05). With the low dose of amino acid, the controls showed movement towards the odour on the left side of the tank (Fig. 37A), but the Mtz-exposed fish showed significantly less horizontal movement (Post-hoc t-test; p<0.05). When the dosage was increased, the control fish's movement increased slightly; but the experimental group increased dramatically; so, there was no longer a difference between the two groups (Post-hoc t-test; p>0.05). The Mtz-treated group responded normally given a high enough concentration.

When vertical movement was examined (Fig. 37B), there was no significant effect of treatment, dose or an interaction effect between treatment and dose (ANOVAs; p>0.05). The controls showed no significant movement in either direction and

remained unchanged with the increase in dosage concentration. The fish did not move

towards the surface but instead occupied mean positions in the centre of the tank;

however, the standard error is quite high which may have indicated an increase in

activity, as described in Chapter 4. With the low dose, the Mtz-exposed fish showed

similar responses to the controls, with average positions in the center of the tank. In

summary, both groups had an average position in the center of the tank vertically. The

Mtz-treated fish showed severely reduced horizontal responses with the low dose but a

mostly normal response when the concentration was increased. This response may

indicate that the fish's detection threshold for amino acids had been affected.

5.3.3 Responses To Cadaverine

When horizontal responses to cadaverine were examined, there was no

significant effect of condition, dose or interaction effect (Fig. 38A; ANOVAs; p>0.05). The

controls showed movement towards the left when exposed to the low dose of

cadaverine, with a large standard of error. Increasing the dosage caused the controls to

move to the right, away from the odour. When the experimental fish were exposed to

low dose cadaverine, they showed no net horizontal movement in either direction, and

when the dosage was increased, there was slight horizontal movement right. Both

groups moved away from the aversive stimulus at the high dose, but this change was

not statistically significant.

In terms of vertical movement (Fig. 38B), there was again no significant effect of

treatment, dose or an interaction effect between treatment and dose (ANOVAs;

p>0.05). The controls showed movement towards the bottom of the tank when exposed

to the low dose, and this increased with the higher dose. The Mtz-exposed fish also showed movement towards the bottom of the tank with the low dose, but this movement remained largely the same with the increase in dose. Both groups showed movement towards the bottom of the tank, and this reaction was consistent with a known stress response in zebrafish: sinking in the water column (Cachat et al., 2010). Given the visual difference between the two groups at the higher dose (Fig. 38B), it was surprising that the difference was not statistically significant. When the data were pooled across treatment, the difference was significant (ANOVA; $p<0.05$). The lack of statistical significance may be attributed to noisy data and may benefit from an increase in sample size. In conclusion, while both groups exhibited conflicting horizontal movement, the Mtz-treated fish showed an appropriate vertical response to cadaverine but one that was slightly blunted when compared with the controls.

5.3.4 Tyrosine Hydroxylase

Upon examination of the experimental brains, there at first appeared to be no immediate visible difference compared to the control brains (Fig. 39). Both the control (Fig. 39A) and experimental (Fig. 39B) olfactory bulbs showed similar anti-TH staining in an overview. Higher magnification images highlighted the lower density of cells in the experimental bulb (Fig. 39C) versus a comparable area in the control (Fig. 39D). When quantified, there was a deficit evident in the Mtz-treated fish. Experimental bulbs contained significantly fewer TH cells than the control bulb (Fig. 40A), decreasing from 1015 to 732 (t-test; $p<0.05$). This decrease was particularly notable in the posterior of the bulb, with the posterior medial (PM) and posterior lateral (PL) quadrants having

significantly fewer cells when compared to the same areas in the control bulbs (Fig.40B; ANOVA; $p < 0.05$; Post-hoc t-test; $p < 0.05$). Neurite length was also affected by the Mtz, with treated brains possessing neurites that were on average 9 µm shorter than those in the control brains (Fig. 41A). When the origin of the neurites was investigated there was a significant effect of quadrant (Fig. 41B; ANOVA; $p < 0.05$), where the experimental AL and PM quadrants were significantly different from each other (Post-hoc t-test; $p < 0.05$). This indicated that the percentage of neurites in AL decreased while PM increased when compared to the controls. When neurite length was broken down by region, further differences emerged. Neurites lengths in anterior and posterior regions were significantly different between experimental and controls (Fig. 41C; ANOVA; $p < 0.05$). A post-hoc analysis revealed that while there was no difference between neurite lengths in the anterior region, neurites in the posterior region were significantly shorter in the experimental group (Post-hoc t-test; $p < 0.05$). Comparison of the lateral and medial region produced a similar result. These regions were significantly different between experimental and control groups (Fig. 41D; ANOVA; $p < 0.05$), and a post-hoc analysis revealed no difference between lengths in the lateral region, but neurites in the medial region were significantly shorter in the experimental group (Post-hoc t-test; $p < 0.05$). As the mechanism by which Mtz was entering the brain is not well understood, a population of TH+ cells in the posterior forebrain was characterized to determine if the exposure affected other brain regions. When compared to the control brains (Fig. 42B) these TH+ cells in experimental brains appeared unaffected (Fig. 42A). After quantification, there was no statistical difference between the number of cells in the

posterior population in the control and experimental conditions (Fig. 42C; t-test; p>0.05). In summary, Mtz exposure decreased the number of TH+ cells in the brain by 30%, with most of the loss focused in the posterior of the bulb. Most surviving neurites were in the PM quadrant, and there was a decrease in neurite length, mostly in the posterior medial regions.

5.3.5 Keyhole Limpet Hemocyanin

Anti-KLH staining of the control OBs revealed normal bulb morphology with all regions evident, innervation with smoothly bundled OSNs and properly formed glomeruli (Fig.43A; See Chapter 2 for detailed description of normal anatomy). Axons of OSNs were bundled and smooth (Fig. 43A$_I$), and the glomeruli were identifiable and spherical; and the synapses of the OSNs were clearly visible within (Fig. 43A$_{II}$). All ten of the bulbs exhibited normal anatomy. Conversely, the OBs of the Mtz-treated fish showed some disturbances in OSN organization. The general structure of the bulb was largely unchanged in about half of the ten bulbs, but OSN axons appeared to be missing to varying degrees in others (Fig. 43B). In general, when the axons of the OSNs were present, they were unbundled, or the bundle appeared wavy and frayed (Fig. 43B$_{II}$). Glomeruli, if present, were misshapen with most of the fine nerve endings of the OSNs not clearly visible (Fig. 43B$_{II}$). It was difficult to choose a representative example because there was so much variation between bulbs (Fig. 44). Some bulbs possessed near normal staining except for some slightly degraded glomeruli (Fig. 44A). Others were missing some OSNs, but there was no consistency in the regions of the bulb where this occurred

(Fig. 44B). In some bulbs, OSNs were largely absent with small blebs that may have been

the remnants of glomeruli (Fig. 44C & D).

5.4 Discussion

5.4.1 Behaviour

During the metronidazole (Mtz) exposure, every effort was made to reduce stress on the fish. Because the exposure was only 24-hrs, the fish spent minimal time in stagnant water before being moved to a recirculating tank for seven days. Control fish exhibited no stress behaviours, but the exposed fish did display anxiety-like behaviour. The experimental fish had a lower baseline position than the controls, which may indicate stress in zebrafish (Cachat et al., 2010). In response to a low dose of amino acids the Mtz-exposed fish showed no horizontal response, but they displayed a normal movement towards the odour in response to a higher dose. This may indicate that the Mtz-treatment had reduced the odour detection threshold of the fish, rather than affecting other olfactory abilities, like discrimination. Both the control and experimental groups showed no net vertical movement in response to either the low or high dose of amino acids but instead had an average mean position in the center of the tank. The standard error was quite large, possibly suggesting that the fish moved up and down in the tank while moving towards the odour horizontally. As mentioned in the Discussion of Chapter 4, the tanks used in this experiment are considered small in size (3 L) for odour exposure experiments. Therefore, fish may respond slightly differently than they would in a larger custom tank.

In response to the death-associated odourant cadaverine, both groups demonstrated conflicting results. The expected result of exposing zebrafish to cadaverine is immediate movement to the bottom of the tank (Hussain et al., 2013). If

possible, the fish will also try to leave the area containing the odour (Godoy et al., 2020). Both groups showed an average horizontal position near the center of the tank when exposed to the low dose and a non-significant movement away from the odour when the dose was increased. This suggested that the fish were moving back and forth in the tank, possibly trying to escape the odour. In terms of the vertical movement, the experimental fish did have a comparable response to controls, although it remained the same when the dose increased, whereas the controls sank farther in the tank, albeit non-significantly. Again, this may have been due to a reduced capacity to detect odours, or the increased anxiety-like behaviour displayed by the experimental fish. During the statistical analysis, it was noted that some values were approaching significance and would benefit from an increase in the sample size. Due to the highly variable nature of animal behaviour, sometimes larger sample sizes are preferred to minimize the standard error (Charan and Kantharia, 2013).

In summary, the Mtz-exposed fish had a diminished response to the low dose of amino acids but a normal response to the high dose. The response to cadaverine was normal at the low dose and possibly blunted at the higher dose. Both findings may imply a deficit in the odour detection threshold of the fish. However, it was difficult to determine the extent to which the reactions were caused by potentially reduced olfactory capacity or due to stress.

5.4.2 Anatomy

A 24-hr exposure of wild-type zebrafish to Mtz caused a significant reduction in the number of TH+ cells in the olfactory bulb. Approximately 30% of the cells were

depleted mostly in the posterior region of the bulb. Neurites were also negatively

impacted, with numbers generally decreasing in the anterior of the bulb and length

significantly shorter in the posterior medial regions. This conclusion complicates the use

of Mtz in the chemogenetic ablation technique that has been used to target

dopaminergic neurons in the zebrafish brain (Godoy et al., 2015, 2020). As mentioned in

the introduction, a transgenic line of zebrafish was developed to express nitroreductase

(NTR), a bacterial enzyme derived from *Escherichia coli*, under the control of the

dopamine transporter (DAT). This resulted in a fish that expressed NTR in the

telencephalon, diencephalon, olfactory bulb and caudal hypothalamus. When Mtz is

applied to the fish, it is converted into a cytotoxic metabolite, only in those cells where

NTR is present (Curado et al., 2008). This method was supposed to specifically ablate the

targeted cells and leave others unaffected, but the results of this experiment clearly

contradicted that hypothesis.

There was also the unexpected disruption of the olfactory sensory neurons

(OSNs), which were affected to varying degrees. Some had mild disturbances in OSN

organization, mainly with glomeruli that were sparse or missing. In more moderately

affected bulbs, OSNs were absent in some areas with glomeruli gone entirely. The most

impacted bulbs possessed only a few OSNs and small clusters of bright blebs,

hypothesized to be the remnants of glomeruli. With these distributions, it was difficult

to determine if the olfactory deficits noted in the behavioural study were caused by the

reduction in TH+ cells or the disruptions in the OSNs. A previous study using this method

noted various behavioural changes including increased freezing and almost total

anosmia. Adult transgenic zebrafish exposed to Mtz for 24-hrs had an almost 70%

reduction in TH+ cells and displayed no response to the aversive odour cadaverine

(Godoy et al., 2020). While the reduction in TH+ cells in this experiment was modest in

comparison to the more efficient chemogenetic model, Mtz clearly affects the olfactory

bulb outside of this system and has detrimental effects on other olfactory cells.

The question then arises how the Mtz is affecting the olfactory cells without the

benefit of the chemogenetic system. Metronidazole, developed in 1959, has long been

used as a well-tolerated treatment for parasitic and bacterial infections (Leitsch, 2019).

Despite its widespread use, it has been associated with neurotoxicity in rare cases

(Hernández Ceruelos et al., 2019). The mechanism by which this occurs is poorly

understood, but it is thought that Mtz first enters cells through passive diffusion where

its nitro group is reduced, transforming it into a reactive intermediate that attacks

targets within the cell (Leitsch, 2019). Therefore, a reasonable assumption is that given

enough time, Mtz could negatively impact many types of cells in the zebrafish brain. It is

unclear given its method of transport whether Mtz is traveling directly up the olfactory

nerve or entering through another route. The unaffected population of TH+ cells in the

forebrain of Mtz-treated would imply that it was preferentially entering through the

nose. Although it may be affecting the nose because of its general sensitivity to

environmental pathogens (Zhou et al., 2023).

In conclusion, Mtz-exposed fish had deficits in their odour detection threshold,

but it was difficult to clearly separate these responses from anxiogenic behaviour. The

experimental fish had a 30% depletion in TH+ cells mostly concentrated in the posterior

of the bulb. Neurites were fewer in number towards the anterior region but shorter in

length in the posterior medial region. OSNs were variably affected, with the mildest

having disrupted glomeruli to the most severe possessing few OSNs and no glomeruli.

Therefore, Mtz application with or without the chemogenetic system may not be the

most appropriate method of specifically ablating dopaminergic neurons in the zebrafish,

particularly in the olfactory bulb, given its obvious effect on the OSNs.

Figure 36: Average horizontal and vertical position of groups of Mtz-treated fish before administration of an amino acid mixture or cadaverine. (A) Both groups began each trial roughly in the same position, with no significant difference between them (ANOVA; p>0.05). Zero indicates the origin of the odour (left side of the tank) and 21.0 cm is the far-right side of the tank. (N=10. Error bars = ± S.E.M.) **(B)** The Mtz-exposed fish began each trial near the bottom of the tank, while the controls maintained a significantly higher average position in the middle of the tank (ANOVA; p<0.05). Zero indicates the bottom of the tank and 13.0 cm is the top of the tank (water's surface). (N=10. Error bars = ± S.E.M.)
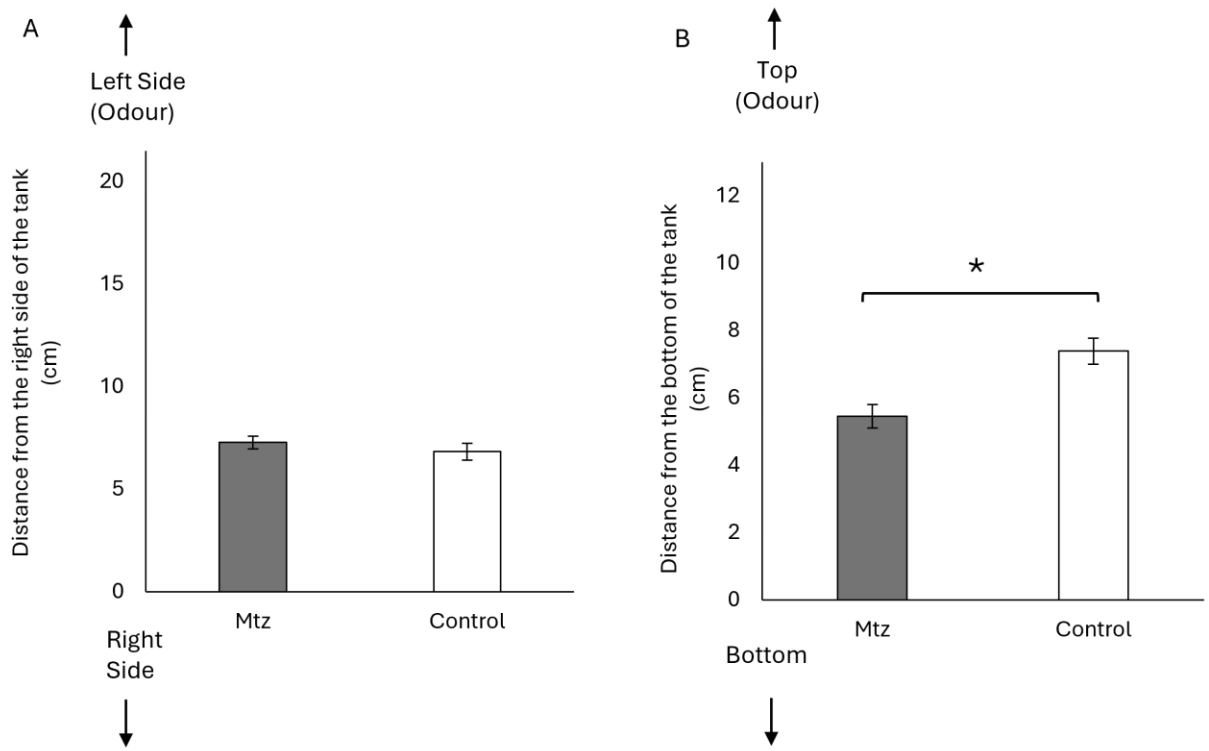
Figure 36: Average horizontal and vertical position of groups of Mtz-treated fish before administration of an amino acid mixture or cadaverine.

Figure 37: Horizontal and vertical movement of Mtz-treated zebrafish in response to two different concentrations of amino acid mixture. (A) Positive values indicate horizontal movement towards the left side of the tank where the odour was introduced. There was a significant effect of condition (ANOVA; p<0.05) but no effect of dose or an interaction effect between treatment and dose (ANOVAs; P>0.05). Mtz-treated fish showed no response to low dose amino acid mixture, while the controls exhibited a significantly larger movement towards the left (odour; Post-hoc t-test; p<0.05). Controls increased their movement in response to the higher concentration of amino acid. The Mtz-treated fish displayed a substantial increase in movement towards the left when the dose increased, and they were no longer significantly different than the control group (Post-hoc t-test; p>0.05). Data points are mean horizontal distance from the odour source (left) before amino acid delivery minus mean distance from the odour source during amino acid delivery (N=10. Error bars = ± S.E.M.). **(B)** Positive values indicate vertical movement towards the top of the tank where the odour was introduced. There was no significant effect of treatment, dose or an interaction effect between treatment and dose (ANOVAs; p>0.05). Neither group showed net movement in either direction in response to the lower or higher concentration of amino acids. Data points are mean vertical distance from the odour source (top) before amino acid delivery minus mean distance from the odour source during amino acid delivery (N=10. Error bars = ± S.E.M.).
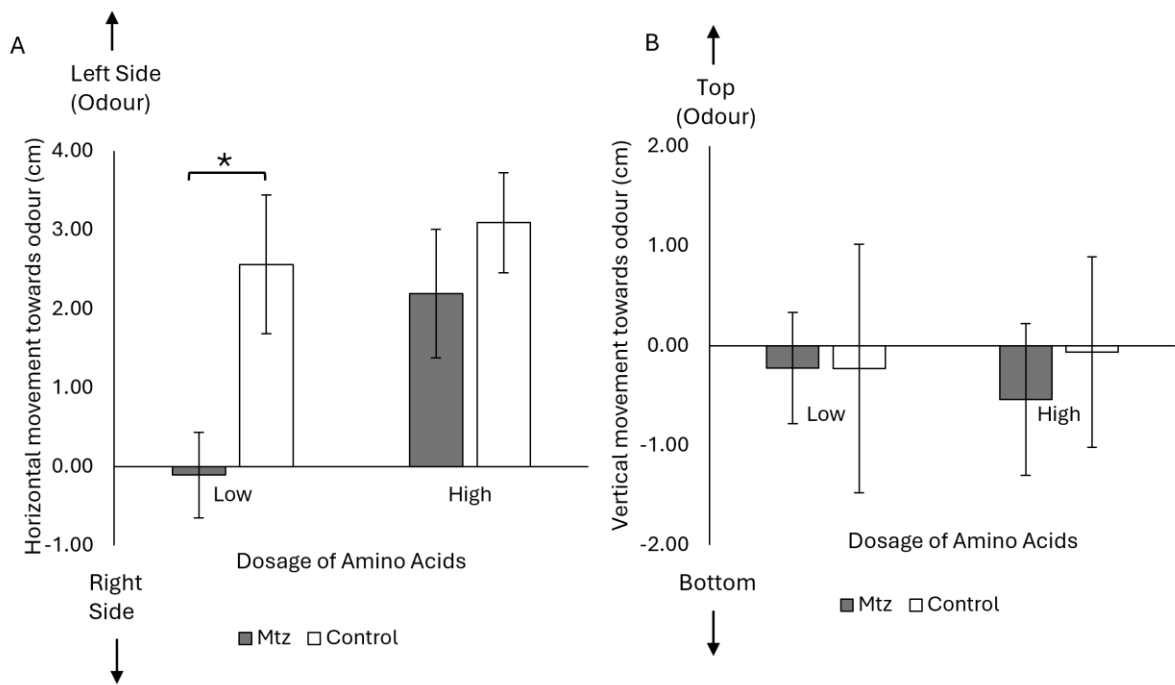
Figure 37: Horizontal and vertical movement of Mtz-treated zebrafish in response to two different concentrations of amino acid mixture.

Figure 38: Horizontal and vertical movement of Mtz-treated zebrafish in response to two different concentrations of the aversive odour, cadaverine. (A) Positive values indicate horizontal movement towards the left side of the tank where the odour was introduced. There was no significant effect of condition, dose or interaction effect (ANOVAs; $p > 0.05$). In response to the lower cadaverine dose, the Mtz-treated fish and facility controls exhibited no net movement in either direction. When the concentration increased, the Mtz-treated fish and controls moved right away from the odour source. Data points are mean horizontal distance from the odour source (left) before cadaverine delivery minus mean distance from the odour source during cadaverine delivery (N=10. Error bars = ± S.E.M.). **(B)** Positive values indicate vertical movement towards the top of the tank where the odour was introduced. There was again no significant effect of treatment, dose or an interaction effect between treatment and dose (ANOVAs; $p > 0.05$). Both groups demonstrated similar movement towards the bottom of the tank in response to the lower dose of cadaverine. When the dose increased, the control fish showed increased movement towards the bottom of the tank, but the Mtz-treated fish remained unchanged. Given the appearance of the two bars at the higher dose it was unusual that the difference was not statistically significant. When the data was pooled across treatment the difference was significant (ANOVA; $p < 0.05$). It is possible that more tanks are required to reach significance. Data points are mean vertical distance from the odour source (top) before cadaverine delivery minus mean distance from the odour source during cadaverine delivery. N=10. Error bars = ± S.E.M.
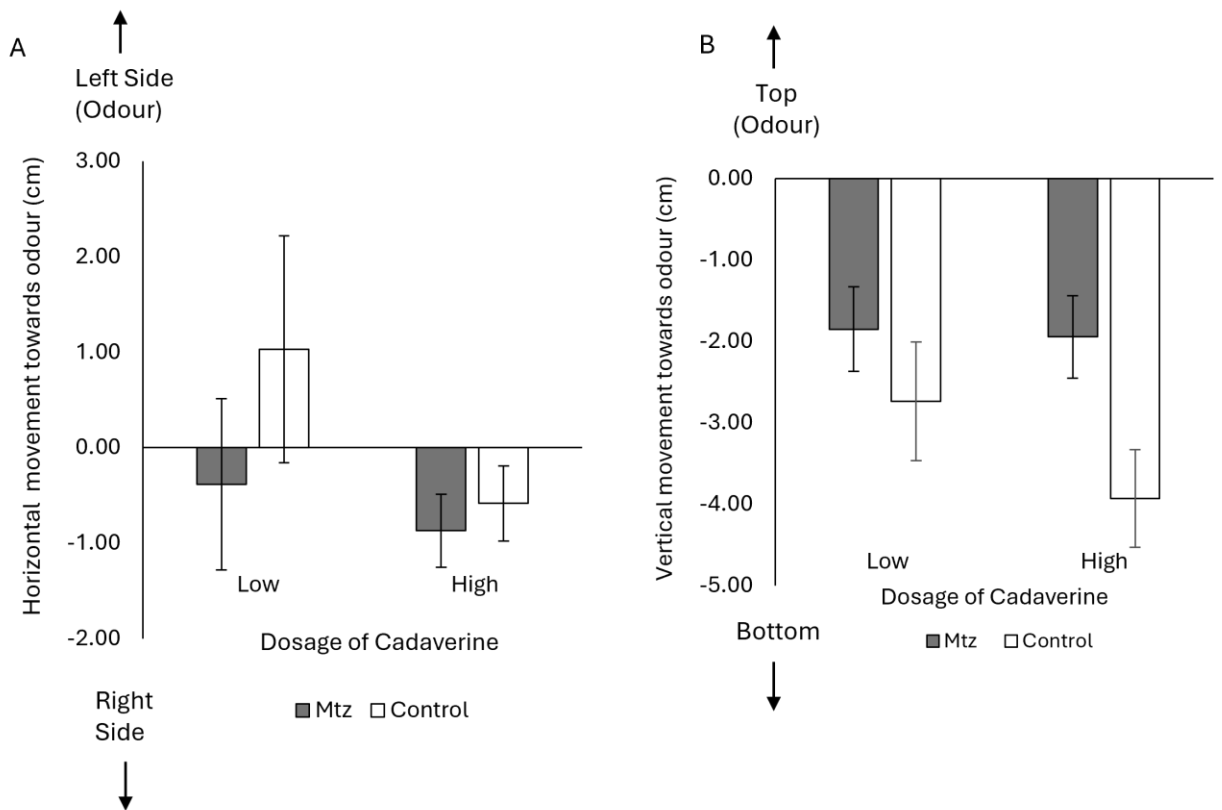
Figure 38: Horizontal and vertical movement of Mtz-treated zebrafish in response to two different concentrations of the aversive odour, cadaverine.

Figure 39: Anti-tyrosine hydroxylase (TH) staining of Mtz-treated zebrafish olfactory bulbs. (A) The Mtz-treated olfactory bulbs showed a slight all-over depletion of TH+ cells. (B) Control fish exhibited normal bulb anatomy with TH+ cells in abundance. (C) In a higher magnification image, the lower density of TH+ cells was evident in the Mtz-treated olfactory bulbs. (D) In contrast, the control bulb had more numerous, densely packed cells.
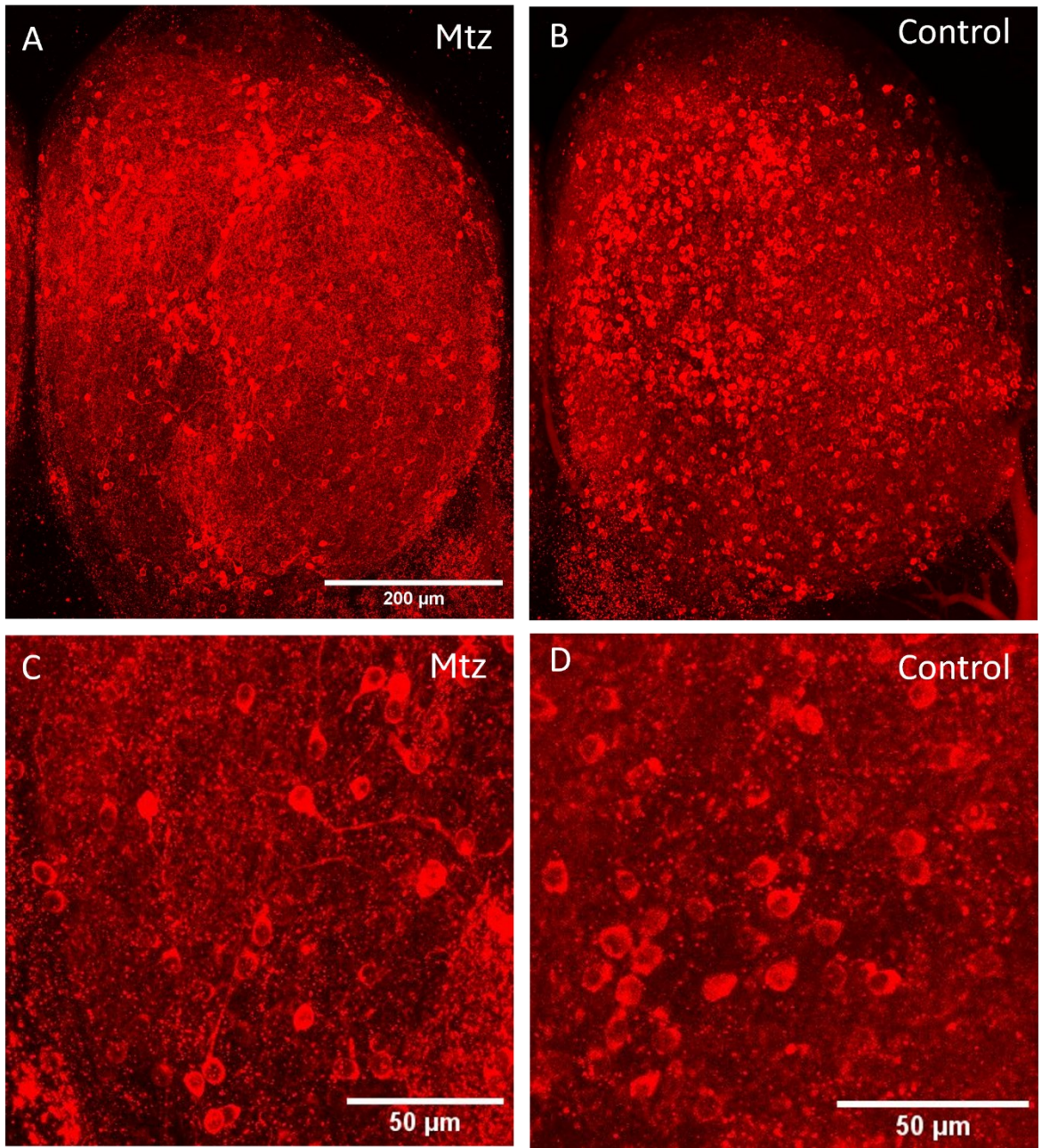
Figure 39: Anti-tyrosine hydroxylase (TH) staining of Mtz-treated zebrafish olfactory bulbs.

Figure 40: Quantification of TH+ cells in the olfactory bulb (OB) of Mtz-treated versus control zebrafish. (A) Mtz-treated OBs had significantly fewer cells than the controls (ANOVA; $p < 0.05$), dropping from 1015 cells to 732 (approx. 30%). (B) The TH+ cells were depleted in all four quadrants: Anterior Lateral (AL), Anterior Medial (AM), Posterior Lateral (PL) and Posterior Medial (PM). There was a significant difference between the Mtz-treated fish and the controls (ANOVA; $p < 0.05$), with a significant decrease noted in the PM and PL quadrants.
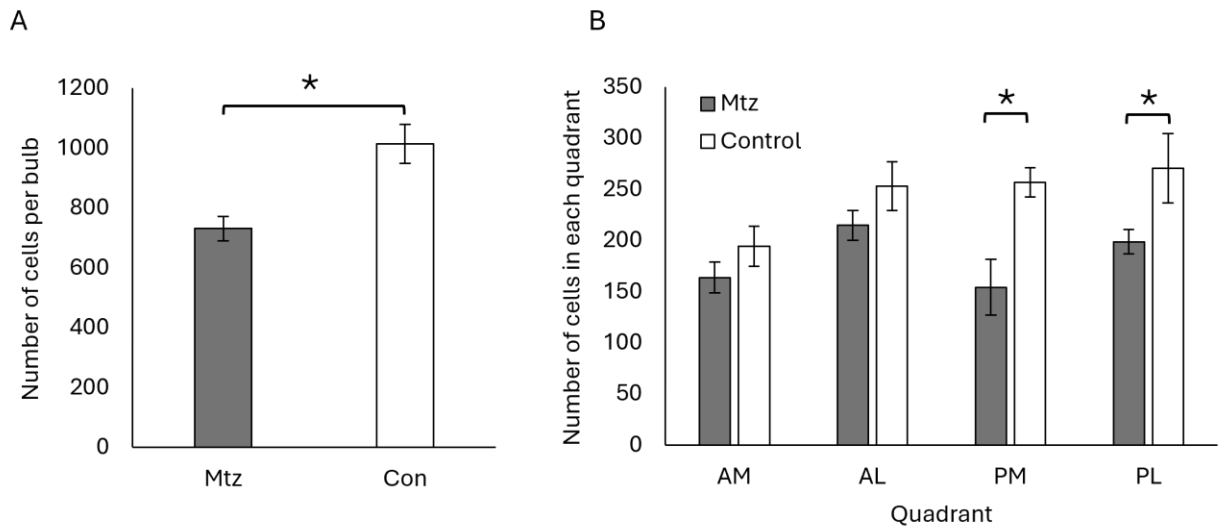
Figure 40: Quantification of TH+ cells in the olfactory bulb (OB) of Mtz-treated versus control zebrafish.

Figure 41: Quantification of TH+ neurites in the olfactory bulb (OB) of Mtz-treated versus control zebrafish. (A) When the neurites were analyzed, they were significantly shorter in the Mtz-treated OBs than the control OBs (t-test; p<0.05). (B) Neurite lengths decreased unevenly throughout the bulb as there was a difference between the anterior and posterior regions within each condition (ANOVA; p<0.05). Further analysis revealed that neurites in the posterior region were significantly shorter in the Mtz-treated fish than in the control fish (Post-hoc t-test; p<0.05). (D) There were similar results between the lateral and medial regions. There was a significant difference between the neurite lengths of the Mtz-treated fish and the controls (ANOVA; p<0.05), with neurites in medial region were significantly shorter in the Mtz-treated fish than in the control fish (Post-hoc t-test; p<0.05). [N=10. Error bars = ± S.E.M.]
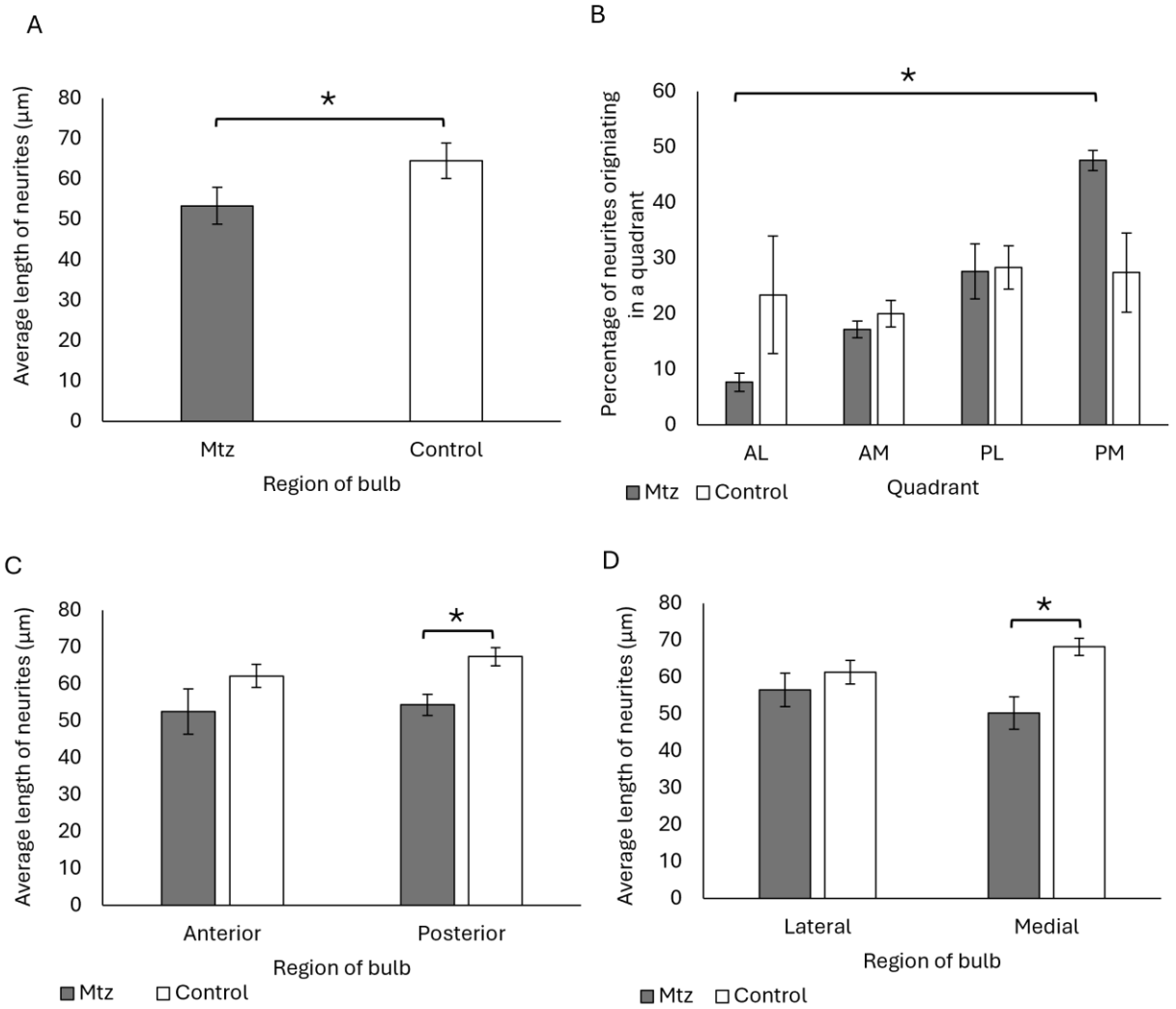
Figure 41: Quantification of TH+ neurites in the olfactory bulb (OB) of Mtz-treated versus control zebrafish.

Figure 42: Examination of TH+ cells in posterior forebrain of Mtz-treated versus control zebrafish. (A) The Mtz-treated forebrain showed no depletion of TH+ cells and was not visibly different from the (B) forebrain population of the control fish. (C) When the cells were quantified, there was no significant difference between the experimental and control brains (t-test; p>0.05) [N=6 for each group Error bars = ± S.E.M.]
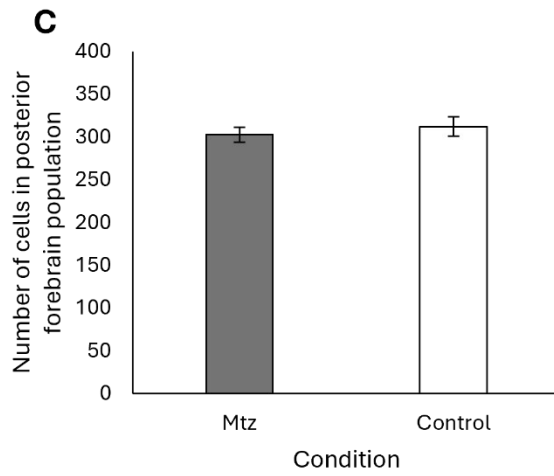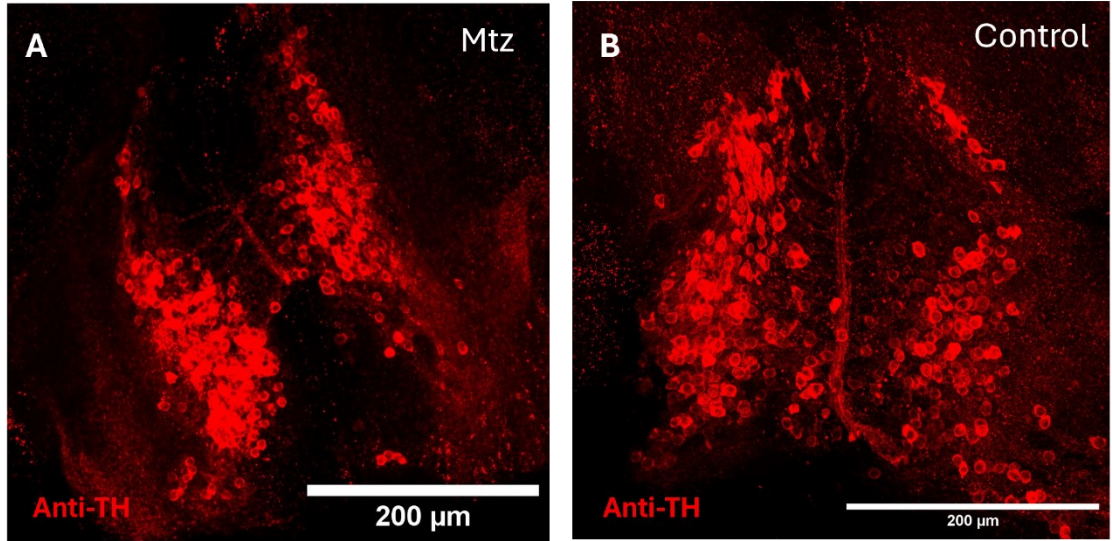
Figure 42: Examination of TH+ cells in posterior forebrain of Mtz-treated versus control zebrafish.

Figure 43: Anti-Keyhole Limpet Hemocyanin staining of olfactory sensory neurons (OSNs) in 24-hr Mtz-treated zebrafish olfactory bulbs (OBs). Anti-KLH staining of the control OBs revealed normal bulb morphology with all regions evident, innervation with smoothly bundled OSNs and properly formed glomeruli (A). Axons of OSNs were bundled and smooth (A_I) and the glomeruli were identifiable, spherical and the synapses of the OSNs were clearly visible within (A_{II}). All ten of the bulbs exhibited normal anatomy. Conversely, the OBs of the Mtz-treated fish showed some disturbances in OSN organization. The general structure of the bulb was largely unchanged in about half of the ten bulbs, but OSNs were missing to varying degrees in others (B). In general, when the axons of the OSNs were present they were unbundled, wavy and frayed (B_I). Glomeruli, if present, were misshapen with most of the fine nerve endings of the OSNs not clearly visible (B_{II}).
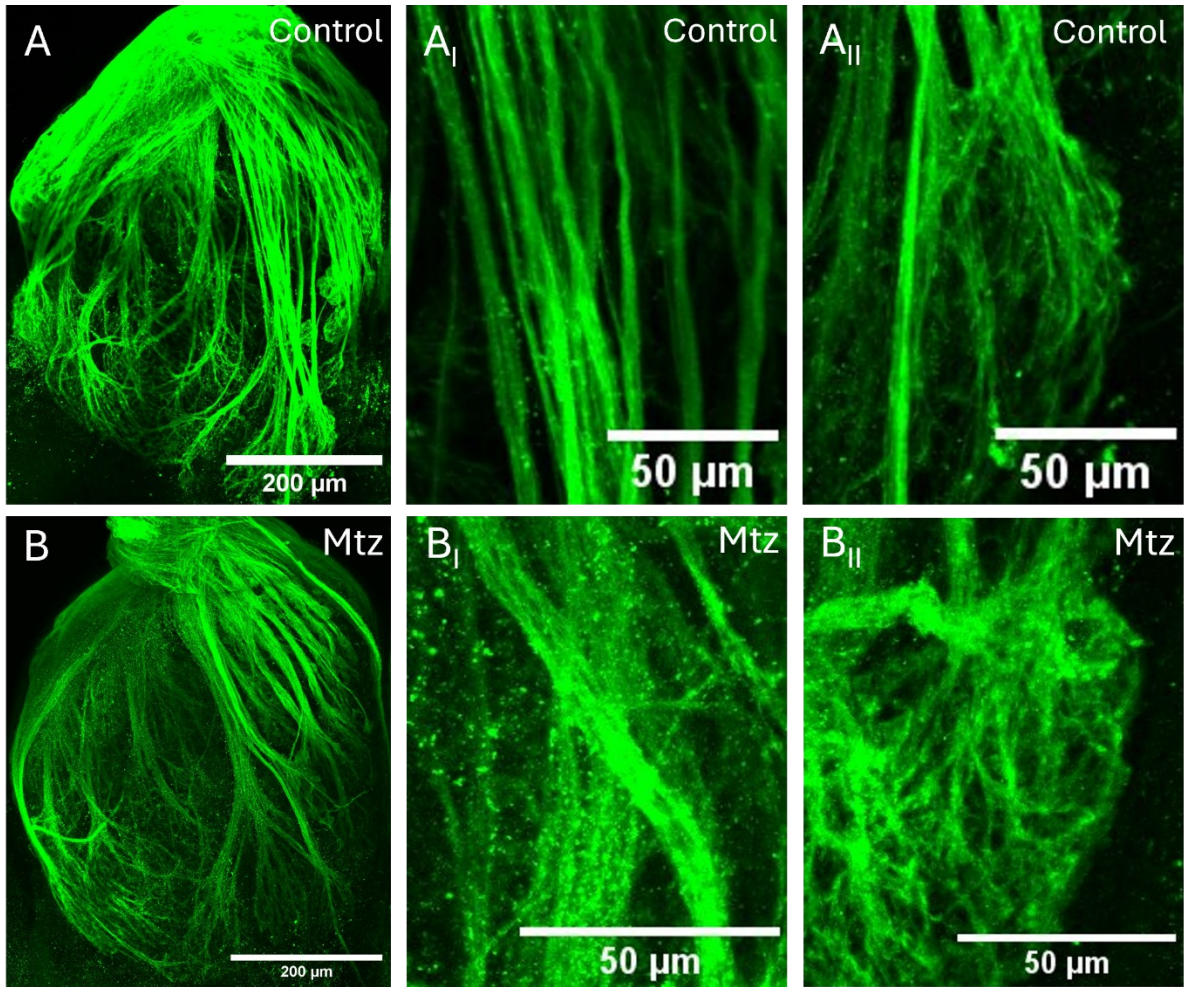
Figure 43: Anti-Keyhole Limpet Hemocyanin staining of olfactory sensory neurons (OSNs) in 24-hr Mtz-treated zebrafish olfactory bulbs (OBs).

Figure 44: Anti-Keyhole Limpet Hemocyanin staining of olfactory sensory neurons (OSNs) in an assortment of Mtz-treated olfactory bulbs (OBs). It was difficult to choose a representative example because there was so much variation between bulbs. Some bulbs possessed near normal staining except for some slightly degraded glomeruli (A). Others were missing some OSNs, but there was no consistency on the regions of the bulb where this occurred (B). In some bulbs, OSNs were largely absent with small blebs which may have been the remnants of glomeruli (C & D).
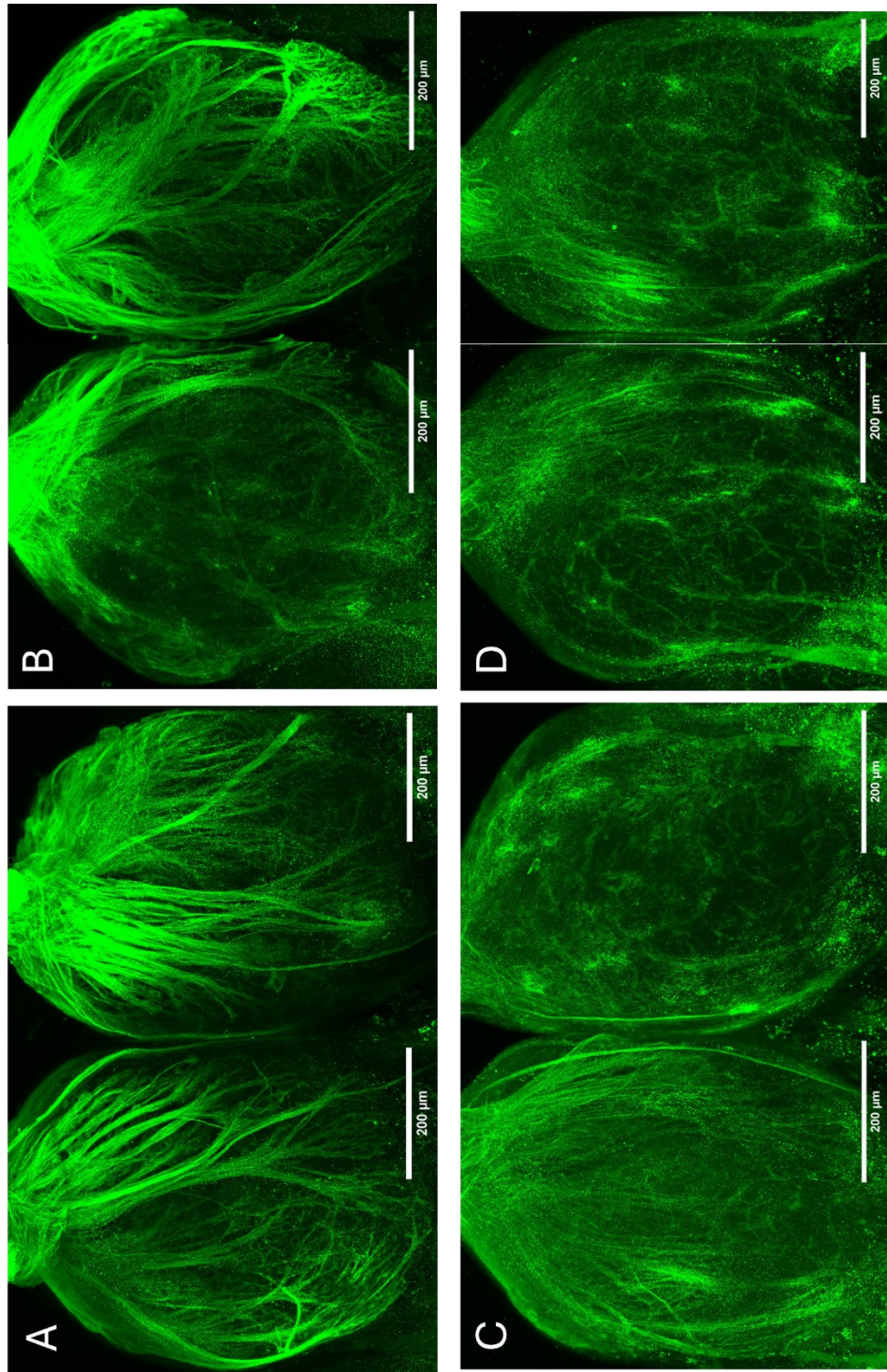
Figure 44: Anti-Keyhole Limpet Hemocyanin staining of olfactory sensory neurons (OSNs) in an assortment of Mtz-treated olfactory bulbs (OBs).

Chapter 6: General Discussion

6.1 Summary

The goal of this thesis was to investigate the dopaminergic neurons of the zebrafish olfactory bulb using various methods including immunohistochemistry, behaviour analysis and administration of environmental toxins. In Chapter 2, I described the normal anatomy of the TH+ cells in the olfactory bulb, and how it changed during development of the fish. I identified four cell types/subtypes which appear to have specific functions and noted differences in the lateral and medial regions of the bulb, specifically the uniquely dopaminergic innervation of the medial olfactory tract. In Chapter 3, I developed an appetitive olfactory learning paradigm which successfully trained fish to respond to the odour of phenylethyl alcohol after four days of conditioning. I then used the apparatus and baseline food odour response to examine the effects of environmental manganese exposure on olfactory behaviours in Chapter 4. I also showed that manganese exposure reduced the number TH+ cells by 50% and majorly disrupted the olfactory sensory neurons (OSNs) of the bulb. Given the sensitivity of the olfactory system to environmental contaminants shown in Chapter 4, I questioned whether an additional control was needed for a recently published report on a metronidazole (Mtz)-based chemogenetic ablation technique, which claimed to specifically target TH+ cells in the olfactory bulb of zebrafish. Thus, in Chapter 5, I concluded that exposure to Mtz alone causes a 30% reduction in TH+ cells and variable disruptions to the OSNs. In addition, anxiogenic behaviour was noted along with reduced olfactory responses to odours.

6.2 Description Of TH+ Cell Types

There were four cell types identified in Chapter 2. By far the most common type were cells without axons or with axons that were undetectable using the methods described. These cells were evenly distributed in all regions of the bulb. The second most numerous cells were unipolar cells having a single neurite that did not branch within 10 μm of the soma, which were also found all evenly throughout the bulb. Next was technically a subpopulation of unipolar cells that possessed a neurite branch within 10 μm of the cell body. In this study, they were only noted near the division between the forebrain and olfactory bulb, with the cell body usually near the division between the two regions and the two branches projecting into the forebrain and olfactory bulb, respectively. Given the location and morphology, it is likely that these cells are involved in modulating the mitral cell relay between the bulb and the olfactory tract. Not all cells in this area possessed these branched neurites, in fact those cells were in the minority with less than a dozen distinguishable in the adult bulb. The final type are multipolar cells, typically possessing two neurites; however, several cells had three neurites. Initially, multipolar cells seemed to be located mostly in the medial bulb, but in older animals, they were noted all over the bulb. In some reptiles, both unipolar and multipolar TH+ cells were observed, with the unipolar cells but not the multipolar cells being closely associated with glomeruli (Kosaka et al., 1991). In rodents, TH+ cells were divided by soma size, with large cells innervating multiple glomeruli and small cells only innervating one (Kosaka and Kosaka, 2009). One could reasonably hypothesize that at least some of the unipolar cells in zebrafish are associated with glomeruli, like in reptiles,

given their location (Fig. 3); and the multipolar cells could be responsible for intra- or inter-region connectivity. However, further investigation into the specific types of dopaminergic receptors in the bulb is needed before conclusions can be drawn.

Noted differences in the lateral vs medial olfactory bulb

There were apparent differences in the lateral and medial regions of the bulb throughout development. The medial region generally possessed more TH+ cell bodies and a larger percentage of neurites than the lateral side. The neurites on the medial side also tended to be longer than the lateral neurites. There are several possible explanations for these differences. As noted in Chapter 2, the medial cells appeared earlier in development than many of the lateral cells, and were therefore more mature. Another reason, also discussed in Chapter 2, was that different regions of the bulb are responsible for the processing of different odours. Lateral glomeruli are activated when amino acids are detected by the fish, and they are largely associated with food. Zebrafish are largely visual animals and rely on vision for food identification; it is therefore possible that specific identification and discrimination of amino acids is not as crucial for successful feeding. Furthermore, for the first week of life, larvae do not eat but instead rely on their remaining yolk sac for nourishment (Parichy et al., 2009). Shorter neurites may also indicate that the TH+-cells are closely associated with a particular glomerulus and not involved in crosstalk or inhibition between regions. Medial glomeruli are mainly responsible for the detection of social cues, like shoaling, mating and danger detection. Longer neurites in this region may indicate communication between distinct areas of the bulb, as most of the noted longer neurites

were relatively straight, without turns or convolutions. The most notable difference was the uniquely dopaminergic innervation of the medial olfactory tract. By adulthood, the medial posterior region of the bulb is continuous with the medial olfactory tract. As mentioned above, not only do some cells innervate in both directions, but many unbranched neurites are also present in this area.

6.3 Environmental Toxins Cause Olfactory Deficits But Also Side Effects

The manganese-exposed fish showed reduced sensitivity at low dose amino acids and inappropriate responses at high dose by dropping to the bottom of the tank. However, it is unclear what portion of the response was due to the loss of the TH+ cells, OSNs or both. Other studies examining the effects of TH+ cell loss on olfactory behaviour also did not examine the OSNs, so there is little available information for comparison. As discussed in Chapter 4, other heavy metals are known to disrupt OSNs in zebrafish, so it would be conservative to hypothesize that this is also true of manganese. These studies did note that manganese-exposed fish exhibit anxiety-like behaviour including spending more time at the bottom of the tank, which was confirmed in my study as well. Therefore, it is difficult to determine the extent to which the behavioural changes were caused by specific loss of the TH+ cells or due to stress and general degradation of the bulb. The Mtz study compounded this problem. There was a loss of TH+ cells, albeit smaller than produced by the long-term manganese exposure, but still a discernable disruption of OSNs. The behavioural responses of these fish to both studied odours were slightly blunted, possibly indicating that the detection threshold for these odours may have been affected. Even the Mtz-treated fish exhibited some anxiety-like

behaviour, namely resting lower in the tank than the controls. Therefore, it seemed that specific ablation of the olfactory TH+ cells without impacting other cells may be harder to achieve than originally determined. The stress of exposure may have had a larger impact on olfactory behaviour than anticipated and obscured the true effect of cell loss. It was also difficult to determine the true source of the stress responses. The direct effect of the chemical or the exposure process could be responsible, but anosmia or hyposmia has also been noted to cause anxiety-like behaviour in zebrafish (Abreu et al., 2016).

6.4 Benefits Of Easily Adaptable Olfactory Learning Paradigms

The learning paradigm developed in Chapter 3, while not fully utilized in Chapters 4 and 5, would be largely beneficial for further investigation of olfactory behaviour. This was a simple, cost-effective setup with reasonable water requirements that could be operated in any zebrafish facility. Though this experiment used a flow-through system, it could easily be switched to recirculation for the night to reduce water needs. In fact, depending on the scent used and its chemical makeup, the system could be modified to break down or filter out the odourant so the experiments could be run completely on recirculated water. Some of our earlier learning paradigms that utilized auditory or visual cues operated quite successfully using recirculated water from a standard 10-gallon (38 L) aquarium reservoir with a charcoal and particulate filter to run four 3 L tanks at a time (Doyle et al., 2017). These adjustments would make this paradigm readily accessible to any researcher.

This paradigm would be useful for further examination of the effects of various substances on the olfactory system. In addition to using the paradigm for odourant exposures, as in Chapters 4 and 5, it can also be used to examine if the fish are able to detect the odour enough to form an association. Also, it may be unclear whether the chemical exposure has affected the ability of the fish to form associations in the first place. This paradigm can also be combined with our visual and auditory-based paradigms to determine if the fish are still capable of learning or if only the olfactory system is affected (Doyle et al., 2017). Olfactory discrimination experiments would be easily designed using this method as well. Fish exposed to ablative chemicals could be appetitively conditioned to a particular odour and then exposed to another odour after training. This could determine their ability to differentiate between the two odours or whether the fish respond to both in a similar fashion. Hyposmic fish may also misidentify odours and respond incorrectly, as seen in Chapter 4 when the manganese-exposed fish displayed a stress response to amino acids.

6.5 Future Directions: Can Ablation Really Be Specific?

This thesis demonstrates that it is difficult to specifically ablate the dopaminergic neurons without affecting other cells in the olfactory bulb. As seen in Chapters 4 and 5, this may have had confounding effects on the fish's response to odours and even their general behaviour. Here I examined the effects of both manganese and metronidazole; however, other potential chemicals to specifically ablate dopaminergic neurons also exist. The hydroxylated analogue of dopamine, 6-hydroxydopamine (6-OHDA), has a high affinity for the dopamine transporter, which carries 6-OHDA inside of the

dopaminergic neurons, where it accumulates and causes cell death (Blandini and Armentero, 2012). Intramuscular injections of 6-OHDA in zebrafish caused locomotor defects and decreased dopamine levels in the brain, which indicate that 6-OHDA can cross the blood-brain barrier (BBB) even more readily in zebrafish than in mammals (Murray et al., 1975; Anichtchik et al., 2004). When 6-OHDA was administered to larval and adult zebrafish, there was a significant reduction in the number of TH positive neurons in the diencephalon, hypothalamus, posterior tuberculum, ventral thalamus and pretectum (Parng et al., 2007; Vijayanathan et al., 2017). The challenge with 6-OHDA lies with the method of exposure. Only larvae have been successfully exposed using a bath application method due to the increased permeability of zebrafish embryos to the environment (Lam et al., 2005). In adults, the substance must be directly injected into the area of interest or there is a risk of affecting other areas of the brain and consequently other behaviours. Targeting the olfactory bulb via injection without major physical damage would be difficult due to its small size.

Another alternative is 1-methyl-4-phenyl-1,2,3,6-tetrahydropyridine (MPTP), a well-documented method of inducing dopaminergic neurodegeneration in a variety of animals (Dauer et al., 2002). The highly lipophilic MPTP crosses the blood brain barrier and is converted to the metabolite 1-methyl-4phenylpyridinium ion (MPP+) by the enzyme monoamine oxidase B (Blandini and Armentero, 2012). MPP+ has a high affinity for the dopamine transporter and is carried into the dopaminergic neurons of the substantia nigra in mammals where it blocks mitochondrial Complex I activity (Blandini and Armentero, 2012).

When exposed to MPTP, zebrafish exhibit a loss of dopaminergic neurons in the diencephalon, and adult zebrafish showed decreases in swimming responses (Bretaud et al., 2004; Lam et al., 2005; Babu et al., 2016). Like 6-OHDA, bath applications have only been successful in larvae, and injections must be localized to the bulb to avoid side effects. One solution is to place a small amount of MPTP into the olfactory pit to exploit the possibility that it could travel up the olfactory nerve to the bulb given its highly lipophilic nature. As discussed in Chapters 1 and 4, some substances can travel up the olfactory nerve to the bulb, but it is unknown if 6-OHDA and MPTP are capable of the same function. If this method is effective, it would prove an easier, less traumatic way of administering these chemicals to the olfactory bulbs specifically, with potentially minimum off-target effects.

6.6 Conclusions

This thesis provided a solid foundation of the description of the TH+ cells in the zebrafish olfactory bulb both in adults and throughout development, which further builds on the previous work of cataloguing other olfactory cells and provides a jumping off point for deeper studies into the intricacies of these interneurons. It has also provided insight into the difficulty of specifically targeting TH+ cells in the bulb without other confounding factors like stress or other affected cells. These findings also highlight the need for alternative exposure methods with little or no off-target effects, considering the general environmental sensitivity of the olfactory system. This thesis also underlines the importance of olfactory research in early detection of human diseases, like Alzheimer's and Parkinson's Disease. A thorough understanding of the

olfactory system could facilitate the development of treatments for olfactory

dysfunction, which is particularly topical with the widespread cases of COVID-19-

induced anosmia.

References

Abreu, M. S., Giacomini, A. C. V. V., Kalueff, A. V., and Barcellos, L. J. G. (2016). The smell of "anxiety": Behavioral modulation by experimental anosmia in zebrafish. *Physiol. Behav.* 157, 67–71. doi:10.1016/j.physbeh.2016.01.030.

Agetsuma, M., Aoki, T., Aoki, R., and Okamoto, H. (2012). Cued fear conditioning in zebrafish (Danio rerio). *Zebrafish Protoc. Neurobehav. Res.* 66, 257–264. doi:10.1007/978-1-61779-597-8_19.

Ahuja, G., Nia, S. B., Zapilko, V., Shiriagin, V., Kowatschew, D., Oka, Y., et al. (2015). Kappe neurons, a novel population of olfactory sensory neurons. *Sci. Rep.* 4. doi:10.1038/SREP04037.

Alamdari, H. H., Kilcup, N., Ford, Z., Wilfart, F., Roach, D. C., and Schmidt, M. (2018). Design and Development of a High-Throughput System for Learning and Memory Research on Zebrafish. *J. Behav. Brain Sci.* 08, 351–368. doi:10.4236/jbbs.2018.86023.

Altenhofen, S., Wiprich, M. T., Nery, L. R., Leite, C. E., Vianna, M. R. M. R., and Bonan, C. D. (2017). Manganese(II) chloride alters behavioral and neurochemical parameters in larvae and adult zebrafish. *Aquat. Toxicol.* 182, 172–183. doi:10.1016/J.AQUATOX.2016.11.013.

Anichtchik, O. V., Kaslin, J., Peitsaro, N., Scheinin, M., and Panula, P. (2004). Neurochemical and behavioural changes in zebrafish Danio rerio after systemic administration of 6-hydroxydopamine and 1-methyl-4-phenyl-1,2,3,6-tetrahydropyridine. *J. Neurochem.* 88, 443–453. doi:10.1111/j.1471-4159.2004.02190.x.

Arduino (2014). Classic Arduino IDE 1.06. Available at: https://www.arduino.cc/en/Main/OldSoftwareReleases#previous.

Argo, S., Weth, F., and Korsching, S. I. (2003). Analysis of penetrance and expressivity during ontogenesis supports a stochastic choice of zebrafish odorant receptors from predetermined groups of receptor genes. *Eur. J. Neurosci.* 17, 833–843. doi:10.1046/J.1460-9568.2003.02505.X.

Attems, J., Walker, L., and Jellinger, K. A. (2015). Olfaction and Aging: A Mini-Review. *Gerontology* 61, 485–490. doi:10.1159/000381619.

Avdesh, A., Martin-Iverson, M. T., Mondal, A., Chen, M., Askraba, S., Morgan, N., et al. (2012). Evaluation of color preference in zebrafish for learning and memory. *J. Alzheimer's Dis.* 28, 459–469. doi:10.3233/JAD-2011-110704.

Babu, N. S., Murthy, C. L. N., Kakara, S., Sharma, R., Brahmendra Swamy, C. V., and Idris, M. M. (2016). 1-Methyl-4-phenyl-1,2,3,6-tetrahydropyridine induced Parkinson's disease in zebrafish. *Proteomics* 16, 1407–1420. doi:10.1002/pmic.201500291.

Baier, H., and Korsching, S. (1994). Olfactory glomeruli in the zebrafish form an invariant pattern and are identifiable across animals. *J. Neurosci.* 14, 219–230. Available at: http://www.jneurosci.org/content/jneuro/14/1/219.full.pdf [Accessed February 18, 2017].

Bang, Y., Lim, J., and Choi, H. J. (2021). Recent advances in the pathology of prodromal non-motor symptoms olfactory deficit and depression in Parkinson's disease: clues to early diagnosis and effective treatment. *Arch. Pharm. Res.* 44, 588–604. doi:10.1007/s12272-021-01337-3.

Barker, H. A. (1981). Amino Acid Degradation by Anaerobic Bacteria. *Annu. Rev. Biochem.* 50, 23–40. doi:10.1146/annurev.bi.50.070181.000323.

Barth, A. L., Justice, N. J., and Ngai, J. (1996). Asynchronous Onset of Odorant Receptor Expression in the Developing Zebrafish Olfactory System.

Best, J. D., and Alderton, W. K. (2008). Zebrafish: An in vivo model for the study of neurological diseases. *Neuropsychiatr. Dis. Treat.* 4, 567–576. doi:10.1006/dbio.2001.0201.

Biechl, D., Tietje, K., Gerlach, G., and Wullimann, M. F. (2016). Crypt cells are involved in kin recognition in larval zebrafish. *Sci. Rep.* 6, 24590. doi:10.1038/srep24590.

Biechl, D., Tietje, K., Ryu, S., Grothe, B., Gerlach, G., and Wullimann, M. F. (2017). Identification of accessory olfactory system and medial amygdala in the zebrafish. *Sci. Rep.* 7, 1–17. doi:10.1038/srep44295.

Bilotta, J., Risner, M. L., Davis, E. C., and Haggbloom, S. J. (2005). Assessing appetitive choice discrimination learning in zebrafish. *Zebrafish* 2, 259–268. doi:10.1089/zeb.2005.2.259.

Bjørklund, G., Chartrand, M. S., and Aaseth, J. (2017). Manganese exposure and neurotoxic effects in children. *Environ. Res.* 155, 380–384. doi:10.1016/J.ENVRES.2017.03.003.

Blandini, F., and Armentero, M.-T. (2012). Animal Models of Parkinson's Disease. *FEBS J.* 279, 1156–1166. doi:https://doi.org/10.1111/j.1742-4658.2012.08491.x.

Blank, M., Guerim, L. D., Cordeiro, R. F., and Vianna, M. R. M. (2009). A one-trial inhibitory avoidance task to zebrafish: Rapid acquisition of an NMDA-dependent long-term memory. *Neurobiol. Learn. Mem.* 92, 529–534. doi:10.1016/j.nlm.2009.07.001.

Blaser, R. E., and Rosemberg, D. B. (2012). Measures of Anxiety in Zebrafish (Danio rerio): Dissociation of Black/White Preference and Novel Tank Test. *PLoS One* 7, e36931. doi:10.1371/journal.pone.0036931.

Blechinger, S. R., Kusch, R. C., Haugo, K., Matz, C., Chivers, D. P., and Krone, P. H. (2007). Brief embryonic cadmium exposure induces a stress response and cell death in the

developing olfactory system followed by long-term olfactory deficits in juvenile zebrafish. *Toxicol. Appl. Pharmacol.* 224, 72–80. doi:10.1016/J.TAAP.2007.06.025.

Boesveldt, S., Postma, E. M., Boak, D., Welge-Luessen, A., Schöpf, V., Mainland, J. D., et al. (2017). Anosmia-A Clinical Review. *Chem. Senses* 42, 513–523. doi:10.1093/chemse/bjx025.

Bouchard, M. F., Sauvé, S., Barbeau, B., Legrand, M., Brodeur, M. È., Bouffard, T., et al. (2011). Intellectual impairment in school-age children exposed to manganese from drinking water. *Environ. Health Perspect.* 119, 138–143. doi:10.1289/ehp.1002321.

Bové, J., Prou, D., Perier, C., and Przedborski, S. (2005). Toxin-Induced Models of Parkinson's Disease. *Am. Soc. Exp. Neurother.* 2, 484–494. doi:10.4061/2011/520640.

Boyd, J. D., and Delaney, K. R. (2002). Tyrosine hydroxylase-immunoreactive interneurons in the olfactory bulb of the frogs Rana pipiens and Xenopus laevis. *J. Comp. Neurol.* 454, 42–57. doi:10.1002/cne.10428.

Braubach, O. R. (2011). Development, organization and plasiticty of the zebrafish olfactory system. [Doctoral dissertation, Dalhousie University]. Dalhousie Institutional Repository. https://dalspace.library.dal.ca/handle/10222/13342

Braubach, O. R, and Croll, R. P. (2021). The glomerular network of the zebrafish olfactory bulb. *Cell Tissue Res.* 383, 255–271. doi:10.1007/S00441-020-03394-4/FIGURES/7.

Braubach, O. R., Fine, A., and Croll, R. P. (2012). Distribution and functional organization of glomeruli in the olfactory bulbs of zebrafish (Danio rerio). *J. Comp. Neurol.* 520, 2317–2339. doi:10.1002/cne.23075.

Braubach, O. R., Miyasaka, N., Koide, T., Yoshihara, Y., Croll, R. P., and Fine, A. (2013). Experience-dependent versus experience-independent postembryonic development of distinct groups of zebrafish olfactory glomeruli. *J. Neurosci.* 33, 6905–16. doi:10.1523/JNEUROSCI.5185-12.2013.

Braubach, O. R., Wood, H., Gadbois, S., Fine, A., and Croll, R. P. (2009). Olfactory conditioning in the zebrafish. *Behav. brain …* 18, 9977–9988. doi:doi:10.1016/j.bbr.2008.10.044.

Braubach, O. R., Wyeth, R. C., Murray, A., Fine, A., and Croll, R. P. (2011). "A simple and effective method to condition olfactory behaviors in groups of zebrafish," in *Neuromethods*, 85–97. doi:10.1007/978-1-60761-953-6_7.

Braubach, O., Tombaz, T., Geiller, T., Homma, R., Bozza, T., Cohen, L. B., et al. (2018). Sparsened neuronal activity in an optogenetically activated olfactory glomerulus. *Sci. Rep.* 8. doi:10.1038/s41598-018-33021-w.

Bretaud, S., Lee, S., and Guo, S. (2004). Sensivity of zebrafish to environmental toxins implicated in Parkinson's disease. in *Neurotoxicology and Teratology*, 857–864.

doi:10.1016/j.ntt.2004.06.014.

Briggs, J. P. (2002). The zebrafish: A new model organism for integrative physiology. *Am. J. Physiol. - Regul. Integr. Comp. Physiol.* 282. doi:10.1152/AJPREGU.00589.2001.

Broglio, C., Rodríguez, F., Gómez, A., Arias, J. L., and Salas, C. (2010). Selective involvement of the goldfish lateral pallium in spatial memory. *Behav. Brain Res.* 210, 191–201. doi:10.1016/j.bbr.2010.02.031.

Buatois, A., Siddiqi, Z., Naim, S., Marawi, T., and Gerlai, R. (2024). A simple semi-automated home-tank method and procedure to explore classical associative learning in adult zebrafish. *Behav. Res. Methods* 56, 736–749. doi:10.3758/s13428-023-02076-7.

Buck, L., and Axel, R. (1991). A novel multigene family may encode odorant receptors: A molecular basis for odor recognition. *Cell* 65, 175–187. doi:10.1016/0092-8674(91)90418-X.

Bundschuh, S., Zhu, P., Schärer, Y.-P., and Friedrich, R. (2012). Dopaminergic Modulation of Mitral Cells and Odor Responses in the Zebrafish Olfactory Bulb. *J. Neurosci.* 32, 6830–6840. doi:10.1523/JNEUROSCI.6026-11.2012.

Buske, C., and Gerlai, R. (2011). Shoaling develops with age in Zebrafish (Danio rerio). *Prog. Neuro-Psychopharmacology Biol. Psychiatry* 35, 1409–1415. doi:10.1016/j.pnpbp.2010.09.003.

Byrd, C. A. (2000). Deafferentation-induced changes in the olfactory bulb of adult zebrafish. *Brain Res.* 866, 92–100. doi:10.1016/S0006-8993(00)02252-6.

Byrd, C. A., and Brunjes, P. C. (1995). Organization of the olfactory system in the adult zebrafish: Histological, immunohistochemical, and quantitative analysis. *J. Comp. Neurol.* 358, 247–259. doi:10.1002/cne.903580207.

Byrd, C. A., Jones, J. T., Quattro, J. M., Rogers, M. E., Brunjes, P. C., and Vogt, R. G. (1996). Ontogeny of odorant receptor gene expression in zebrafish, Danio rerio. *J. Neurobiol.* 29, 445–458. doi:10.1002/(SICI)1097-4695(199604)29:4<445::AID-NEU3>3.0.CO;2-8.

Cachat, J., Stewart, A., Grossman, L., Gaikwad, S., Kadri, F., Chung, K. M., et al. (2010). Measuring behavioral and endocrine responses to novelty stress in adult zebrafish. *Nat. Protoc.* 5, 1786–1799. doi:10.1038/nprot.2010.140.

Calderon-Garciduenas, L., Rodriguez-Alcaraz, A., Villarreal-Calderon, A., Lyght, O., Janszen, D., and Morgan, K. T. (1998). Nasal epithelium as a sentinel for airborne environmental pollution. *Toxicol. Sci.* 46, 352–364. doi:10.1006/toxs.1998.2549.

Calne, D. B., Chu, N. S., Huang, C. C., Lu, C. S., and Olanow, W. (1994). Manganism and idiopathic parkinsonism: Similarities and differences. *Neurology* 44, 1583–1586. doi:10.1212/wnl.44.9.1583.

Calvo-Ochoa, E., and Byrd-Jacobs, C. A. (2019). The Olfactory System of Zebrafish as a Model for the Study of Neurotoxicity and Injury: Implications for Neuroplasticity and Disease. *Int. J. Mol. Sci.* 20. doi:10.3390/ijms20071639.

Caramillo, E. M., and Echevarria, D. J. (2017). Alzheimer's disease in the zebrafish: Where can we take it? *Behav. Pharmacol.* 28, 179–186. doi:10.1097/FBP.0000000000000284.

Carvan, M. J., Loucks, E., Weber, D. N., and Williams, F. E. (2004). Ethanol effects on the developing zebrafish: Neurobehavior and skeletal morphogenesis. in *Neurotoxicology and Teratology*, 757–768. doi:10.1016/j.ntt.2004.06.016.

Chacko, A., Delbaz, A., Walkden, H., Basu, S., Armitage, C. W., Eindorf, T., et al. (2022). Chlamydia pneumoniae can infect the central nervous system via the olfactory and trigeminal nerves and contributes to Alzheimer's disease risk. *Sci. Rep.* 12, 2759. doi:10.1038/s41598-022-06749-9.

Chacon, D. M., and Luchiari, A. C. (2014). A dose for the wiser is enough: The alcohol benefits for associative learning in zebrafish. *Prog. Neuro-Psychopharmacology Biol. Psychiatry* 53, 109–115. doi:10.1016/j.pnpbp.2014.03.009.

Champagne, D. L., Hoefnagels, C. C. M., de Kloet, R. E., and Richardson, M. K. (2010). Translating rodent behavioral repertoire to zebrafish (Danio rerio): Relevance for stress research. *Behav. Brain Res.* 214, 332–342. doi:10.1016/J.BBR.2010.06.001.

Charan, J., and Kantharia, N. (2013). How to calculate sample size in animal studies? *J. Pharmacol. Pharmacother.* 4, 303–306. doi:10.4103/0976-500X.119726.

Chen, K., Wang, C. Q., Fan, Y. Q., Xie, Y. S., Yin, Z. F., Xu, Z. J., et al. (2014). The evaluation of rapid cooling as an anesthetic method for the zebrafish. *Zebrafish* 11, 71–75. doi:10.1089/zeb.2012.0858.

Chen, P., Culbreth, M., and Aschner, M. (2016). Exposure, epidemiology, and mechanism of the environmental toxicant manganese. *Environ. Sci. Pollut. Res.* 23, 13802–13810. doi:10.1007/s11356-016-6687-0.

Chen, Y. C., Priyadarshini, M., and Panula, P. (2009). Complementary developmental expression of the two tyrosine hydroxylase transcripts in zebrafish. *Histochem. Cell Biol.* 132, 375–381. doi:10.1007/s00418-009-0619-8.

Chia, J. S. M., Wall, E. S., Wee, C. L., Rowland, T. A. J., Cheng, R. K., Cheow, K., et al. (2019). Bacteria evoke alarm behaviour in zebrafish. *Nat. Commun.* 10. doi:10.1038/s41467-019-11608-9.

Christou, M., Kavaliauskis, A., … E. R.-S. of the T., 2020, undefined, Ropstad, E., William, T., et al. (2019). DMSO effects larval zebrafish (Danio rerio) behavior, with additive and interaction effects when combined with positive controls. *Elsevier*. doi:10.1016/j.scitotenv.2019.134490.

Clark, K. J., Urban, M. D., Skuster, K. J., and Ekker, S. C. (2011). "Transgenic zebrafish using transposable elements," in *Methods in Cell Biology* (Academic Press), 137–149. doi:10.1016/B978-0-12-374814-0.00008-2.

Clarke, C., and Upson, S. (2017). A global portrait of the manganese industry—A socioeconomic perspective. *Neurotoxicology* 58, 173–179. doi:10.1016/j.neuro.2016.03.013.

Coggeshall, R. E., and Lekan, H. A. (1996). Methods for determining numbers of cells and synapses: A case for more uniform standards of review. *J. Comp. Neurol.* 364, 6–15. doi:10.1002/(SICI)1096-9861(19960101)364:1<6::AID-CNE2>3.0.CO;2-9.

Colwill, R. M., and Creton, R. (2011). Imaging escape and avoidance behavior in zebrafish larvae. *Rev. Neurosci.* 22, 63–73. doi:10.1515/RNS.2011.008.

Colwill, R. M., Raymond, M. P., Ferreira, L., and Escudero, H. (2005). Visual discrimination learning in zebrafish (Danio rerio). *Behav. Processes* 70, 19–31. doi:10.1016/j.beproc.2005.03.001.

Cummings, J. L. (2004). Treatment of Alzheimer's disease: current and future therapeutic approaches. *Rev. Neurol. Dis.* 1, 60–9. Available at: http://www.ncbi.nlm.nih.gov/pubmed/16400259 [Accessed November 11, 2018].

Cuoghi, B., and Mola, L. (2007). Microglia of teleosts: Facing a challenge in neurobiology. *Eur. J. Histochem.* 51, 231–239. Available at: https://search-proquest-com.ezproxy.library.dal.ca/docview/876292801?accountid=10406 [Accessed November 21, 2018].

Curado, S., Stainier, D. Y. R., and Anderson, R. M. (2008). Nitroreductase-mediated cell/tissue ablation in zebrafish: A spatially and temporally controlled ablation method with applications in developmental and regeneration studies. *Nat. Protoc.* 3, 948–954. doi:10.1038/nprot.2008.58.

Dauer, W., Kholodilov, N., Vila, M., Trillat, A.-C., Goodchild, R., Larsen, K. E., et al. (2002). Resistance of α-synuclein null mice to the parkinsonian neurotoxin MPTP. *Proc. Natl. Acad. Sci.* 99, 14524–14529. doi:10.1073/pnas.172514599.

De Koning, C., Beekhuijzen, M., Van De Waart, B., Tobor-Kapłon, M., De Vries-Buitenweg, S., Schoutsen, D., et al. (2015). Visualizing compound distribution during zebrafish embryo development: the effects of lipophilicity and DMSO. *Wiley Online Libr.* 104, 253–272. doi:10.1002/bdrb.21166.

Dieris, M., Ahuja, G., Krishna, V., and Korsching, S. I. (2017). A single identified glomerulus in the zebrafish olfactory bulb carries the high-Affinity response to death-Associated odor cadaverine. *Sci. Rep.* 7. doi:10.1038/srep40892.

Dinis-Oliveira, R. J., Remião, F., Carmo, H., Duarte, J. A., Navarro, A. S., Bastos, M. L., et al. (2006). Paraquat exposure as an etiological factor of Parkinson's disease. *Neurotoxicology* 27, 1110–1122. doi:10.1016/j.neuro.2006.05.012.

dos Santos, T. G., Mussulini, B. H. M., Frangipani, L. A., and de Oliveira, D. L. (2020). Differential impact of shorter and longer periods of environmental enrichment on adult zebrafish exploratory activity (Danio rerio) in the novel tank paradigm. *Behav. Processes* 181, 104278. doi:10.1016/j.beproc.2020.104278.

Doty, R. L. (1976). *Mammalian olfaction, reproductive processes, and behavior*. First. New York: Academic Press Available at: https://books.google.ca/books?hl=en&lr=&id=PWwCnplyxYYC&oi=fnd&pg=PP1&dq=olfaction+review+mammals&ots=nOAZT-MbfF&sig=8X4Y29H5U1v8gzvDu1EUKFGJK6Y#v=onepage&q=olfaction review mammals&f=false [Accessed March 3, 2017].

Doyle, J. M., and Croll, R. P. (2022). A Critical Review of Zebrafish Models of Parkinson's Disease. *Front. Pharmacol.* 13. doi:10.3389/fphar.2022.835827.

Doyle, J. M., Merovitch, N., Wyeth, R. C., Stoyek, M. R., Schmidt, M., Wilfart, F., et al. (2017). A simple automated system for appetitive conditioning of zebrafish in their home tanks. *Behav. Brain Res.* 317, 444–452. doi:10.1016/j.bbr.2016.09.044.

Duka, Y. D., Ilchenko, S. I., Kharytonov, M. M., and Vasylyeva, T. L. (2011). Impact of open manganese mines on the health of children dwelling in the surrounding area. *Emerg. Health Threats J.* 4, 7110. doi:10.3402/ehtj.v4i0.7110.

E3 medium (for zebrafish embryos) (2011). *Cold Spring Harb. Protoc.* 2011, pdb.rec66449. doi:10.1101/pdb.rec066449.

Edwards, J. G., and Michel, W. C. (2002). Odor-stimulated glutamatergic neurotransmission in the zebrafish olfactory bulb. *J. Comp. Neurol.* 454, 294–309. doi:10.1002/cne.10445.

Engeszer, R. E., Da Barbiano, L. A., Ryan, M. J., and Parichy, D. M. (2007). Timing and plasticity of shoaling behaviour in the zebrafish, Danio rerio. *Anim. Behav.* 74, 1269–1275. doi:10.1016/j.anbehav.2007.01.032.

Fasano, G., Godoy, R. S., Angiulli, E., Consalvo, A., Franco, C., Mancini, M., et al. (2021). Effects of low-dose methylcyclopentadienyl manganese tricarbonyl-derived manganese on the development of diencephalic dopaminergic neurons in zebrafish. *Environ. Pollut.* 287, 117151. doi:10.1016/j.envpol.2021.117151.

Fatuzzo, I., Niccolini, G. F., Zoccali, F., Cavalcanti, L., Bellizzi, M. G., Riccardi, G., et al. (2023). Neurons, Nose, and Neurodegenerative Diseases: Olfactory Function and Cognitive Impairment. *Int. J. Mol. Sci.* 24. doi:10.3390/ijms24032117.

Friedrich, R. W., and Korsching, S. I. (1997). Combinatorial and chemotopic odorant coding in the zebrafish olfactory bulb visualized by optical imaging. *Neuron* 18, 737–752. doi:10.1016/S0896-6273(00)80314-1.

Friedrich, R. W., and Korsching, S. I. (1998). Chemotopic, Combinatorial, and Noncombinatorial Odorant Representations in the Olfactory Bulb Revealed Using a

Voltage-Sensitive Axon Tracer. *J. Neurosci.* 18, 9977–9988.

Fujita, I., Sorensen, P. W., Stacey, N. E., and Hara, T. J. (1991). The olfactory system, not the terminal nerve, functions as the primary chemosensory pathway mediating responses to sex pheromones in male goldfish. *Brain. Behav. Evol.* 38, 313–321. doi:10.1159/000114397.

Fullard, M. E., Morley, J. F., and Duda, J. E. (2017). Olfactory Dysfunction as an Early Biomarker in Parkinson's Disease. *Neurosci. Bull.* 33, 515–525. doi:10.1007/s12264-017-0170-x.

Fuller, C. L., and Byrd, C. A. (2005). Ruffed cells identified in the adult zebrafish olfactory bulb. *Neurosci. Lett.* 379, 190–194. doi:10.1016/j.neulet.2004.12.062.

Fuller, C. L., Yettaw, H. K., and Byrd, C. A. (2006). Mitral cells in the olfactory bulb of adult zebrafish (Danio rerio): morphology and distribution. *J. Comp. Neurol.* 499, 218–230. doi:10.1002/CNE.21091.

Gayoso, J. A., Castro, A., Anadon, R., and Manso, M. J. (2011). Differential bulbar and extrabulbar projections of diverse olfactory receptor neuron populations in the adult zebrafish (Danio rerio). *J. Comp. Neurol.* 519, 247–276. doi:10.1002/cne.22518.

Gerlach, G., Tietje, K., Biechl, D., Namekawa, I., Schalm, G., and Sulmann, A. (2019). Behavioural and neuronal basis of olfactory imprinting and kin recognition in larval fish. *J. Exp. Biol.* 222. doi:10.1242/jeb.189746.

Gerlai, R. (2010). High-throughput behavioral screens: The first step towards finding genes involved in vertebrate brain function using zebrafish. *Molecules* 15, 2609–2622. doi:10.3390/molecules15042609.

Gobba, F. (2006). Olfactory toxicity: Long-term effects of occupational exposures. *Int. Arch. Occup. Environ. Health* 79, 322–331. doi:10.1007/s00420-005-0043-x.

Gobba, F., and Abbacchini, C. (2012). ANOSMIA AFTER EXPOSURE TO A PYRETHRIN-BASED INSECTICIDE: A CASE REPORT. *Int. J. Occup. Med. Environ. Health* 25, 506–512. doi:10.2478/S13382-012-0060-4.

Godoy, R., Hua, K., Kalyn, M., Cusson, V. M., Anisman, H., and Ekker, M. (2020). Dopaminergic neurons regenerate following chemogenetic ablation in the olfactory bulb of adult Zebrafish (Danio rerio). *Sci. Rep.* 10, 12825. doi:10.1038/s41598-020-69734-0.

Godoy, R., Noble, S., Yoon, K., Anisman, H., and Ekker, M. (2015). Chemogenetic ablation of dopaminergic neurons leads to transient locomotor impairments in zebrafish larvae. *J. Neurochem.* 135, 249–260. doi:10.1111/jnc.13214.

Goetz, R. U., and Zilberman, D. (2000). The dynamics of spatial pollution: The case of phosphorus runoff from agricultural land. *J. Econ. Dyn. Control* 24, 143–163.

doi:10.1016/s0165-1889(98)00067-0.

Gong, Y., Zhao, D., and Wang, Q. (2018). An overview of field-scale studies on remediation of soil contaminated with heavy metals and metalloids: Technical progress over the last decade. *Water Res.* 147, 440–460. doi:10.1016/j.watres.2018.10.024.

Guarneros, M., Ortiz-Romo, N., Alcaraz-Zubeldia, M., Drucker-Colín, R., and Hudson, R. (2013). Nonoccupational environmental exposure to manganese is linked to deficits in peripheral and central olfactory function. *Chem. Senses* 38, 783–791. doi:10.1093/chemse/bjt045.

Hajikhani, B., Calcagno, T., Nasiri, M. J., Jamshidi, P., Dadashi, M., Goudarzi, M., et al. (2020). Olfactory and gustatory dysfunction in COVID-19 patients: A meta-analysis study. *Physiol. Rep.* 8, e14578. doi:10.14814/PHY2.14578.

Halpern, M. E., Rhee, J., Goll, M. G., Akitake, C. M., Parsons, M., and Leach, S. D. (2008). Gal4/UAS transgenic tools and their application to zebrafish. *Zebrafish* 5, 97–110. doi:10.1089/zeb.2008.0530.

Han, A. Y., Mukdad, L., Long, J. L., and Lopez, I. A. (2020). Anosmia in COVID-19: Mechanisms and Significance. *Chem. Senses* 45, 423–428. doi:10.1093/CHEMSE/BJAA040.

Hansen, A., and Zeiske, E. (1993). Development of the olfactory organ in the zebrafish, Brachydanio rerio. *J. Comp. Neurol.* 333, 289–300. doi:10.1002/CNE.903330213.

Hara, T. J. (1994). Olfaction and gustation in fish: an overview. *Acta Physiol. Scand.* 152, 207–217. doi:10.1111/j.1748-1716.1994.tb09800.x.

Harden, M. V., Newton, L. A., Lloyd, R. C., and Whitlock, K. E. (2006). Olfactory imprinting is correlated with changes in gene expression in the olfactory epithelia of the zebrafish. *J. Neurobiol.* 66, 1452–1466. doi:10.1002/neu.20328.

Harrass, S., Yi, C., and Chen, H. (2021). Chronic rhinosinusitis and alzheimer's disease—a possible role for the nasal microbiome in causing neurodegeneration in the elderly. *Int. J. Mol. Sci.* 22. doi:10.3390/ijms222011207.

Harro, J. (2018). Animals, anxiety, and anxiety disorders: How to measure anxiety in rodents and why. *Behav. Brain Res.* 352, 81–93. doi:10.1016/J.BBR.2017.10.016.

Hasler, A., Scholz, A., and Horrall, R. (1978). Olfactory Imprinting and Homing in Salmon: Recent experiments in which salmon have been artificially imprinted to a synthetic chemical verify the olfactory hypothesis for salmon homing. *Am. Sci.* 66, 347–355.

Hassenklöver, T., and Manzini, I. (2013). Olfactory wiring logic in amphibians challenges the basic assumptions of the unbranched axon concept. *J. Neurosci.* 33, 17247–17252. doi:10.1523/JNEUROSCI.2755-13.2013.

Hernández Ceruelos, A., Romero-Quezada, L. C., Ruvalcaba Ledezma, J. C., and López

Contreras, L. (2019). Therapeutic uses of metronidazole and its side effects: An update. *Eur. Rev. Med. Pharmacol. Sci.* 23, 397–401. doi:10.26355/eurrev_201901_16788.

Hillman, E. M. C., Voleti, V., Li, W., and Yu, H. (2019). Light-Sheet Microscopy in Neuroscience. *Annu. Rev. Neurosci.* 42, 295–313. doi:10.1146/annurev-neuro-070918-050357.

Howe, D. G., Bradford, Y. M., Eagle, A., Fashena, D., Frazer, K., Kalita, P., et al. (2017). The Zebrafish Model Organism Database: New support for human disease models, mutation details, gene expression phenotypes and searching. *Nucleic Acids Res.* 45, D758–D768. doi:10.1093/nar/gkw1116.

Hoyberghs, J., Bars, C., Ayuso, M., Van Ginneken, C., Foubert, K., and Van Cruchten, S. (2021). DMSO Concentrations up to 1% are Safe to be Used in the Zebrafish Embryo Developmental Toxicity Assay. *Front. Toxicol.* 3. doi:10.3389/FTOX.2021.804033/FULL.

Hsia, A. Y., Vincent, J. D., and Lledo, P. M. (1999). Dopamine depresses synaptic inputs into the olfactory bulb. *J. Neurophysiol.* 82, 1082–1085. doi:10.1152/jn.1999.82.2.1082.

Hussain, A., Saraiva, L. R., Ferrero, D. M., Ahuja, G., Krishna, V. S., Liberles, S. D., et al. (2013). High-affinity olfactory receptor for the death-associated odor cadaverine. *Proc Natl Acad Sci U S A* 110, 19579–19584. doi:10.1073/pnas.1318596110.

Imamura, F., Ito, A., and LaFever, B. J. (2020). Subpopulations of Projection Neurons in the Olfactory Bulb. *Front. Neural Circuits* 14, 561822. doi:10.3389/fncir.2020.561822.

Jesuthasan, S. J., and Mathuru, A. S. (2008). The Alarm Response in Zebrafish: Innate Fear in a Vertebrate Genetic Model. *J. Neurogenet.* 22, 211–228. doi:10.1080/01677060802298475.

Jesuthasan, S., Krishnan, S., Cheng, R. K., and Mathuru, A. (2021). Neural correlates of state transitions elicited by a chemosensory danger cue. *Prog. Neuro-Psychopharmacology Biol. Psychiatry* 111, 110110. doi:10.1016/j.pnpbp.2020.110110.

Jiang, T., and Holley, A. (1992). Morphological variations among output neurons of the olfactory bulb in the frog (Rana ridibunda). *J. Comp. Neurol.* 320, 86–96. doi:10.1002/cne.903200106.

Jones, S. V., Choi, D. C., Davis, M., and Ressler, K. J. (2008). Learning-dependent structural plasticity in the adult olfactory pathway. *J. Neurosci.* 28, 13106–11. doi:10.1523/JNEUROSCI.4465-08.2008.

Kalueff, A. V, Gebhardt, M., Stewart, A. M., Cachat, J. M., Brimmer, M., Chawla, J. S., et al. (2013). Towards a comprehensive catalog of zebrafish behavior 1.0 and beyond.

Zebrafish 10, 70–86. doi:10.1089/zeb.2012.0861.

Karnik, I., and Gerlai, R. (2012). Can zebrafish learn spatial tasks? An empirical analysis of place and single CS-US associative learning. *Behav. Brain Res.* 233, 415–421. doi:10.1016/j.bbr.2012.05.024.

Khan, K. M., Collier, A. D., Meshalkina, D. A., Kysil, E. V, Khatsko, S. L., Kolesnikova, T., et al. (2017). Zebrafish models in neuropsychopharmacology and CNS drug discovery. *Br. J. Pharmacol.* 174, 1925–1944. doi:10.1111/bph.13754.

Kimmel, C. B., Ballard, W. W., Kimmel, S. R., Ullmann, B., and Schilling, T. F. (1995). Stages of embryonic development of the zebrafish. *Dev. Dyn.* 203, 253–310. doi:10.1002/aja.1002030302.

Koide, T., Miyasaka, N., Morimoto, K., Asakawa, K., Urasaki, A., Kawakami, K., et al. (2009). Olfactory neural circuitry for attraction to amino acids revealed by transposon-mediated gene trap approach in zebrafish. *Proc. Natl. Acad. Sci. U. S. A.* 106, 9884–9889. doi:10.1073/pnas.0900470106.

Kosaka, K., and Kosaka, T. (2007). Chemical properties of type 1 and type 2 periglomerular cells in the mouse olfactory bulb are different from those in the rat olfactory bulb. *Brain Res.* 1167, 42–55. doi:10.1016/J.BRAINRES.2007.04.087.

Kosaka, T., and Hama, K. (1982). Structure of the mitral cell in the olfactory bulb of the goldfish Carassius auratus. *J. Comp. Neurol.* 212, 365–384. doi:10.1002/cne.902120405.

Kosaka, T., and Kosaka, K. (2009). Two types of tyrosine hydroxylase positive GABAergic juxtaglomerular neurons in the mouse main olfactory bulb are different in their time of origin. *Neurosci. Res.* 64, 436–441. doi:10.1016/j.neures.2009.04.018.

Kosaka, T., Kosaka, K., and Nagatsu, I. (1991). Tyrosine hydroxylase-like immunoreactive neurons in the olfactory bulb of the snake, Elaphe quadrivirgata, with special reference to the colocalization of tyrosine hydroxylase- and GABA-like immunoreactivities. *Exp. Brain Res.* 87, 353–362. doi:10.1007/BF00231852/METRICS.

Kosaka, T., Pignatelli, A., and Kosaka, K. (2020). Heterogeneity of tyrosine hydroxylase expressing neurons in the main olfactory bulb of the mouse. *Neurosci. Res.* 157, 15–33. doi:10.1016/j.neures.2019.10.004.

Kotrschal, K. (2000). Taste(s) and olfaction(s) in fish: a review of spezialized sub-systems and central integration. *Pflügers Arch. - Eur. J. Physiol.* 439, r178–r180. doi:10.1007/s004240000137.

Lam, C. S., Korzh, V., and Strahle, U. (2005). Zebrafish embryos are susceptible to the dopaminergic neurotoxin MPTP. *Eur. J. Neurosci.* 21, 1758–1762. doi:10.1111/j.1460-9568.2005.03988.x.

Langheinrich, U. (2003). Zebrafish: A new model on the pharmaceutical catwalk. *BioEssays* 25, 904–912. doi:10.1002/bies.10326.

Larriva-Sahd, J. (2008). The accessory olfactory bulb in the adult rat: A cytological study of its cell types, neuropil, neuronal modules, and interactions with the main olfactory system. *J. Comp. Neurol.* 510, 309–350. doi:10.1002/cne.21790.

Lazzari, M., Bettini, S., Milani, L., Maurizii, M. G., and Franceschini, V. (2019). Differential nickel-induced responses of olfactory sensory neuron populations in zebrafish. *Aquat. Toxicol.* 206, 14–23. doi:10.1016/j.aquatox.2018.10.011.

Leitsch, D. (2019). A review on metronidazole: An old warhorse in antimicrobial chemotherapy. *Parasitology* 146, 1167–1178. doi:10.1017/S0031182017002025.

Li, J., Mack, J. a, Souren, M., Yaksi, E., Higashijima, S., Mione, M., et al. (2005). Early development of functional spatial maps in the zebrafish olfactory bulb. *J. Neurosci.* 25, 5784–5795. doi:10.1523/JNEUROSCI.0922-05.2005.

Li, P., Shah, S., Huang, L., Carr, A. L., Gao, Y., Thisse, C., et al. (2007). Cloning and spatial and temporal expression of the zebrafish dopamine D1 receptor. *Dev. Dyn.* 236, 1339–1346. doi:10.1002/dvdy.21130.

Lieschke, G. J., and Currie, P. D. (2007). Animal models of human disease: Zebrafish swim into view. *Nat. Rev. Genet.* 8, 353–367. doi:10.1038/nrg2091.

Lindsay, S. M., and Vogt, R. G. (2004). Behavioral Responses of Newly Hatched Zebrafish (Danio rerio) to Amino Acid Chemostimulants. *Chem. Senses* 29, 93–100. doi:10.1093/chemse/bjh009.

Lindsey, B. W., Smith, F. M., and Croll, R. P. (2010). From inflation to flotation: Contribution of the swimbladder to whole-body density and swimming depth during development of the zebrafish (Danio rerio). *Zebrafish* 7, 85–96. doi:10.1089/zeb.2009.0616.

Linney, E., Upchurch, L., and Donerly, S. (2004). Zebrafish as a neurotoxicological model. *Neurotoxicol. Teratol.* 26, 709–718. doi:10.1016/j.ntt.2004.06.015.

Lipton, S. A., and Rosenberg, P. A. (1994). Excitatory amino acids as a final common pathway for neurologic disorders. *N. Engl. J. Med.* 330, 613–622. doi:10.1056/NEJM199403033300907.

Lucore, E. C., and Connaughton, V. P. (2021). Observational learning and irreversible starvation in first-feeding zebrafish larvae: is it okay to copy from your friends? *Zoology* 145, 125896. doi:10.1016/j.zool.2021.125896.

Lynam, D. R., Roos, J. W., Pfeifer, G. D., Fort, B. F., and Pullin, T. G. (1999). Environmental effects and exposures to manganese from use of methylcyclopentadienyl manganese tricarbonyl (MMT) in gasoline. *Neurotoxicology* 20, 145–150. Available at: https://europepmc.org/article/med/10385878 [Accessed

March 27, 2024].

Ma, E. Y., Heffern, K., Cheresh, J., and Gallagher, E. P. (2018). Differential copper-induced death and regeneration of olfactory sensory neuron populations and neurobehavioral function in larval zebrafish. *Neurotoxicology* 69, 141–151. doi:10.1016/j.neuro.2018.10.002.

MacDonald, T. C., Sylvain, N. J., James, A. K., Pickering, I. J., Krone, P. H., and George, G. N. (2016). Effects of inorganic mercury on the olfactory pits of zebrafish larvae. *Metallomics* 8, 514–517. doi:10.1039/c6mt00031b.

Macrides, F., and Schneider, S. P. (1982). Laminar organization of mitral and tufted cells in the main olfactory bulb of the adult hamster. *J. Comp. Neurol.* 208, 419–430. doi:10.1002/cne.902080410.

Manning-Bog, A. B., McCormack, A. L., Purisai, M. G., Bolin, L. M., and Di Monte, D. A. (2003). Alpha-synuclein overexpression protects against paraquat-induced neurodegeneration. *J. Neurosci.* 23, 3095–9. doi:10.1523/JNEUROSCI.23-08-03095.2003.

Mathis, S., Le Masson, G., Soulages, A., Duval, F., Carla, L., Vallat, J.-M., et al. (2021). Olfaction and anosmia: From ancient times to COVID-19. *J. Neurol. Sci.* 425, 117433. doi:10.1016/j.jns.2021.117433.

Merovitch, N. H. (2016). A simple automated system for appetitive conditioning of zebrafish in their home tank and underlying neural activation.

Meyers, J. R. (2018). Zebrafish: Development of a Vertebrate Model Organism. *Curr. Protoc. Essent. Lab. Tech.* 16. doi:10.1002/CPET.19.

Miller, N., and Gerlai, R. (2012). "Automated tracking of zebrafish shoals and the analysis of shoaling behavior," in *Zebrafish Protocols for Neurobehavioral Research* (Humana Press, Totowa, NJ), 217–230. doi:10.1007/978-1-61779-597-8.

Miyasaka, N., Knaut, H., and Yoshihara, Y. (2007). Cxcl12/Cxcr4 chemokine signaling is required for placode assembly and sensory axon pathfinding in the zebrafish olfactory system. *Development* 134, 2459–68. doi:10.1242/dev.001958.

Miyasaka, N., Wanner, A. A., Li, J., Mack-Bucher, J., Genoud, C., Yoshihara, Y., et al. (2012). Functional development of the olfactory system in zebrafish. doi:10.1016/j.mod.2012.09.001.

Modney, B. K., and Hatton, G. I. (1989). Multiple Synapse Formation: A Possible Compensatory Mechanism for Increased Cell Size in Rat Supraoptic Nucleus. *J. Neuroendocrinol.* 1, 21–27. doi:10.1111/j.1365-2826.1989.tb00072.x.

Mohammed, A. S., Kapri, A., and Goel, R. (2011). "Heavy Metal Pollution: Source, Impact, and Remedies," in *Biomanagement of Metal-Contaiminated Soils* (Springer, Dordrecht), 1–28. doi:10.1007/978-94-007-1914-9_1.

Mombaerts, P. (2006). Axonal wiring in the mouse olfactory system. *Annu. Rev. Cell Dev. Biol.* 22, 713–37. doi:10.1146/annurev.cellbio.21.012804.093915.

Mombaerts, P., Wang, F., Dulac, C., Chao, S. K., Nemes, A., Mendelsohn, M., et al. (1996). Visualizing an olfactory sensory map. *Cell* 87, 675–686. doi:10.1016/S0092-8674(00)81387-2.

Moretz, J. A., Martins, E. P., and Robison, B. D. (2007). Behavioral syndromes and the evolution of correlated behavior in zebrafish. *Behav. Ecol.* 18, 556–562. doi:10.1093/beheco/arm011.

Mori, K., Kishi, K., and Ojima, H. (1983). Distribution of dendrites of mitral, displaced mitral, tufted, and granule cells in the rabbit olfactory bulb. *J. Comp. Neurol.* 219, 339–355. doi:10.1002/cne.902190308.

Mori, K., Nagao, H., and Yoshihara, Y. (1999). The olfactory bulb: coding and processing of odor molecule information. *Science (80-.).* 286, 711–5. doi:10.1126/science.286.5440.711.

Morin, C., de Souza Silva, M. A., Müller, C. P., Hardigan, P., and Spieler, R. E. (2013). Active avoidance learning in zebrafish (Danio rerio)-The role of sensory modality and inter-stimulus interval. *Behav. Brain Res.* 248, 141–143. doi:10.1016/j.bbr.2013.04.009.

Mueller, K. P., and Neuhauss, S. C. F. (2012). Automated visual choice discrimination learning in zebrafish (Danio rerio). *J. Integr. Neurosci.* 11, 73–85. doi:10.1142/S0219635212500057.

Mueller, T., Dong, Z., Berberoglu, M. A., and Guo, S. (2011). The dorsal pallium in zebrafish, Danio rerio (Cyprinidae, Teleostei). *Brain Res.* 1381, 95–105. doi:10.1016/j.brainres.2010.12.089.

Mueller, T., and Wullimann, M. F. (2009). An evolutionary interpretation of teleostean forebrain anatomy. in *Brain, Behavior and Evolution* (S. Karger AG), 30–42. doi:10.1159/000229011.

Müller, A., Österlund, H., Marsalek, J., and Viklander, M. (2020). The pollution conveyed by urban runoff: A review of sources. *Sci. Total Environ.* 709. doi:10.1016/j.scitotenv.2019.136125.

Murray, M., Jones, H., Cserr, H. F., and Rall, D. P. (1975). The blood-brain barrier and ventricular system of Myxine glutinosa. *Brain Res.* 99, 17–33. Available at: http://www.ncbi.nlm.nih.gov/pubmed/1188978 [Accessed November 16, 2018].

Musilova, J., Arvay, J., Vollmannova, A., Toth, T., and Tomas, J. (2016). Environmental Contamination by Heavy Metals in Region with Previous Mining Activity. *Bull. Environ. Contam. Toxicol.* 97, 569–575. doi:10.1007/s00128-016-1907-3.

Nadig, A. P. R., Huwaimel, B., Alobaida, A., Khafagy, E. S., Alotaibi, H. F., Moin, A., et al.

(2022). Manganese chloride (MnCl2) induced novel model of Parkinson's disease in adult Zebrafish; Involvement of oxidative stress, neuroinflammation and apoptosis pathway. *Biomed. Pharmacother.* 155. doi:10.1016/j.biopha.2022.113697.

Namekawa, I., Moenig, N. R., and Friedrich, R. W. (2018). Rapid olfactory discrimination learning in adult zebrafish. *Exp. Brain Res.* 236, 2959–2969. doi:10.1007/S00221-018-5352-X/FIGURES/5.

Nellore, J., and Nandita, P. (2015). Paraquat exposure induces behavioral deficits in larval zebrafish during the window of dopamine neurogenesis. *Toxicol. Reports* 2, 950–956. doi:10.1016/j.toxrep.2015.06.007.

Newman, M., Ebrahimie, E., and Lardelli, M. (2014). Using the zebrafish model for Alzheimer's disease research. *Front. Genet.* 5, 189. doi:10.3389/fgene.2014.00189.

Northcutt, R. G. (2011). Do teleost fishes possess a homolog of Mammalian isocortex? *Brain. Behav. Evol.* 78, 136–138. doi:10.1159/000330830.

Nussbaum, R., and Ellis, C. (2003). Alzheimer's disease and Parkinson's disease. *N. Engl. J. Med.* 348, 1356–1364. doi:10.1056/NEJM2003ra020003.

Oka, Y. (1983). Golgi, electron-microscopic and combined golgi-electron-microscopic studies of the mitral cells in the goldfish olfactory bulb. *Neuroscience* 8, 723–742. doi:10.1016/0306-4522(83)90006-4.

Oliva, A. M., Jones, K. R., and Restrepo, D. (2008). Sensory-dependent asymmetry for a urine-responsive olfactory bulb glomerulus. *J. Comp. Neurol.* 510, 475–483. doi:10.1002/cne.21800.

Olsén, K. H. (2011). "Effects of pollutants on olfactory mediated behaviors in fish and crustaceans," in *Chemical Communication in Crustaceans* (Springer New York), 507–529. doi:10.1007/978-0-387-77101-4_26.

Olsén, K. H. (2015). "Effects of Pollutants on Olfactory Detection and Responses to Chemical Cues Including Pheromones in Fish," in *Fish Pheromones and Related Cues* (Wiley Blackwell), 217–236. doi:10.1002/9781118794739.ch10.

Panula, P., Sallinen, V., Sundvik, M., Kolehmainen, J., Torkko, V., Tiittula, A., et al. (2006). Modulatory neurotransmitter systems and behavior: towards zebrafish models of neurodegenerative diseases. *Zebrafish* 3, 235–247. Available at: https://www.liebertpub.com/doi/abs/10.1089/zeb.2006.3.235 [Accessed October 11, 2018].

Parichy, D. M., Elizondo, M. R., Mills, M. G., Gordon, T. N., and Engeszer, E. (2009). Normal Table of Post-Embryonic Zebrafish Development: Staging by Externally Visible Anatomy of the Living Fish. *Dev. Dyn.* 238, 2975–3015. doi:10.1002/dvdy.22113.Normal.

Parng, C., Roy, N. M., Ton, C., Lin, Y., and McGrath, P. (2007). Neurotoxicity assessment

using zebrafish. *J. Pharmacol. Toxicol. Methods* 55, 103–112. doi:10.1016/j.vascn.2006.04.004.

Pather, S., and Gerlai, R. (2009). Shuttle box learning in zebrafish (Danio rerio). *Behav. Brain Res.* 196, 323–327. doi:10.1016/j.bbr.2008.09.013.

Pisharath, H., and Parsons, M. J. (2009). Nitroreductase-mediated cell ablation in transgenic zebrafish embryos. *Methods Mol. Biol.* 546, 133–143. doi:10.1007/978-1-60327-977-2_9.

Portavella, M., Torres, B., and Salas, C. (2004). Avoidance Response in Goldfish: Emotional and Temporal Involvement of Medial and Lateral Telencephalic Pallium. *J. Neurosci.* 24, 2335–2342. doi:10.1523/JNEUROSCI.4930-03.2004.

Potter, S. M., Zheng, C., Koos, D. S., Feinstein, P., Fraser, S. E., and Mombaerts, P. (2001). Structure and emergence of specific olfactory glomeruli in the mouse. *J. Neurosci.* 21, 9713–23. doi:21/24/9713 [pii].

Pressler, T. R., and Strowbridge, B. W. (2020). Activation of granule cell interneurons by two divergent local circuit pathways in the rat olfactory bulb. *J. Neurosci.* 40, 9701–9714. doi:10.1523/JNEUROSCI.0989-20.2020.

Racette, B. A., Nelson, G., Dlamini, W. W., Hershey, T., Prathibha, P., Turner, J. R., et al. (2022). Environmental manganese exposure and cognitive control in a South African population. *Neurotoxicology* 89, 31–40. doi:10.1016/j.neuro.2022.01.004.

Rana, A. Q., Ahmed, U. S., Chaudry, Z. M., and Vasan, S. (2015). Parkinson's disease: A review of non-motor symptoms. *Expert Rev. Neurother.* 15, 549–562. doi:10.1586/14737175.2015.1038244.

Reid, W. (2023). Neurodegenerative Diseases due to Neurotoxins passing through the Nose-to-Brain Pathway. *Med. Res. Arch.* 11. doi:10.18103/mra.v11i6.3898.

Riddle, D. R., and Oakley, B. (1992). Immunocytochemical identification of primary olfactory afferents in rainbow trout. *J. Comp. Neurol.* 324, 575–589. doi:10.1002/cne.903240410.

Riel, D. Van, Verdijk, R., and Kuiken, T. (2015). The olfactory nerve: A shortcut for influenza and other viral diseases into the central nervous system. *J. Pathol.* 235, 277–287. doi:10.1002/path.4461.

Rink, E., and Wullimann, M. F. (2002). Connections of the ventral telencephalon and tyrosine hydroxylase distribution in the zebrafish brain (Danio rerio) lead to identification of an ascending dopaminergic system in a teleost. in *Brain Research Bulletin*, 385–387. doi:10.1016/S0361-9230(01)00696-7.

Riojas-Rodríguez, H., Solís-Vivanco, R., Schilmann, A., Montes, S., Rodríguez, S., Ríos, C., et al. (2010). Intellectual function in Mexican children living in a mining area and environmentally exposed to manganese. *Environ. Health Perspect.* 118, 1465–1470.

doi:10.1289/ehp.0901229.

Rodríguez, F., López, J. C., Vargas, J. P., Gómez, Y., Broglio, C., and Salas, C. (2002). Conservation of Spatial Memory Function in the Pallial Forebrain of Reptiles and Ray-Finned Fishes. *J. Neurosci.* 22, 2894–2903. doi:10.1523/jneurosci.22-07-02894.2002.

Rolle-McFarland, D., Liu, Y., Mostafaei, F., Zauber, S. E., Zhou, Y., Li, Y., et al. (2019). The association of bone, fingernail and blood manganese with cognitive and olfactory function in Chinese workers. *Sci. Total Environ.* 666, 1003–1010. doi:10.1016/j.scitotenv.2019.02.208.

Ruan, Y., Zheng, X. Y., Zhang, H. L., Zhu, W., and Zhu, J. (2012). Olfactory dysfunctions in neurodegenerative disorders. *J. Neurosci. Res.* 90, 1693–1700. doi:10.1002/jnr.23054.

Rubinstein, A. L. (2006). Zebrafish assays for drug toxicity screening. *Expert Opin. Drug Metab. Toxicol.* 2, 231–240. doi:10.1517/17425255.2.2.231.

Ruzicka, L., Howe, D. G., Ramachandran, S., Toro, S., Van Slyke, C. E., Bradford, Y. M., et al. (2019). The Zebrafish Information Network: New support for non-coding genes, richer Gene Ontology annotations and the Alliance of Genome Resources. *Nucleic Acids Res.* 47, D867–D873. doi:10.1093/nar/gky1090.

Sager, J. J., Bai, Q., and Burton, E. A. (2010). Transgenic zebrafish models of neurodegenerative diseases. *Brain Struct. Funct.* 214, 285–302. doi:10.1007/s00429-009-0237-1.

Salas, C., Broglio, C., Durán, E., Gómez, A., Ocaña, F. M., Jiménez-Moya, F., et al. (2006). Neuropsychology of learning and memory in teleost fish. *Zebrafish* 3, 157–171. doi:10.1089/zeb.2006.3.157.

Santamaria, A. B., and Sulsky, S. I. (2010). Risk assessment of an essential element: Manganese. in *Journal of Toxicology and Environmental Health - Part A: Current Issues* (Taylor & Francis Group), 128–155. doi:10.1080/15287390903337118.

Satou, M. (1990). Synaptic organization, local neuronal circuitry, and functional segregation of the teleost olfactory bulb. *Prog. Neurobiol.* 34, 115–142. doi:10.1016/0301-0082(90)90004-Z.

Scangas, G. A., and Bleier, B. S. (2017). Anosmia: Differential Diagnosis, Evaluation, and Management. *https://doi.org/10.2500/ajra.2017.31.4403* 31, e3–e7. doi:10.2500/AJRA.2017.31.4403.

Schaefer, M. L., Finger, T. E., and Restrepo, D. (2001). Variability of position of the P2 glomerulus within a map of the mouse olfactory bulb. *J. Comp. Neurol.* 436, 351–362. doi:10.1002/cne.1072.

Scott, G. R., and Sloman, K. A. (2004). The effects of environmental pollutants on

complex fish behaviour: Integrating behavioural and physiological indicators of toxicity. *Aquat. Toxicol.* 68, 369–392. doi:10.1016/j.aquatox.2004.03.016.

Shao, X., Lakhina, V., Dang, P., Cheng, R. P., Marcaccio, C. L., and Raper, J. A. (2017). Olfactory sensory axons target specific protoglomeruli in the olfactory bulb of zebrafish. *Neural Dev.* 12. doi:10.1186/s13064-017-0095-0.

Sherer, T. B., Betarbet, R., Testa, C. M., Seo, B. B., Richardson, J. R., Kim, J. H., et al. (2003). Mechanism of toxicity in rotenone models of Parkinson's disease. *J Neurosci* 23, 10756–10764. doi:23/34/10756 [pii].

Shiba, K., Arai, T., Sato, S., Kubo, S. ichiro, Ohba, Y., Mizuno, Y., et al. (2009). Parkin stabilizes PINK1 through direct interaction. *Biochem. Biophys. Res. Commun.* 383, 331–335. doi:10.1016/j.bbrc.2009.04.006.

Silva, L., and Antunes, A. (2017). Vomeronasal Receptors in Vertebrates and the Evolution of Pheromone Detection. *Annu. Rev. Anim. Biosci.* 5, 353–370. doi:10.1146/annurev-animal-022516-022801.

Sison, M., and Gerlai, R. (2010). Associative learning in zebrafish (Danio rerio) in the plus maze. *Behav. Brain Res.* 207, 99–104. doi:10.1016/j.bbr.2009.09.043.

Sison, M., and Gerlai, R. (2011). Associative learning performance is impaired in zebrafish (Danio rerio) by the NMDA-R antagonist MK-801. *Neurobiol. Learn. Mem.* 96, 230–237. doi:10.1016/j.nlm.2011.04.016.Associative.

Sobel, N., Thomason, M. E., Stappen, I., Tanner, C. M., Tetrud, J. W., Bower, J. M., et al. (2001). An impairment in sniffing contributes to the olfactory impairment in Parkinson's disease. *Proc. Natl. Acad. Sci. U. S. A.* 98, 4154–4159. doi:10.1073/pnas.071061598.

Sousa, N., Almeida, O. F. X., and Wotjak, C. T. (2006). A hitchhiker's guide to behavioral analysis in laboratory rodents. *Genes, Brain Behav.* 5, 5–24. doi:10.1111/j.1601-183X.2006.00228.x.

Spence, R., Gerlach, G., Lawrence, C., and Smith, C. (2008). The behaviour and ecology of the zebrafish, Danio rerio. *Biol. Rev.* 83, 13–34. doi:10.1111/j.1469-185X.2007.00030.x.

Starcevic, S. L., and Zielinski, B. S. (1997). Glutathione and glutathione S-transferase in the rainbow trout olfactory mucosa during retrograde degeneration and regeneration of the olfactory nerve. *Exp. Neurol.* 146, 331–340. doi:10.1006/exnr.1997.6548.

Stewart, A. M., Grieco, F., Tegelenbosch, R. A. J., Kyzar, E. J., Nguyen, M., Kaluyeva, A., et al. (2015). A novel 3D method of locomotor analysis in adult zebrafish: Implications for automated detection of CNS drug-evoked phenotypes. *J. Neurosci. Methods* 255, 66–74. doi:10.1016/j.jneumeth.2015.07.023.

Stoddart, D. M. (1980). "The olfactory system of vertebrates," in *The Ecology of Vertebrate Olfaction* (Dordrecht: Springer Netherlands), 1–33. doi:10.1007/978-94-009-5869-2_1.

Stoyek, M. R., Croll, R. P., and Smith, F. M. (2015). Intrinsic and extrinsic innervation of the heart in zebrafish (Danio rerio). *J. Comp. Neurol.* 523, 1683–1700. doi:10.1002/cne.23764.

Sunderman, F. W. (2001). Nasal toxicity, carcinogenicity, and olfactory uptake of metals. *Ann. Clin. Lab. Sci.* 31, 3–24. Available at: http://www.annclinlabsci.org/content/31/1/3.short [Accessed March 22, 2024].

Susaki, E. A., Tainaka, K., Perrin, D., Kishino, F., Tawara, T., Watanabe, T. M., et al. (2014). Whole-brain imaging with single-cell resolution using chemical cocktails and computational analysis. *Cell* 157, 726–739. doi:10.1016/j.cell.2014.03.042.

Susaki, E. A., Tainaka, K., Perrin, D., Yukinaga, H., Kuno, A., and Ueda, H. R. (2015). Advanced CUBIC protocols for whole-brain and whole-body clearing and imaging. *Nat. Protoc.* 10, 1709–1727. doi:10.1038/nprot.2015.085.

Takeda, A. (2003). Manganese action in brain function. *Brain Res. Rev.* 41, 79–87. doi:10.1016/S0165-0173(02)00234-5.

Takesono, A., Dimitriadou, S., Clark, N. J., Handy, R. D., Mourabit, S., Winter, M. J., et al. (2023). Zinc oxide nanoparticles disrupt development and function of the olfactory sensory system impairing olfaction-mediated behaviour in zebrafish. *Environ. Int.* 180, 108227. doi:10.1016/j.envint.2023.108227.

Tierney, K. B. (2011). Behavioural assessments of neurotoxic effects and neurodegeneration in zebrafish. *Biochim. Biophys. Acta - Mol. Basis Dis.* 1812, 381–389. doi:10.1016/j.bbadis.2010.10.011.

Tierney, K. B., Baldwin, D. H., Hara, T. J., Ross, P. S., Scholz, N. L., and Kennedy, C. J. (2010). Olfactory toxicity in fishes. *Aquat. Toxicol.* 96, 2–26. doi:10.1016/J.AQUATOX.2009.09.019.

Tierney, K. B., Sekela, M. A., Cobbler, C. E., Xhabija, B., Gledhill, M., Ananvoranich, S., et al. (2011). Evidence For Behavioral Preference Toward Environmental Concentrations Of Urban-Use Herbicides In A Model Adult Fish. *Environ. Toxicol. Chem.* 30, 2046–2054. Available at: https://onlinelibrary.wiley.com/doi/full/10.1002/etc.588 [Accessed June 27, 2022].

Tissingh, G., Berendse, H. W., Bergmans, P., DeWaard, R., Drukarch, B., Stoof, J. C., et al. (2001). Loss of olfaction in De Novo and treated Parkinson's disease: Possible implications for early diagnosis. *Mov. Disord.* 16, 41–46. doi:10.1002/1531-8257(200101)16:1<41::AID-MDS1017>3.0.CO;2-M.

Tjälve, H., and Tallkvist, J. (2003). "The Olfactory Pathway as a Route of Entry of Metals into the Brain," in *Metal Ions and Neurodegenerative Disorders* (WORLD

SCIENTIFIC), 67–98. doi:10.1142/9789812796691_0003.

Toledo-Ibarra, G. A., Rojas-Mayorquín, A. E., and Girón-Pérez, M. I. (2013). Influence of the cholinergic system on the immune response of teleost fishes: Potential model in biomedical research. *Clin. Dev. Immunol.* 2013, 536534. doi:10.1155/2013/536534.

Valentinčič, T., Wegert, S., and Caprio, J. (1994). Learned olfactory discrimination versus innate taste responses to amino acids in channel catfish (Ictalurus punctatus). *Physiol. Behav.* 55, 865–873. doi:10.1016/0031-9384(94)90072-8.

Vaz, R. L., Outeiro, T. F., and Ferreira, J. J. (2018). Zebrafish as an animal model for drug discovery in Parkinson's disease and other movement disorders: A systematic review. *Front. Neurol.* 9. doi:10.3389/fneur.2018.00347.

Velez, Z., Hubbard, P. C., Alves, A., Costa, R. A., and Guerreiro, P. M. (2024). Environmental salinity modulates olfactory sensitivity in the euryhaline European seabass, Dicentrarchus labrax, acclimated to seawater and brackish water. *J. Exp. Biol.* 227. doi:10.1242/JEB.246448.

Vijayanathan, Y., Lim, F. T., Lim, S. M., Long, C. M., Tan, M. P., Majeed, A. B. A., et al. (2017). 6-OHDA-Lesioned Adult Zebrafish as a Useful Parkinson's Disease Model for Dopaminergic Neuroregeneration. *Neurotox. Res.* 32, 496–508. doi:10.1007/s12640-017-9778-x.

Villemagne, V. L., Burnham, S., Bourgeat, P., Brown, B., Ellis, K. A., Salvado, O., et al. (2013). Amyloid β deposition, neurodegeneration, and cognitive decline in sporadic Alzheimer's disease: A prospective cohort study. *Lancet Neurol.* 12, 357–367. doi:10.1016/S1474-4422(13)70044-9.

Volz, S. N., Hausen, J., Nachev, M., Ottermanns, R., Schiwy, S., and Hollert, H. (2020). Short exposure to cadmium disrupts the olfactory system of zebrafish (Danio rerio) – Relating altered gene expression in the olfactory organ to behavioral deficits. *Aquat. Toxicol.* 226, 105555. doi:10.1016/j.aquatox.2020.105555.

Voulvoulis, N., and Georges, K. (2015). "Industrial and agricultural sources and pathways of aquatic pollution," in *Impact of Water Pollution on Human Health and Environmental Sustainability* (IGI Global), 29–54. doi:10.4018/978-1-4666-9559-7.ch002.

Wager, K., and Russell, C. (2013). Mitophagy and neurodegeneration: The zebrafish model system. *Autophagy* 9, 1693–1709. doi:10.4161/auto.25082.

Wagner, S., Gresser, A. L., Torello, A. T., and Dulac, C. (2006). A Multireceptor Genetic Approach Uncovers an Ordered Integration of VNO Sensory Inputs in the Accessory Olfactory Bulb. *Neuron* 50, 697–709. doi:10.1016/j.neuron.2006.04.033.

Wallace, C. K., Bright, L. A., Marx, J. O., Andersen, R. P., Mullins, M. C., and Carty, A. J. (2018). Effectiveness of Rapid Cooling as a Method of Euthanasia for Young

Zebrafish (Danio rerio). *J. Am. Assoc. Lab. Anim. Sci.* 57, 58–63.

Wang, R., Shafi, M., Ma, J., Zhong, B., Guo, J., Hu, X., et al. (2018a). Effect of amendments on contaminated soil of multiple heavy metals and accumulation of heavy metals in plants. *Environ. Sci. Pollut. Res.* 25, 28695–28704. doi:10.1007/s11356-018-2918-x.

Wang, X. H., Souders, C. L., Zhao, Y. H., and Martyniuk, C. J. (2018b). Paraquat affects mitochondrial bioenergetics, dopamine system expression, and locomotor activity in zebrafish (Danio rerio). *Chemosphere* 191, 106–117. doi:10.1016/j.chemosphere.2017.10.032.

Ward, A. J. W., Duff, A. J., Horsfall, J. S., and Currie, S. (2008). Scents and scents-ability: Pollution disrupts chemical social recognition and shoaling in fish. *Proc. R. Soc. B Biol. Sci.* 275, 101–105. doi:10.1098/rspb.2007.1283.

Weiss, L., Jungblut, L. D., Pozzi, A. G., Zielinski, B. S., O'Connell, L. A., Hassenklöver, T., et al. (2020). Multi-glomerular projection of single olfactory receptor neurons is conserved among amphibians. *J. Comp. Neurol.* 528, 2239–2253. doi:10.1002/CNE.24887.

Whitcroft, K. L., and Hummel, T. (2019). Clinical Diagnosis and Current Management Strategies for Olfactory Dysfunction: A Review. *JAMA Otolaryngol. - Head Neck Surg.* 145, 846–853. doi:10.1001/jamaoto.2019.1728.

White, R. M., Sessa, A., Burke, C., Bowman, T., LeBlanc, J., Ceol, C., et al. (2008). Transparent Adult Zebrafish as a Tool for In Vivo Transplantation Analysis. *Cell Stem Cell* 2, 183–189. doi:10.1016/j.stem.2007.11.002.

Whitlock, K. E., and Westerfield, M. (1998). A transient population of neurons pioneers the olfactory pathway in the zebrafish. *J. Neurosci.* 18, 8919–27. Available at: http://www.ncbi.nlm.nih.gov/pubmed/9786997.

Whitlock, K. E., and Westerfield, M. (2000). The olfactory placodes of the zebrafish form by convergence of cellular fields at the edge of the neural plate. *Development* 127, 3645–3653. doi:10.1242/dev.127.17.3645.

Wiens, J. H. (1980). Agricultural runoff and water pollution. *Can. Water Resour. J.* 5, 78–89. doi:10.4296/cwrj0503078.

Winchester, R. L., and Martyn, K. (2020). Could Early Identification of Changes in Olfactory Function Be an Indicator of Preclinical Neurodegenerative Disease? A Systematic Review. *Neurol. Ther.* 9, 243–263. doi:10.1007/s40120-020-00199-z.

Wolman, M. A., Jain, R. A. R., Liss, L., and Granato, M. (2011). Chemical modulation of memory formation in larval zebrafish. *Proc. Natl. Acad. Sci. U. S. A.* 108, 15468–73. doi:10.1073/pnas.1107156108.

Wu, R., Yao, F., Li, X., Shi, C., Zang, X., Shu, X., et al. (2022). Manganese Pollution and Its

Remediation: A Review of Biological Removal and Promising Combination Strategies. *Microorganisms* 10, 2411. doi:10.3390/microorganisms10122411.

Wullimann, M. F., and Mueller, T. (2004). Teleostean and Mammalian Forebrains Contrasted : Evidence from Genes to. *J. Comp. Neurol.* 162, 143–162. doi:10.1002/cne.20183.

Wullimann, M. F., Rupp, B., and Reichert, H. (1996). The brain of the zebrafish Danio rerio: a neuroanatomical atlas. *Neuroanat. Zebrafish Brain*, 19–87. doi:10.1007/978-3-0348-8979-7_5.

Wullimann, M., and Rink, E. (2001). Detailed immunohistology of Pax6 protein and tyrosine hydroxylase in the early zebrafish brain suggests role of Pax6 gene in development of dopaminergic. *Dev. brain Res.* 131, 173–191. Available at: http://www.sciencedirect.com/science/article/pii/S016538060100270X [Accessed September 6, 2017].

Wyeth, R. C., Braubach, O. R., Fine, A., and Croll, R. P. (2011). Videograms: A method for repeatable unbiased quantitative behavioral analysis without scoring or tracking. *Neuromethods* 51, 15–33. doi:10.1007/978-1-60761-953-6_2.

Xu, X., Scott-Scheiern, T., Kempker, L., and Simons, K. (2007). Active avoidance conditioning in zebrafish (Danio rerio). *Neurobiol. Learn. Mem.* 87, 72–77. doi:10.1016/j.nlm.2006.06.002.

Xydakis, M. S., Albers, M. W., Holbrook, E. H., Lyon, D. M., Shih, R. Y., Frasnelli, J. A., et al. (2021). Post-viral effects of COVID-19 in the olfactory system and their implications. *Lancet Neurol.* 20, 753–761. doi:10.1016/S1474-4422(21)00182-4/ATTACHMENT/24EF7464-1995-4BF8-8135-7F75903AE1AB/MMC1.PDF.

Yasuoka, A., and Abe, K. (2009). Gustation in fish: Search for prototype of taste perception. *Results Probl. Cell Differ.* 47, 239–255. doi:10.1007/400_2008_6.

Yonekura, J., and Yokoi, M. (2008). Conditional genetic labeling of mitral cells of the mouse accessory olfactory bulb to visualize the organization of their apical dendritic tufts. *Mol. Cell. Neurosci.* 37, 708–718. doi:10.1016/j.mcn.2007.12.016.

Zhang, Y., Guldner, I. H., Nichols, E. L., Benirschke, D., Smith, C. J., Zhang, S., et al. (2021). Instant FLIM enables 4D in vivo lifetime imaging of intact and injured zebrafish and mouse brains. *Optica* 8, 885. doi:10.1364/optica.426870.

Zhou, X., Kumar, P., Bhuyan, D. J., Jensen, S. O., Roberts, T. L., and Münch, G. W. (2023). Neuroinflammation in Alzheimer's Disease: A Potential Role of Nose-Picking in Pathogen Entry via the Olfactory System? *Biomolecules* 13. doi:10.3390/biom13111568.

Zielinski, B. S., and Hara, T. J. (2006). Olfaction. *Fish Physiol.* 25, 1–43. doi:10.1016/S1546-5098(06)25001-5.

Zimmermann Prado Rodrigues, G., Beatris Mentges Staudt, L., Griebeler Moreira, M., Garbino dos Santos, T., Santos de Souza, M., Júnior Lúcio, C., et al. (2019). Histopathological, genotoxic, and behavioral damages induced by manganese (II) in adult zebrafish. doi:10.1016/j.chemosphere.2019.125550.

Zimmermann Prado Rodrigues, G., Staudt, L. B. M., Moreira, M. G., dos Santos, T. G., de Souza, M. S., Lúcio, C. J., et al. (2020). Histopathological, genotoxic, and behavioral damages induced by manganese (II) in adult zebrafish. *Chemosphere* 244. doi:10.1016/J.CHEMOSPHERE.2019.125550.

Zou, Y. M., Lu, D., Liu, L. P., Zhang, H. H., and Zhou, Y. Y. (2016). Olfactory dysfunction in Alzheimer's disease. *Neuropsychiatr. Dis. Treat.* 12, 869–875. doi:10.2147/NDT.S104886.

Appendix I – Supplemental Figures & Video

Supplemental Figure 1: Comparison of staining between two anti-tyrosine hydrolyse (TH) antibodies. (A) The two antibodies showed complete overlap in anti-TH staining. (B) Staining of an anti-TH antibody hosted in rabbit. (C) Staining of an anti-TH antibody hosted in mouse. This staining contained fewer artifacts than the rabbit-hosted antibody.
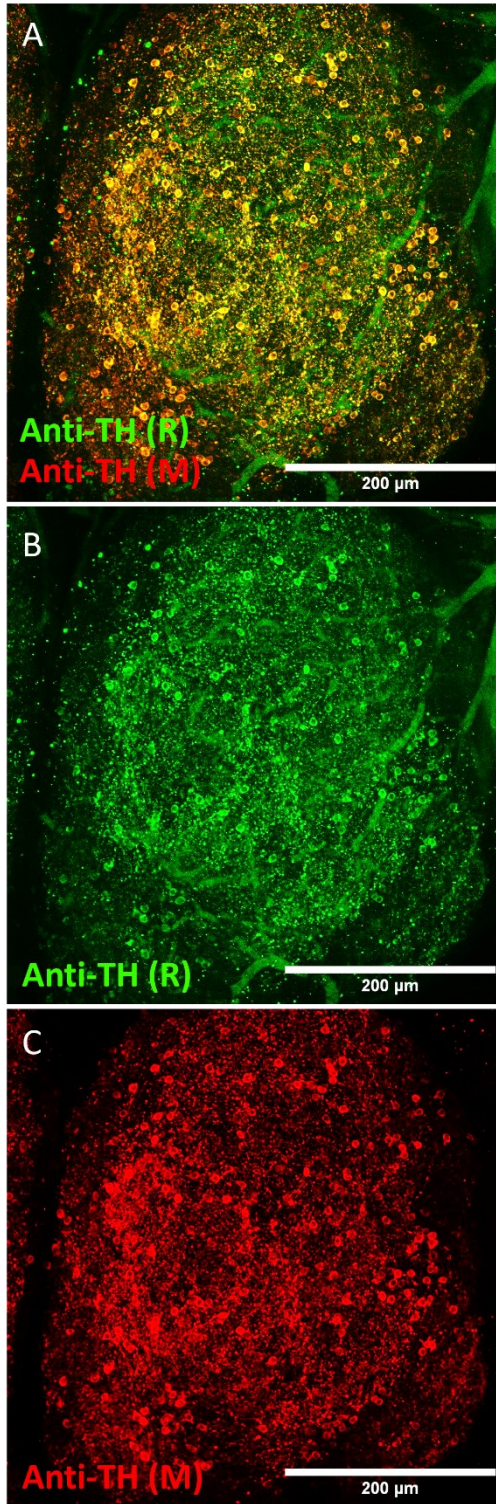
Supplemental Figure 1: Comparison of staining between two anti-tyrosine hydrolyse (TH) antibodies.

Supplemental Video 1: Modelling dispersal of odourant using food dye trial. After

injection, a single bolus of dye was visible for about 15 s and then broke into

concentrated swirls. The concentrated swirls were observable for approximately 120 s

before what appeared to be homogeneous dispersion throughout the tank. During the

dye experiment, all fish in the tank appeared to encounter the concentrated dye within

about 15 s. Thus, if PEA odourant dispersed similarly to the dye, each fish would be

expected to encounter an area of concentrated odourant before the food was

presented.

Supplemental Video 2: Representative video of acquisition trial 48 for auditory

conditioning in an experimental tank. Fish exhibit normal swimming behaviour in the

15 seconds before the presentation of conditioned stimulus. During the presentation of

the conditioned stimulus, indicated by the red light, fish displayed increased activity and

moved towards the food source (upper-left corner of the tank) in anticipation of the

food reward.

Appendix II – Arduino Sketch

```
#Olfactory Training Paradigm

#include <Time.h>

#include <TimeAlarms.h>

#include <DS1307RTC.h>

#include <Wire.h>

#include <Adafruit_MotorShield.h>

#include "utility/Adafruit_PWMServoDriver.h"


Adafruit_MotorShield AFMS = Adafruit_MotorShield();

Adafruit_StepperMotor *Motor1 = AFMS.getStepper(200, 1);

Adafruit_StepperMotor *Motor2 = AFMS.getStepper(200, 1);


void setup() {


 pinMode(5, OUTPUT);
 pinMode(6, OUTPUT);


 Serial.begin(9600);
 while (!Serial) ; // wait until Arduino Serial Monitor opens
 //setTime(9,59,0,9,31,14); // set time to Wednesday 15:18:00pm April 16 2014
  setSyncProvider(RTC.get);   // the function to get the time from the RTC
  Alarm.alarmRepeat(9,45,0, PumpOn);  // Set Alarm For 9:45AM Every Day
  Alarm.alarmRepeat(9,45,10, PumpOff);  // Set Alarm For 9:45:20AM Every Day
  Alarm.alarmRepeat(9,45,20, Feeder1);  // Set Alarm For 9:45:20AM Every Day
  Alarm.alarmRepeat(10,19,0, PumpOn);  // Set Alarm For 10:19AM Every Day
  Alarm.alarmRepeat(10,19,10, PumpOff);  // Set Alarm For 10:19:20AM Every Day
  Alarm.alarmRepeat(10,19,20, Feeder1);  // Set Alarm For 10:19:20AM Every Day
```

```
Alarm.alarmRepeat(11,28,0, PumpOn);  // Set Alarm For 11:28AM Every Day

Alarm.alarmRepeat(11,28,10, PumpOff);  // Set Alarm For 11:28:20AM Every Day

Alarm.alarmRepeat(11,28,20, Feeder1);  // Set Alarm For 11:28:20AM Every Day

Alarm.alarmRepeat(12,20,0, PumpOn);  // Set Alarm For 12:20PM Every Day

Alarm.alarmRepeat(12,20,10, PumpOff);  // Set Alarm For 12:20PM Every Day

Alarm.alarmRepeat(12,20,20, Feeder1);  // Set Alarm For 12:20PM Every Day

Alarm.alarmRepeat(13,48,0, PumpOn);  // Set Alarm For 13:48PM Every Day

Alarm.alarmRepeat(13,48,10, PumpOff);  // Set Alarm For 13:48:20PM Every Day

Alarm.alarmRepeat(13,48,20, Feeder1);  // Set Alarm For 13:48:20PM Every Day

Alarm.alarmRepeat(14,35,0, PumpOn);  // Set Alarm For 14:35PM Every Day

Alarm.alarmRepeat(14,35,10, PumpOff);  // Set Alarm For 14:35:20PM Every Day

Alarm.alarmRepeat(14,35,20, Feeder1);  // Set Alarm For 14:35:20PM Every Day

Alarm.alarmRepeat(16,23,0, PumpOn);  // Set Alarm For 16:23OM Every Day

Alarm.alarmRepeat(16,23,10, PumpOff);  // Set Alarm For 16:23:20PM Every Day

Alarm.alarmRepeat(16,23,20, Feeder1);  // Set Alarm For 16:23:20PM Every Day

Alarm.alarmRepeat(17,59,0, PumpOn);  // Set Alarm For 17:59PM Every Day

Alarm.alarmRepeat(17,59,10, PumpOff);  // Set Alarm For 17:59:20PM Every Day

Alarm.alarmRepeat(17,59,20, Feeder1);  // Set Alarm For 17:59:20PM Every Day

Alarm.alarmRepeat(19,10,0, PumpOn);  // Set Alarm For 19:10PM Every Day

Alarm.alarmRepeat(19,10,10, PumpOff);  // Set Alarm For 19:10:20PM Every Day

Alarm.alarmRepeat(19,10,20, Feeder1);  // Set Alarm For 19:10:20PM Every Day

Alarm.alarmRepeat(20,22,0, PumpOn);  // Set Alarm For 20:22PM Every Day

Alarm.alarmRepeat(20,22,10, PumpOff);  // Set Alarm For 20:22:20PM Every Day

Alarm.alarmRepeat(20,22,20, Feeder1);  // Set Alarm For 20:22:20PM Every Day


AFMS.begin(); // Start the bottom shield

Motor1->setSpeed(500); // Speed in RPM

Motor2->setSpeed(500); // Speed in RPM

}
```

```
void loop() {

 Alarm.delay(1000); // wait one second between clock display

}


void PumpOn() {

 digitalWrite(5, HIGH);

 digitalWrite(6, LOW);


}


void PumpOff() {

 digitalWrite(5, LOW);

 digitalWrite(6, LOW);


}


void Feeder1() {

 Motor1->step(40, BACKWARD, DOUBLE); //Steps, Direction, Step Type (SINGLE, DOUBLE,
INTERLEAVE, MICROSTEP)

 Motor1->release();

}

void Feeder2() {

 Motor2->step(40, BACKWARD, DOUBLE); //Steps, Direction, Step Type (SINGLE, DOUBLE,
INTERLEAVE, MICROSTEP)

 Motor2->release();


}
```

Appendix III – Copyright Release

Doyle, J. M., and Croll, R. P. (2022). A Critical Review of Zebrafish Models of Parkinson's

   Disease. *Front. Pharmacol.* 13. doi:10.3389/fphar.2022.835827.

cinematographic adaptations or any other form in which the Work may be recast, transformed, or adapted including in any form recognizably derived from the original, except that a work that constitutes a Collection will not be considered an Adaptation for the purpose of this License. For the avoidance of doubt, where the Work is a musical work, performance or phonogram, the synchronization of the Work in timed-relation with a moving image ("synching") will be considered an Adaptation for the purpose of this License.

 b. "Collection" means a collection of literary or artistic works, such as encyclopedias and anthologies, or performances, phonograms or broadcasts, or other works or subject matter other than works listed in Section 1(f) below, which, by reason of the selection and arrangement of their contents, constitute intellectual creations, in which the Work is included in its entirety in unmodified form along with one or more other contributions, each constituting separate and independent works in themselves, which together are assembled into a collective whole. A work that constitutes a Collection will not be considered an Adaptation (as defined above) for the purposes of this License.

 c. "Distribute" means to make available to the public the original and copies of the Work or Adaptation, as appropriate, through sale or other transfer of ownership.

 d. "Licensor" means the individual, individuals, entity or entities that offer(s) the Work under the terms of this License.

 e. "Original Author" means, in the case of a literary or artistic work, the individual, individuals, entity or entities who created the Work or if no individual or entity can be identified, the publisher; and in addition (i) in the case of a performance the actors, singers, musicians, dancers, and other persons who act, sing, deliver, declaim, play in, interpret or otherwise perform literary or artistic works or expressions of folklore; (ii) in the case of a phonogram the producer being the person or legal entity who first fixes the sounds of a performance or other sounds; and, (iii) in the case of broadcasts, the organization that transmits the broadcast.

 f. "Work" means the literary and/or artistic work offered under the terms of this License including without limitation any production in the literary, scientific and artistic domain, whatever may be the mode or form of its expression including digital form, such as a book, pamphlet and other writing; a lecture, address, sermon or other work of the same nature; a dramatic or dramatico-musical work; a choreographic work or entertainment in dumb show; a musical composition with or without words; a cinematographic work to which are assimilated works expressed by a process analogous to cinematography; a work of drawing, painting, architecture, sculpture, engraving or lithography; a photographic work to which are assimilated works expressed by a process analogous to photography; a work of applied art; an illustration, map, plan, sketch or three-dimensional work relative to geography, topography, architecture or science; a performance; a broadcast; a phonogram; a compilation of data to the extent it is protected as a copyrightable work; or a work performed by a variety or circus performer to the extent it is not otherwise considered a literary or artistic work.

 g. "You" means an individual or entity exercising rights under this License who has not previously violated the terms of this License with respect to the Work, or who has received

express permission from the Licensor to exercise rights under this License despite a previous violation.

h. "Publicly Perform" means to perform public recitations of the Work and to communicate to the public those public recitations, by any means or process, including by wire or wireless means or public digital performances; to make available to the public Works in such a way that members of the public may access these Works from a place and at a place individually chosen by them; to perform the Work to the public by any means or process and the communication to the public of the performances of the Work, including by public digital performance; to broadcast and rebroadcast the Work by any means including signs, sounds or images.

i. "Reproduce" means to make copies of the Work by any means including without limitation by sound or visual recordings and the right of fixation and reproducing fixations of the Work, including storage of a protected performance or phonogram in digital form or other electronic medium.

2. Fair Dealing Rights. Nothing in this License is intended to reduce, limit, or restrict any uses free from copyright or rights arising from limitations or exceptions that are provided for in connection with the copyright protection under copyright law or other applicable laws.

3. License Grant. Subject to the terms and conditions of this License, Licensor hereby grants You a worldwide, royalty-free, non-exclusive, perpetual (for the duration of the applicable copyright) license to exercise the rights in the Work as stated below:

a. to Reproduce the Work, to incorporate the Work into one or more Collections, and to Reproduce the Work as incorporated in the Collections;

b. to create and Reproduce Adaptations provided that any such Adaptation, including any translation in any medium, takes reasonable steps to clearly label, demarcate or otherwise identify that changes were made to the original Work. For example, a translation could be marked "The original work was translated from English to Spanish," or a modification could indicate "The original work has been modified.";

c. to Distribute and Publicly Perform the Work including as incorporated in Collections; and,

d. to Distribute and Publicly Perform Adaptations.

e. For the avoidance of doubt:

i. Non-waivable Compulsory License Schemes. In those jurisdictions in which the right to collect royalties through any statutory or compulsory licensing scheme cannot be waived, the Licensor reserves the exclusive right to collect such royalties for any exercise by You of the rights granted under this License;

ii. Waivable Compulsory License Schemes. In those jurisdictions in which the right to collect royalties through any statutory or compulsory licensing scheme can be waived, the Licensor waives the exclusive right to collect such royalties for any exercise by You of the rights granted under this License; and,

iii. Voluntary License Schemes. The Licensor waives the right to collect royalties, whether individually or, in the event that the Licensor is a member of a collecting society that administers voluntary licensing schemes, via that society, from any exercise by You of the rights granted under this License.

The above rights may be exercised in all media and formats whether now known or hereafter devised. The above rights include the right to make such modifications as are technically necessary to exercise the rights in other media and formats. Subject to Section 8(f), all rights not expressly granted by Licensor are hereby reserved.

4. Restrictions. The license granted in Section 3 above is expressly made

subject to and limited by the following restrictions:

a. You may Distribute or Publicly Perform the Work only under the terms of this License. You must include a copy of, or the Uniform Resource Identifier (URI) for, this License with every copy of the Work You Distribute or Publicly Perform. You may not offer or impose any terms on the Work that restrict the terms of this License or the ability of the recipient of the Work to exercise the rights granted to that recipient under the terms of the License. You may not sublicense the Work. You must keep intact all notices that refer to this License and to the disclaimer of warranties with every copy of the Work You Distribute or Publicly Perform. When You Distribute or Publicly Perform the Work, You may not impose any effective technological measures on the Work that restrict the ability of a recipient of the Work from You to exercise the rights granted to that recipient under the terms of the License. This Section 4(a) applies to the Work as incorporated in a Collection, but this does not require the Collection apart from the Work itself to be made subject to the terms of this License. If You create a Collection, upon notice from any Licensor You must, to the extent practicable, remove from the Collection any credit as required by Section 4(b), as requested. If You create an Adaptation, upon notice from any Licensor You must, to the extent practicable, remove from the Adaptation any credit as required by Section 4(b), as requested.

b. If You Distribute, or Publicly Perform the Work or any Adaptations or Collections, You must, unless a request has been made pursuant to Section 4(a), keep intact all copyright notices for the Work and provide, reasonable to the medium or means You are utilizing: (i) the name of the Original Author (or pseudonym, if applicable) if supplied, and/or if the Original Author and/or Licensor designate another party or parties (e.g., a sponsor institute, publishing entity, journal) for attribution ("Attribution Parties") in Licensor's copyright notice, terms of service or by other

reasonable means, the name of such party or parties; (ii) the title of the Work if supplied; (iii) to the extent reasonably practicable, the URI, if any, that Licensor specifies to be associated with the Work, unless such URI does not refer to the copyright notice or licensing information for the Work; and (iv) , consistent with Section 3(b), in the case of an Adaptation, a credit identifying the use of the Work in the Adaptation (e.g., "French translation of the Work by Original Author," or "Screenplay based on original Work by Original Author"). The credit required by this Section 4 (b) may be implemented in any reasonable manner; provided, however, that in the case of a Adaptation or Collection, at a minimum such credit will appear, if a credit for all contributing authors of the Adaptation or Collection appears, then as part of these credits and in a manner at least as prominent as the credits for the other contributing authors. For the avoidance of doubt, You may only use the credit required by this Section for the purpose of attribution in the manner set out above and, by exercising Your rights under this License, You may not implicitly or explicitly assert or imply any connection with, sponsorship or endorsement by the Original Author, Licensor and/or Attribution Parties, as appropriate, of You or Your use of the Work, without the separate, express prior written permission of the Original Author, Licensor and/or Attribution Parties.

 c. Except as otherwise agreed in writing by the Licensor or as may be otherwise permitted by applicable law, if You Reproduce, Distribute or Publicly Perform the Work either by itself or as part of any Adaptations or Collections, You must not distort, mutilate, modify or take other derogatory action in relation to the Work which would be prejudicial to the Original Author's honor or reputation. Licensor agrees that in those jurisdictions (e.g. Japan), in which any exercise of the right granted in Section 3(b) of this License (the right to make Adaptations) would be deemed to be a distortion, mutilation, modification or other derogatory action prejudicial to the Original Author's honor and reputation, the Licensor will waive or not assert, as appropriate, this Section, to the fullest extent permitted by the applicable national law, to enable You to reasonably exercise Your right under Section 3(b) of this License (right to make Adaptations) but not otherwise.

5. Representations, Warranties and Disclaimer

UNLESS OTHERWISE MUTUALLY AGREED TO BY THE PARTIES IN WRITING, LICENSOR OFFERS THE WORK AS-IS AND MAKES NO REPRESENTATIONS OR WARRANTIES OF ANY KIND CONCERNING THE WORK, EXPRESS, IMPLIED, STATUTORY OR OTHERWISE, INCLUDING, WITHOUT LIMITATION, WARRANTIES OF TITLE, MERCHANTIBILITY, FITNESS FOR A PARTICULAR PURPOSE, NONINFRINGEMENT, OR THE ABSENCE OF LATENT OR OTHER DEFECTS, ACCURACY, OR THE PRESENCE OF ABSENCE OF ERRORS, WHETHER OR NOT DISCOVERABLE. SOME JURISDICTIONS DO NOT ALLOW THE EXCLUSION OF IMPLIED WARRANTIES, SO SUCH EXCLUSION MAY NOT APPLY TO YOU.

6. Limitation on Liability. EXCEPT TO THE EXTENT REQUIRED BY APPLICABLE LAW, IN NO EVENT WILL LICENSOR BE LIABLE TO YOU ON ANY LEGAL THEORY FOR ANY SPECIAL, INCIDENTAL, CONSEQUENTIAL, PUNITIVE OR EXEMPLARY DAMAGES ARISING OUT OF THIS LICENSE OR THE USE OF THE WORK, EVEN IF LICENSOR HAS BEEN ADVISED OF THE POSSIBILITY OF SUCH DAMAGES.

7. Termination

 a. This License and the rights granted hereunder will terminate automatically upon any breach by You of the terms of this License. Individuals or entities who have received Adaptations or Collections from You under this License, however, will not have their licenses terminated provided such individuals or entities remain in full compliance with those licenses. Sections 1, 2, 5, 6, 7, and 8 will survive any termination of this License.

 b. Subject to the above terms and conditions, the license granted here is perpetual (for the duration of the applicable copyright in the Work). Notwithstanding the above, Licensor reserves the right to release the Work under different license terms or to stop distributing the Work at any time; provided, however that any such election will not serve to withdraw this License (or any other license that has been, or is required to be, granted under the terms of this License), and this License will continue in full force and effect unless terminated as stated above.

8. Miscellaneous

 a. Each time You Distribute or Publicly Perform the Work or a Collection, the Licensor offers to the recipient a license to the Work on the same terms and conditions as the license granted to You under this License.

 b. Each time You Distribute or Publicly Perform an Adaptation, Licensor offers to the recipient a license to the original Work on the same terms and conditions as the license granted to You under this License.

 c. If any provision of this License is invalid or unenforceable under applicable law, it shall not affect the validity or enforceability of the remainder of the terms of this License, and without further action by the parties to this agreement, such provision shall be reformed to the minimum extent necessary to make such provision valid and enforceable.

 d. No term or provision of this License shall be deemed waived and no breach consented to unless such waiver or consent shall be in writing and signed by the party to be charged with such waiver or consent.

 e. This License constitutes the entire agreement between the parties with respect to the Work licensed here. There are no understandings, agreements or representations with respect to the

Work not specified here. Licensor shall not be bound by any additional provisions that may appear in any communication from You. This License may not be modified without the mutual written agreement of the Licensor and You.

 f. The rights granted under, and the subject matter referenced, in this License were drafted utilizing the terminology of the Berne Convention for the Protection of Literary and Artistic Works (as amended on September 28, 1979), the Rome Convention of 1961, the WIPO Copyright Treaty of 1996, the WIPO Performances and Phonograms Treaty of 1996 and the Universal Copyright Convention (as revised on July 24, 1971). These rights and subject matter take effect in the relevant jurisdiction in which the License terms are sought to be enforced according to the corresponding provisions of the implementation of those treaty provisions in the applicable national law. If the standard suite of rights granted under applicable copyright law includes additional rights not granted under this License, such additional rights are deemed to be included in the License; this License is not intended to restrict the license of any rights under applicable law.

Creative Commons Notice

 Creative Commons is not a party to this License, and makes no warranty whatsoever in connection with the Work. Creative Commons will not be liable to You or any party on any legal theory for any damages whatsoever, including without limitation any general, special, incidental or consequential damages arising in connection to this license. Notwithstanding the foregoing two (2) sentences, if Creative Commons has expressly identified itself as the Licensor hereunder, it shall have all rights and obligations of Licensor.

 Except for the limited purpose of indicating to the public that the Work is licensed under the CCPL, Creative Commons does not authorize the use by either party of the trademark "Creative Commons" or any related trademark or logo of Creative Commons without the prior written consent of Creative Commons. Any permitted use will be in compliance with Creative Commons' then-current trademark usage guidelines, as may be published on its website or otherwise made available upon request from time to time. For the avoidance of doubt, this trademark restriction does not form part of this License.

 Creative Commons may be contacted at https://creativecommons.org/.